LARGE IN SITU DIRECT SHEAR TESTS ON ROCK PILES AT THE QUESTA MINE, TAOS COUNTY, NEW MEXICO

By

Kwaku Boakye

Advisors: Dr. Virginia McLemore and Dr. Ali Fakhimi

Submitted in Partial Fulfillment
of the Requirement for the

Master of Science degree in Mineral Engineering with specialty in Geotechnical Engineering

Socorro, New Mexico

May, 2008

This thesis is dedicated to God who has been by my side all through, to my dad Mr. Asamoah Boakye, my Mom Mrs. Esther Boakye for taking care of me and loving me as a son, love to you all, to my siblings and my extended Family

ABSTRACT

The purpose of this study is to perform in situ and laboratory direct shear tests to evaluate the shear strength parameters of rock piles deposited during surface mining operation at the Chevron Mining Inc. (formerly Molycorp Inc.) located in Taos County, New Mexico and evaluate the effect of weathering on these shear strength parameters. Weathering of rock piles is an important process that can change the shear strength (cohesion and friction angle) of these materials. A modified in situ direct shear test apparatus was designed and used to evaluate in situ cohesion and friction angle of rock pile materials. Two test apparatuses were constructed; a 30 cm square metal shear box and a 60 cm square metal shear box. In addition to the shear box, the testing apparatus has a metal top plate, a fabricated roller plate, normal and shear dial gages with wooden supports, and two hydraulic jacks and cylinders with a maximum oil pressure of 70 MPa (10,000 psi) and a load capacity of 10 tonnes. The main difference between the in-situ shear box and its conventional laboratory equivalent is that the in-situ shear box consists of a single box that confines an excavated block of rock pile material. The lower half of the block consists of the rock pile material underneath the shear plane that is a semi-infinite domain. This modification in the shear test apparatus reduces the time needed for block preparation, helps perform several tests at different levels of the same sample

block, and allows for accommodating large shear displacement with no reduction in the area of the shear plane. The range of normal stresses for the in-situ tests was 15 to 70 kPa, while for the laboratory shear testing a wider range of 20 to 650 kPa was used. The results showed that the cohesion of some rock pile materials has increased with increase in weathering but not all weathered samples have high values of cohesion. This increase in cohesion is due to gravitational compaction of these materials since their placement, due to the presence of the cementing agents within the rock pile materials that are a result of weathering products, and due to matric suction. The results indicate that no reduction of the friction angle with increase in weathering has occurred so far in the rock piles at the test locations.

ACKNOWLEDGEMENTS

I would like to express my deepest gratitude to the following institutions for their financial and kind support: Molycorp Corporation now Chevron Mining, Inc in the form of a Research Assistantship; WAIME (The Woman's Auxiliary to the American Institute of Mining, Metallurgical, and Petroleum Γ ˙ eers) for financial support; and the New Mexico Bureau of Geology and Mineral Resc for much assistance. I gratefully acknowledge your support.

I would like to express my sincere appreciation to Dr. McLemore and Dr. Fakhimi for providing guidance, insight, and support throughout the course of this research. Appreciation is also extended to Dr. Mojtabai who is on my thesis advisory committee and who encouraged me to do my thesis research at New Mexico Tech. I would like to thank many people who provided support and suggestions on this research, including Lynne Kurilovitch and other members of the weathering study project. I especially want to thank all of the students who assisted me with my in situ testing and laboratory testing program. Last but not least, I would like to thank all the Ghanaian community on campus for all their support by reviewing my thesis a thousand times, and literally going through this experience with me.

TABLE OF CONTENTS

LIST OF FIGURES

LIST OF TABLES

THIS THESIS IS ACCEPTED ON BEHALF OF THE FACULTY OF THE INSTITUTE BY THE FOLLOWING COMMITTEE:

Advisor Signature Date

_____

_____

_____

_____

I release this document to the New Mexico Institute of Mining and Technology.

_____

Student Signature Date

1.0 INTRODUCTION

1.1 Background

This thesis evaluate the shear strength parameters of the surface layer of Questa Molybdenum mine rock piles with conventional laboratory direct shear test and in-situ direct shear test and evaluate the effect of weathering on the shear strength of mine rock pile materials. Using laboratory test methods to determine the shear strength parameters of rock pile material has become popular compared to in-situ testing because the laboratory tests are less expensive and easier to perform. Even with very sophisticated techniques for simulating in-situ conditions, sample disturbance is difficult to eliminate, which causes variations in laboratory results as compared to in-situ testing results. Even with the best sampling technique it is practically impossible to prevent sample disturbance when collecting for laboratory shear tests, especially in rock piles that contain large boulders and rock fragments. The exact amount of disturbance that a sample undergoes is difficult to quantify. Nevertheless, most studies of the shear strength of rock piles involve the use of conventional laboratory analysis performed on disturbed samples. These laboratory tests are considered standard engineering practice for design purposes, but they do not always take into account the existence of cohesion within the rock pile. In fact cohesion is usually considered to be zero for laboratory direct shear testing. Yet cohesion could affect the overall stability of rock piles. For example, previous studies have identified the influence of microstructures such as cementation on shear strength (El-Sohby et al. 1987; Pereira 1996; Pereira and Fredlund 1999).

In order to evaluate the effect of cohesion on the slope stability of rock piles and to allow larger particles to be included in the tests with no disturbance, a modified in-situ

shear testing apparatus was developed and implemented. The in-situ shear tests performed in this project are similar to the methods used by Fakhimi et al. (2004). They used in-situ shear tests on soil material in a tunnel in Tehran where the reaction of the normal force was transferred to the tunnel roof. Subsequent sections of this document give detailed design, methodology, and results for the modified in-situ shear tests performed during this research work.

In addition to in-situ shear testing, laboratory shear tests were conducted on the disturbed dry samples. The results of in-situ and laboratory shear tests are compared in this thesis. The effect of weathering on the shear strength of Questa rock pile material will be addressed as well. All appendices of this research study are on a CD attached to the thesis.

1.2 Thesis Overview

This thesis is organized into seven chapters as follows:

Chapter 1: Introduction to the general concept of the research project, the project background and site description

Chapter 2: Review of previous shear strength studies and index parameters of the rock piles.

Chapter 3: Literature review of concepts related to this research

Chapter 4: Methodology adopted to address our objectives

Chapter 5: Presentation of in situ, laboratory, and index parameters results

Chapter 6: Discussions of all tests results

Chapter 7: Conclusions and recommendations

1.3 Project Scope and Objective

Early in July 2006, a program was undertaken to use an in-situ direct shear device to evaluate the in-situ shear strength parameters of rock piles deposited during surface mining at the Chevron Mining Company's Questa molybdenum mine. Conventional laboratory tests were also conducted for each corresponding in-situ tests. The mine area's most conspicuous features are the nine rock piles constructed from 31,750,000,000 kg (31.75 million metric tons) of overburden removed during the surface mining period (URS Corporation, 2000). The rock piles are heterogeneous with particle sizes ranging from minute clay-size fractions up to boulders (Gutierrez, 2006). Three questions arise in evaluating the shear strength parameters for these rock pile materials:

1. What are the cohesion values of the rock piles? In order to measure the cohesion, in situ-shear testing was needed as disturbing the samples can destroy the interlocking and other mechanisms between the particles.
2. What is the shear strength parameters for the analog sites and how do they compare to the rock pile material?
3. What is the effect of weathering on the shear strength parameters of the rock pile after 40 years since their emplacement?

The evaluation program for the two shear testing methods was undertaken in three steps:

1. Design and construct an in-situ direct shear device large enough to test the natural particle sizes and heterogeneities of the rock piles effectively.
2. Use the new in-situ direct shear test apparatus on the rock piles to determine their shear strength parameters.

3. Conduct laboratory shear tests on the smaller size fractions of the same rock pile materials as that tested in situ to compare the two direct shear test methods and their results.

1.4 Site Description

1.4.1 Location of the Questa Mine

The Questa molybdenum mine is located in a region with a long history of mining 5.6 km (3.5 miles) east of the village of Questa in Taos County, north central New Mexico (Figure 1.1). The mine is on the south-facing slopes of the north side of the Red River valley between an east-west trending ridgeline of the Sangre de Cristo Mountains and State Highway 38 adjacent to the Red River at elevation 2,438 m (8,000 ft) (URS Corporation, 2000).

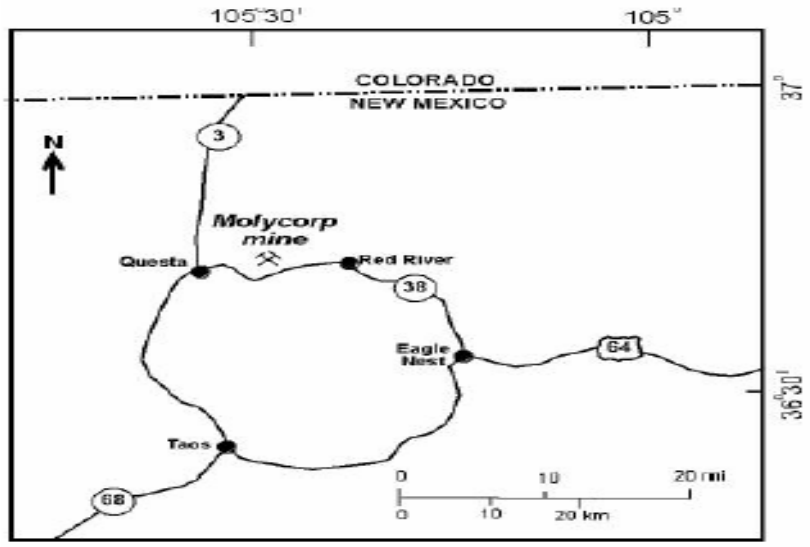

Figure 1.1. This image shows the location map of Chevron Mining Co.'s Questa molybdenum mine, which is in northern Taos County, New Mexico (Gutierrez, 2006).

1.4.2 Mine History

The Questa Molybdenum Mine has existed for 83 years since the first discovery of molybdenum in the area in 1914. Molybdenum was discovered by two local prospectors who later staked multiple claims in an area of the Sangre de Cristo Mountains called Sulphur Gulch. Prospectors first thought that the unknown, dark, metallic material was graphite and was used for a myriad of functions from lubricating wagon axles to shoe polish. Samples were sent for assay in 1917 to identify the "gold and silver mineral" composition, but the outcome was instead an abundance of molybdenum. Molybdenum is also a strategic mineral, and was particularly important during World Wars I and II.

The property was acquired by R and S Molybdenum Mining Company in 1918 and they initiated underground mining of the high-grade molybdenum veins. R and S Molybdenum Mining Company changed their name to the Molybdenum Corporation of America in 1920. The Molybdenum Corporation of America was acquired by Union Oil Company of California in August of 1977 and became Molycorp, Inc., and subsequently was acquired by Chevron Mining Co., Inc. in October 2007. Molybdenum Corporation of America operated the Junebug mill in 1923 that milled 25 tons of ore daily. The mill was fed with molybdenite (MoS_2) with some grades running as high as 35% molybdenum. The mill operated for the duration of the first underground mine operatiosn until that ceased in 1956. In 1963 the mill was dismantled to make way for a new mill.

Molybdenum Corporation of America initiated extensive exploration work from 1957 to 1960 under contract through the U. S. Defense Minerals Exploration Act. With the completion of the contract in 1960, Molybdenum Corporation of America continued exploration by core drilling from the surface and underground with the hope of starting

an open pit if large deposits of molybdenum were found in the subsurface. The program was accelerated because the need of more molybdenum production was inevitable. By 1964, sufficient reserves had been defined to justify the development of an open pit mine and the construction of a mill that could handle 10,000 tons per day. Open mine stripping started in 1964, and the first ore from the pit was delivered to the new mill in January 1966.

Renewed development of the existing underground mine began with the sinking of two vertical shafts approximately 396 m (1,300 ft) deep, and a 1.6 km -long decline was driven from the existing mill area to the haulage level. The treatment of the molybdenum ore was modernized to increase the percentage of recovery. This also helped to accommodate the underground higher grade ore.

Open pit operations ceased in 1983 with the opening of the new underground mine, which used block caving mining methods. In 1986, the "soft" market price of molybdenum caused the shutdown of the mine, but the mine was reopened in 1989 when the price of Mo rose again. The operation of the mine continued until January 1992 when the mine was shut down again due to the low price of molybdenum. The mine reopened in 1995 and most of that year was devoted to mine dewatering and repair. Production began in 1996 and over the next several years approximately 13.6 million kg (30 million pounds) of molybdenum concentrate were produced. In 1998, development of a new orebody started and three adjacent orebodies were defined. The mine continues to be one of the molybdenum producers in the United States, increasing their employment each year.

1.4.3 Mine Features

The mine encompasses three main tributary valleys: Capulin Canyon, Goathill Gulch, and Sulphur Gulch from east to west, respectively (Shaw, 2002). During the period of open pit mining (1969-1981), approximately 31,750,000,000 kg (31.75 million metric tons) of mine waste rock and overburden was removed. This material was placed in nine valley-fill and side-hill rock piles using end dumping methods. The piles, including Sugar Shack South, Middle and Old Sulphur (or Sulphur Gulch South), were deposited along the sides of the mountain ridges and within and along narrow mountain drainages, ultmately forming large rock piles along State Highway 38. These piles are referred to as the Front Rock Piles or Roadside Rock Piles and are on the west-facing slope of the mountain. Capulin, Goathill North, and Goathill South rock piles are on the west-facing mountain slope on the west side of the open pit. On the east side of the pit, the Spring Gulch and Blind Gulch/Sulphur Gulch North rock piles are located. Figure 1.2 is an aerial photograph of the mine site showing the locations of all of the rock piles. The mine rocks piles are characterized by high heights standing at an angle of repose from the Red River at elevations from 2,440 m (8,005 ft) to 2,930m (9,613 ft), making them some of the highest elevation mine rock piles in North America (Shaw, 2002). These rock piles also are typically at the angle of repose of about approximately 37º and have long slope lengths (up to 610 m (2000 ft)), and comparatively shallow depths (366 – 732 m) (1200.79 ft – 2401.57 ft) (Lefebrve et al., 2002). Other features on the mine site are the offices which are situated on the southwestern corner of the mine property and the Mill Site on the southeastern corner.

Figure 1.2 Aerial Photograph – Questa Molybdenum Mine, New Mexico

Circa 2003

Scale
~2,500 feet

North

Sense of Elevation: ~7875' at Administration Bldg (Admin) to ~ 9800' along road between the Open Pit and the D-Orebody Subsidence Area

1.4.4 Geology and Mineralogy of the Red River Valley

The geology and the mineralogy of the area have been reported by many authors (Schilling, 1956; Carpenter, 1968; Clark, 1968; Lipman and Reed, 1989; Meyer and Leonardson, 1990; Roberts et al., 1990; Meyer, 1991). The geology and mineralogy of the Red River Valley area is complex. The Red River Valley is located along the southern edge of the Questa caldera and contains complex structural features (Caine, 2003) and has undergone extensive hydrothermal alteration. The lithologies are likewise diverse, ranging from metamorphic rocks to volcanic rocks, granite to shale, to limestone and sandstone. The area has experienced multiple geologic and tectonic events. The regional geology of the area can be subdivided into five general tectonic periods: Proterozoic, Paleozoic Ancestral Rocky Mountains, Laramide Orogeny, Rio Grand Rift Volcanism (including the Questa caldera), and recent Rio Grande Rift Fill. The Rio-Grand rift-related volcanic rocks are considered to be the most important rocks in the area. The volcanic rocks are extrusive rocks ranging in composition from basaltic and quartz-latitic flow to welded ash-flow sheets of high silica alkaline rhyolite (Amalia Tuff) that erupted from the Questa caldera. Volcanic and intrusive rocks are of Tertiary age and they are underlain by metamorphic rocks of Precambrian age that were intruded by granitic stocks. They are primarily intermediate to felsic composition (andesite to rhyolite) granites and porphyries. The porphyritic granitic rocks have intruded the entire sequence. The porphyries are the ultimate source of the hydrothermal fluids and molybdenite mineralization.

Nordstrom et al. (2005) reported that other common geological features of the Red River valley area are the alteration scars and debris flows. They also indicated that

andesitic volcanic and volcaniclastic rocks are present in most scar-area bedrock outcrops and are the predominant bedrock units in the Straight Creek, South and Southeast Straight Creek, South Goat Hill, Sulphur Gulch, and Southwest Hansen alteration scars. The rock type of the Goat Hill and Hansen scars is predominantly of quartz latite porphyry.

Mutschler et al., (1981) describe the molybdenum deposits of the Red River Valley area as being primarily Climax-type ore deposits that are associated with silica and fluorine-rich rhyolite porphyries and granitic intrusions. Alteration assemblages with a central zone of fluorine-rich potassic alteration, a quartz-sericite pyrite (QSP) zone (locally with a carbonate-fluorite veinlet overprint), and a propylitic zone are mostly produced by Climax-type hydrothermal alteration. In the potassic zone, the rocks are mostly altered to a mixture of biotite, potassium feldspar, quartz, fluorite, and molybdenite; these rocks usually contain less than 3 percent sulfide (including molybdenite). A mixture of quartz, pyrite (as much as 10 percent), and fine-grained mica (sericite or illite) are identified as the Quartz-sericite-pyrite (QSP) alteration. Other minerals typically found in the Red River Valley are chlorite, epidote, and albite.

Minerals associated with the ore deposits in the Red River Valley are predominantly quartz, molybdenite, pyrite, fluorite, calcite, manganiferous calcite, dolomite, ankerite, and rhodochrosite. Minerals that exist in small amounts are galena, sphalerite, chalcopyrite, magnetite, and hematite. In the overburden rock, there are minerals like chlorite, gypsum, illite, illite-smectite, jarosite, kaolinite, and muscovite (Gale and Thompson, 2001).

1.4.5 Climate, Vegetation and Drainage

The climate in the area of the mine is semi-arid with mild, dry summers and cold, wet winters. The mine is located in an area of high relief with a complex distribution pattern of precipitation and net infiltration. As a result of the difference in snow pack at different elevations, there is a general trend of increasing net precipitation with increasing elevation (Shaw et al, 2002). The annual average precipitation and snowfall are approximately 50 cm (1.64 ft) and 370 cm (12.17 ft), respectively. Average winter temperature of the region is approximately 4^{o}C. The Western Regional Climate Center (2003) reported daily temperature generally fluctuating by 18^{o}C throughout the year.

The orographic effect of the mountainous topography leads to precipitation on the windward slopes and localized storms within tributary valleys. Knight (1990) reported that the vegetation along the Red River Valley is mostly of altitude zone (1,800-2,300 m (5,906 – 7,546 ft) in altitude), mixed with conifer woodland (2,300-2,700 m (7,546 – 8,858 ft) in altitude), and spruce-fir woodland (2,700-3700 m (8,858 – 12,139 ft) in altitude). The Sangre de Cristo Mountains are drained by intermittent tributaries of the Red River including Bitter, Hottentot, Straight, Hansen, and Cabresto Creeks (Figure 1.3). Along the banks of the Red River are vegetation like willows, cottonwoods, shrubs, perennial grasses, and followers. Widely spaced pinon pines and junipers extend from the river. Nordstrom et al. (2005) indicated that the rise in abundance of ponderosa and limber pines is due to the presence of gain in altitude. At higher altitudes, there are Douglas and white-firs.

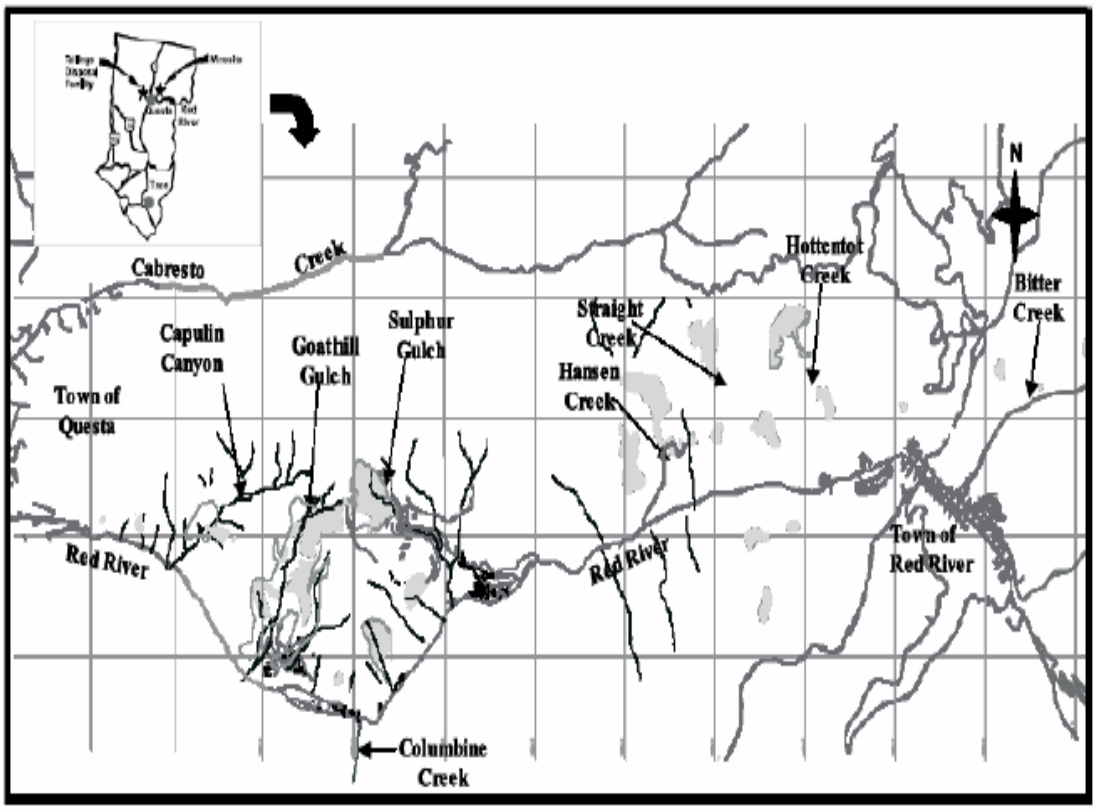

Figure1.3. Drainage patterns of the Questa Red River Area (Shaw et al., 2003)

1.4.6 Motivation for Research Study

The rock piles at the Questa mine have existed for more than three decades. Foundation sliding in the northern portion of the Goathill north rock pile (GHN), one of the nine (9) rock piles at the mine, initiated mitigation efforts in 2002 (Norwest Corporation, 2004). Studies were conducted by Norwest Corporation (2004) on the GHN, in which they indicated that the foundation movement associated with the initial development of the slide occurred in 1969 and 1973.

The stability of the rock piles at the mine has always been a concern to the management. The foundation sliding of the Goathill north rock pile (GHN) initiated the concern of management to assess the long term stability of other rock piles and to evaluate the effect of weathering on the slope stability of these rock piles. In 2002, Molycorp solicited letters of intent from qualified university researchers and other research groups for the purpose of investigating the potential effect of weathering on the long term stability of the rock piles at the mine (Molycorp Inc., 2002).

The University of Utah put together, a team of researchers and consultants from the United States and Canada to undertake the weathering study of the rock piles and evaluate the effect of weathering on the stability of the rock piles. The team consisted of geologists, geophysicists, geochemists, hydrologists, biologists, geotechnical engineers, students and other supporting staffs from different academia and consulting organizations. This research work forms part of the overall research program undertaken by the University of Utah team.

2. REVIEW OF SHEAR STRENGTH STUDIES OF THE QUESTA ROCK PILES

2.1 Current Study of the Shear Strength of Questa Mine Rock Piles

Present work on the rock piles is being performed as part of the Chevron Rock pile Stability Study by a multidisciplinary group of engineers and scientists with the following main objectives:

- Understanding the weathering processes, both at the surface and within the rock piles.
- Measuring the rate at which such weathering processes occur over time.
- Determining the changes in geotechnical properties of alteration scars, colluvium/weathered bedrock and debris flow analogs over time. These sites are analog sites because they are similar in mineralogy and geochemistry and have similar weathering processes.
- Determining the effect of weathering on the cohesion of the rock pile by performing in-situ direct shear tests to evaluate the cohesion of the rock piles.

Early in July 2006, a program was undertaken to use an in-situ direct shear device to evaluate the shear strength parameters of rock piles deposited during surface mining at the Questa molybdenum mine and comparing the results with conventional laboratory direct shear testing methods. The motivation for performing in-situ shear tests was to obtain the shear strength properties of undisturbed rock pile blocks. Disturbed samples may not provide reliable information especially the cementation extent of the material. The field test program ended in August 2007.

2.2 Previous Shear Strength Results for the Rock Piles

A comprehensive geotechnical characterization of the mine rock piles has been carried out at the Questa site over the last several years to evaluate their current conditions. All previous tests for determining the rock pile strength parameters were performed in laboratories. These projects included stability evaluations and the development of closeout and mitigation plans. The geotechnical characterization work included laboratory particle size distribution, Atterberg limits, dry unit weight, specific gravity, moisture content, and shear strength. To perform these tests, representative samples were collected from surface test pits or from drill holes within the rock piles and trenches for GHN and elsewhere throughout the mine site (McLemore, 2005). The drill holes depths range from 9 to 70.4 m (30 to 231 ft) (Norwest Corporation, 2004). Published literature review on geotechnical characterization of the mine rock piles has been performed by Gutierrez (2006), Norwest Corporation (2004, 2005), Robertson GeoConsultants (2000) and URS Corporation (2000).

Gutierrez (2006) investigated the influence of physical, geological, mineralogical and chemical properties on shear strength properties of the Goathill North rock pile at the Questa molybdenum mine, New Mexico. Representative samples were collected based upon visible changes in the weathering characteristics. Shear strength was evaluated in the laboratory using a 5cm by 5cm (2in by 2in) shear box with a deformation rate of 0.0085cm/sec (0.0033in/sec) on air dried samples. In her interpretation results zero cohesion was assumed.

The sample density for the direct shear tests was based on field measurements at the sampling location from a nuclear gage, sand cone, water replacement and sand

replacement tests. Gutierrez (2006) reported average dry density of 1.7 g/cm^3 and standard deviation of 0.15g/cm^3. An average wet density of 1.8 g/cm^3 and standard deviation of 0.18 g/cm^3. Therefore, a dry density of 1.7 ± 0.2g/cm^3 was selected for the Gutierrez (2006) shear box tests. The range of normal stresses used for the direct shear test was between 50kPa and 800kPa.

From these tests Gutierrez (2006) concluded that the majority of samples tested from the Goathill North rock pile are classified as poorly to well graded gravels with fines and sand. Most of the fines (silt and clay) sized are classified as inorganic clay with low swelling potential. Her plots between internal friction angle and percent of fine, liquid limit (LL), or plasticity index (PI) all showed a slight negative correlation. Gutierrez (2006) indicated that the peak internal friction angle ranged from 40^o to 47^o. These high values observed for internal friction angle and residual friction angles were attributed to the angularity and subangularity of the particles of the samples tested. Gutierrez (2006) and Gutierrez et al. (2008) concluded that friction angle of some of the GHN rock pile samples decreased as the degree of weathering increased, but not in all samples. However, the decreases were still small and suggest that 40 years of weathering have not substantially affected the shear strength properties of these rock pile materials. Collectively, the results by Gutierrez (2006), coupled with high slake durability and point load indices by Viterbo (2007) suggest that near future weathering will not substantially decrease the shear strength of the rock piles with time.

In 2005, Norwest Corporation conducted operational geotechnical stability evaluation study on the front rock piles (Middle Rock Pile, Spring Gulch Rock Pile and Sulfur Gulch Rock Pile) to assess their stability in the future (Norwest Corporation,

2005). The shear strength of these rock piles was evaluated by reviewing the results obtained by Robertson GeoConsultant (RGC) Inc. (2000) on bulk samples obtained from pits/trenches. Two type of shear boxes results were summarized by Norwest: a relatively large 30cm by 30cm shear box with sample height of 20 to 23 cm and a smaller 6cm (2.36in) diameter shear box with 2.54cm (1in) sample height.

Norwest's (2005) summarized field grain size distributions for all mine rock pile test samples of Robertson GeoConsultant (RGC) Inc. (2000) and other previous geotechnical study of the rock piles indicated that the material is sandy gravel with varying fines contents mostly between 5 to 20% with maximum sieve size of 75 mm. One sample showed greater fines content of about 32%. The average moisture content of samples tested was less than 10%. Norwest (2005) summarized shear tests results evaluated as follows:

- The isotropically consolidated undrained triaxial test results for large strain provide a lower bound strength envelope of 36^{o}. The triaxial tests were carried out with a much higher confining stress than the direct shear tests, up to 2760kPa, which corresponds to a stress level equivalent to a depth of 140m.
- The results obtained for large box (30cm) direct shear tests fall above the triaxial test strength envelope at 36^{o}. Several of the individual test results indicate a slight strain softening response at the end of the test.
- The results obtained by Norwest (2005) for the small shear box fall in a tight grouping around (above and below) the 36^{o} friction angle line. Testing was carried out with up to 6.4 mm (0.25 inch) horizontal displacement (i.e. 10% strain). The

stress/strain curve for many of the small box tests show a strong strain hardening response at the end of the test.

Based on their findings, Norwest (2005) concluded that a constant volume friction angle of 36^o is the preferred angle for design to ensure stability of the rock piles.

The geotechnical characterization of the properties of the GHN rock pile (Norwest 2004) included laboratory tests of particle size distribution, Atterberg limits, specific gravity, moisture content and shear strength tests. Particle size analysis indicated that the Goathill North rock pile has a wide variation ranging from cobble-sized material to silty and clayey sands using a maximum sieve size of 75 mm. The rock pile material can be described as mostly sandy gravel with less than 20% fines, clay content less than 12%, and the plasticity indexes (PI) is less than 20%. The rock pile dry unit weight of 21 samples indicates an average of 1.8 g/cm^3 with standard deviation of 0.1 g/cm^3. The specific gravity of the mine rock, based on 15 samples, ranges from 2.7 to 2.8. The shear strength of the material tested indicated an average internal friction angle of 36^o. The friction angle was obtained by performing consolidated undrained triaxial tests.

URS Corporation conducted an erosion and stability evaluation of the mine rock piles at Questa in 2003 (URS Corporation, 2003) which was a comprehensive study of the mine rock piles. They studied the shear strength of these rock piles by conducting laboratory direct shear tests using two types of shear boxes, a relatively large 30 cm by 30 cm shear box and a smaller direct shear box of size 6 × 6 cm. Material used for the 6cm by 6cm shear box was first passed through the No. 4 sieve. The 30 cm by 30 cm shear was used to test material less than1.5 inch in size. Material preparation for the 6 cm by 6 cm shear box involved compaction of the material to achieve a dry density between

1.5 g/cm^3 and 2.3 g/cm^3 at a moisture content of 10 to 14 percent. The 30 cm by 30 cm shear box samples were generally prepared to result in a dry density ranging from 1.5 g/cm^3 to 1.7 g/cm^3 at a moisture contents ranging from 8 to 11%. The plasticity index of these materials ranges from 5 to 26 %. Most materials were classified as gravel to sand with some percent of clay. URS's shear test results showed a friction angle between 33^o and 49^o for the large and small box direct shear tests. A high percentage of fines in some of the material accounted for the low friction angles.

2.2 Summary of Previous Shear Strength of Questa Mine Rock Piles

All previous tests for determining the rock pile strength parameters were performed in laboratories. Gutierrez (2006) performed laboratory shear tests to determine internal friction angles using 5cm – 10cm (2- to 4-in) shear boxes on dry samples from the Goathill North (GHN) Rock Pile. She reported a peak friction angle range of 40^o to 47^o and a residual friction angle range of 37^o to 41^o. URS (2003) and Robertson GeoConsultants (2000) reported the same range of shear strength properties for the Questa rock piles. Norwest Corporation compiled a report in 2004 and 2005 of the shear strength of the GHN and front rock piles indicating that the rock piles constant volume friction angle is 36^o. Results obtained from our study were compared to previous studies.

To obtain more reliable shear strength parameters of the rock pile material, an in situ shear apparatus was designed as part of this thesis research and used to measure the in situ shear strength properties of the rock piles. This testing procedure eliminated the uncertainties related to using conventional laboratory testing methods and also prevented the need to collect intact samples which is difficult due to presence of large rock fragments in the rock pile material.

3. LITERATURE REVIEW OF CONCEPTS RELATED TO THIS RESEARCH

3.1 Mine Rock Piles

Rock piles refer to man-made structures consisting of non-ore material removed during the extraction of ore. These materials, referred to in older literature as mine waste, mine soils, overburden, sub-ore, or proto-ore, and do not include the tailings material that consists of non-ore waste remaining after milling. Robertson (1982) described mine rock piles as some of the largest man-made structures at a mine by volume and height. Mine rock piles and tailings piles are two major facilities that contain geological materials that are considered "waste" in mining and milling operations (Robertson, 1985; Sracek et al., 2004). Mine rock pile materials are broken up and removed from their original location, and placed in piles in which the conditions of oxidation, seepage, leaching, and erosion differ considerably from their original locations. The International Commission on Large Dams (ICOLD) in 1996 estimated that the amount of mine rock piles and tailings disposed of globally likely exceeds 5,000,000,000 metric tonnes per annum (Blight et al, 2005). It is important to note that most of these materials are dam materials.

3.1.1 Type of Mine Rock Piles Deposition

The shape of mine rock piles is primarily based on the nature and topography of where they are emplaced. Mine rock piles contain overburden material and can take the shape of one of, or a combination of, many different configurations such as valley-fill, cross-valley, side-hill, ridge, and heaped, depending on the topography of the area (Zahl

et al., 1992). As the name indicates, the valley-fill rock piles are constructed so that the rock pile fills a valley. The valley-fill rock pile has its top surface sloped to eliminate water ponding. Construction of the valley-fill rock pile begins at the upstream end of the valley and dumping proceeds along the downstream face. The method of construction of the embankment also can be started as a cross-valley structure where the area is subsequently filled upstream. Side-hill rock piles are mostly created along the side of a hill or valley but do not cross the valley bottom. Most ridge rock pile embankments straddle the crest of a ridge, and overburden material is placed along both sides of the area. Figure 3.1 shows the various configurations of rock piles depending on the underlying topography.

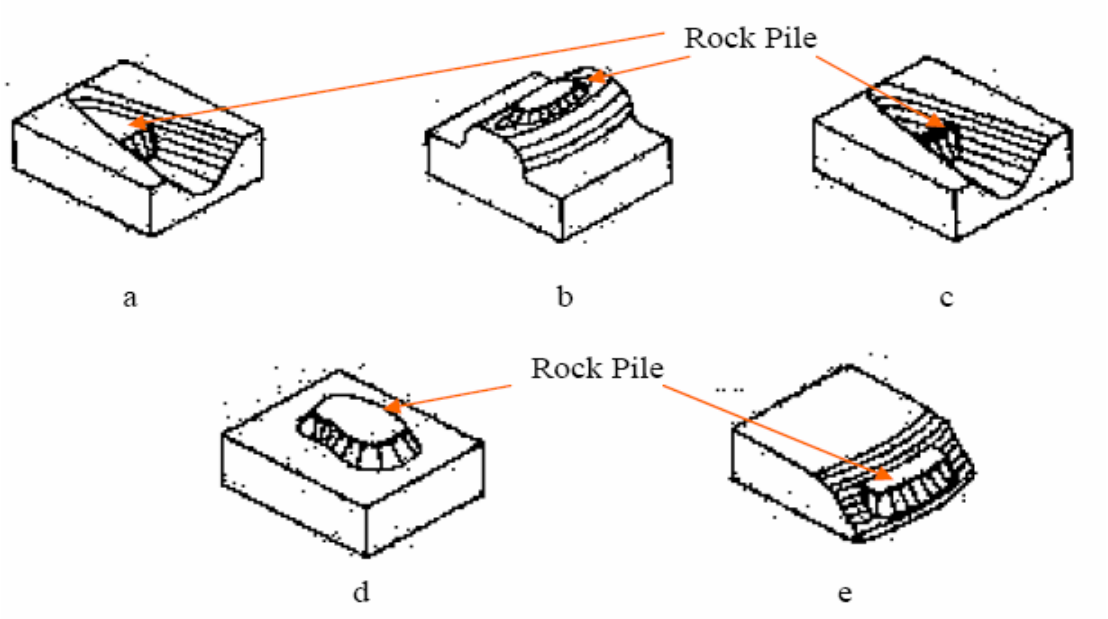

Figure 3.1. Rock Piles Configuration based on Topography, (a) Valley-fill (b) Ridge, (c) Cross-valley, (d) Heaped, (e) Side-hill (Zahl et al., 1992).

Robertson (1982) described different modes of defining rock piles based on the method of dumping. They are grouped into two main groups: end-dumped and layer-placed embankments. End-dumped rock piles are advanced by tipping the rock from the crest of a hill and allowing it to roll down the slope and settle, with the surface and the resulting layers roughly paralleling the angle of repose and sub-parallel to the original slope. Side-hill piles are a common type of end-dumped rock piles. Common features of end-dumped rock piles are continuous raveling and sheet failure along the rock pile slope during the dumping process (Nichols, 1987; Morin et al., 1991, 1997; McLemore et al., 2005). The process of end-dumping results in segregation of materials with finer-grained material at the top and coarser-grained material at the base. Figure 3.2 illustrates the size and layer segregation in the Goathill North rock pile at the Questa molybdenum mine (McLemore et al., 2005). Because they were end-dumped, there are similarities in the nature and features of all the rock piles at the Questa mine and segregation can visually be seen in most of the rock piles. This segregation has been recononized by Swanson et al. 2000. For example, the rock pile at the Libiola mine near Sestri Levante, Genova is reddish-yellow, generally coarse-grained, and stratified (Dinelli et al., 2001). The rock piles at Golden Sunlight are heterogeneous and stratified (Herasymuik, 1996). The waste stockpiles at Ajo mine, Arizona are stratified (Savci and Williamson, 2002). The Goldstrike deposits in Nevada are very complex and stratified (Martin et al., 2005).

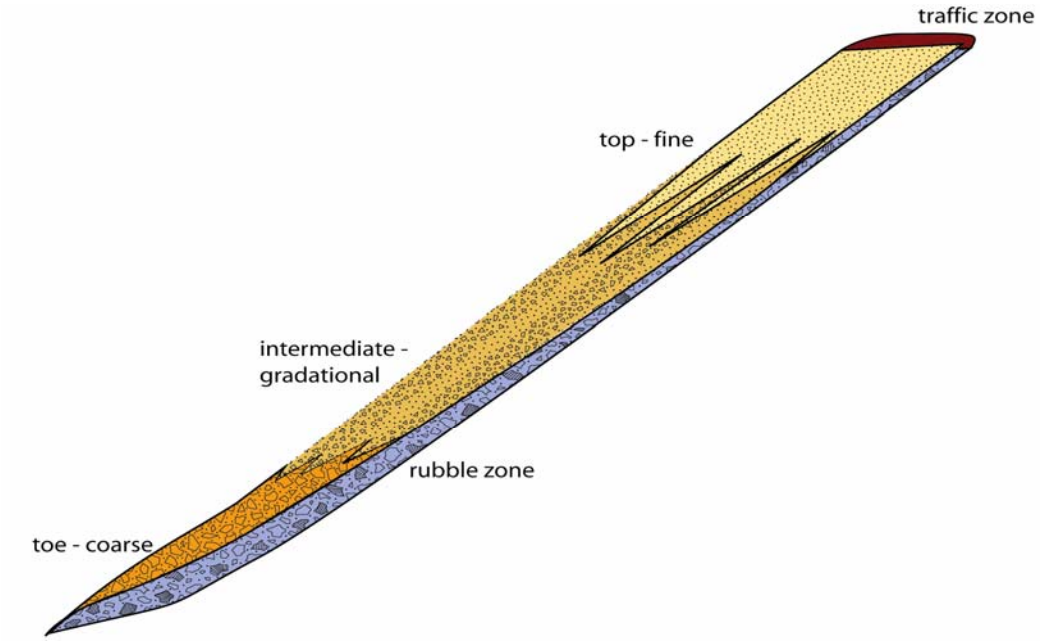

Figure 3.2. Conceptual model of the particle-size distribution of a rock pile constructed by end dumping over the crest of a natural slope of a hill, similar to the construction of GHN and many rock piles in the world (from field studies at GHN and Nichols, 1987, Morin et al., 1991, 1997,). See McLemore et al. (2005) for detailed explanation of zones.

3.1.2 Environmental Issues Related to Mine Rock Piles

Environmental issues related to mine rock piles and mine waste have been the subject of the public regulatory authorities and industry since 1970. This is because of the potential negative environmental impact of these man-made structures on the ecosystem. Generally mining changes the topography and land use capabilities. Open pit mining operation result in a large quantity of mine waste production. It is desirable that following reclamation, the facilities blend into or are compatible with surrounding terrain and that the surface of the facility be capable of a land use equivalent to or better than the original surface. Unfortunately most historic mines consist of abandoned mine waste facilities that

result in degradation of the ecosystem. Environmental issues that arise from mine waste can be grouped into two categories: stability and erosion; and acid mine drainage (AMD) (Robertson, 1985).

The stability of mine rock piles must be carefully evaluated and monitored during operation phases of the mining or after the mine operation. The next section discusses detail insights into slope stability of mine rock piles.

3.1.3 Mine Rock Pile Stability

Mine rock piles deposited at their angle of repose by crest end-dumping have intrinsic stability or directly after of placement (Robertson, 1982). The stability conditions can change with time as a result of time-dependent changes in the strength along potential failure surfaces and the force, principally water pressure, acting on these potential failure surfaces (Robertson, 1982).

The stability of mine rock piles also can decrease as a result of raising the water table due to groundwater accumulation, due to changes in the permeability of the rock pile materials resulting from weathering and the washing in of fines, and due to a possible decrease in pile material strength from weathering. Many tragic rock pile failures occur due to one or more of these changes and therefore long term stability analyses must take into account their potential long-term strength and phreatic surface changes (Robertson, 1985).

Mine rock pile failures are uncontrolled or unscheduled and occur by the rock pile failing beyond its confined zone (Robertson, 1985). Most failures are in weaker

sedimentary rocks, such as those found in coal deposits. The pile failure at coal mines is caused by disruptive actions as a result of:

- Liquefaction of mine rock piles due to events such as floods, earthquakes, volcanic eruption or action, and glaciation, which apply forces exceeding the values for which the impoundments were originally designed (Hutchinson, 1988).
- Rock piles or mine pit slope failure occur due to slow but perpetual actions of wind and water erosion, frost action, other forms of weathering and decomposition, chemical reaction and biological actions such as intrusion by roots, animals and man.
- Foundation failure or failure through weak foundation.
- Subsidence

Caldwell et al. (1981) and others defined different modes of failure that occur in mine rock piles. In most surface or edge slides, material moves along the slope of the mine rock pile to the base. This mode of failure mostly occurs in crest-tipped embankments. If sufficient seepage of water into the mine rock pile creates weak planes and causes flow of material parallel to the face, a shallow flow slide may occur. Rock piles placed on flat ground with competent soil are the least likely to fail. On the other hand, end-dumped and layer-placed embankments are most likely to fail. Block translation can occur where a dump is formed on inclined ground and the soil cover is relatively thin and weak. An unusually high water table in the embankment, earthquakes, or decay of organic material beneath the dump may start such failure. Circular arc failure through dump material is most common where the dump material contains a significant percentage of fine-grained

soil. Similarity, circular arc failure can be deep seated in fine-grained soils (Caldwell and Moss, 1981).

3.2 Factors that Affect Shear Strength of Mine Rock Pile Materials

Characterizing the gravitational stability of mine rock piles is complicated because the factors affecting slope stability can be challenging to differentiate and measure, especially the rock piles' physical properties and their effect on shear strength parameters. With rock piles or soils the shear strength of the material is defined as the resistance of soil to movement along a plane when shearing forces are applied. The stability of a material is controlled principally by the shear strength of the material. McCarthy (1993) refers to soil or mine rock pile stability as being governed by other factors like strength, durability, permeability and small volume changes, but especially by its shear strength.

Shear strength, like other soil properties, is related to several factors. These factors are grouped into compositional factors and environmental factors (Mitchell, 1993). Compositional factors include: the soil particle size distribution and shape, the type and amounts of minerals making up the material, the type of adsorbed anions available, and the composition of the pore water. Environmental factors include: moisture content, density, confining pressure, temperature, soil structure, and availability of water.

Weathering also has an influence on the shear strength of mine rock piles or soils. For instance, Pasamehmetoglu et al. (1981) observed a decrease in strength of weathered andesites, when they studied rock piles in Ankara, Turkey. They noted that there is a large decrease in strength with weathering of the otherwise intact rocks. These changes in

strength are due to the variation in mineral composition and porosity that occurs in andesites during weathering and that these changes affect the slope stability. Abramson (2001) noted the effect of weathering on rock piles by noticing the significant alteration of clay (argillic) to slaking and physical weathering due to the freeze-thaw and wet-dry cycles.

Other researches (Lohnes and Demirel, 1973; Chigira and Oyama, 1999; Pernichele and Kahle, 1971) also indicate that rocks mined from different alteration zones and placed in rock piles undergo weathering at different rates, which can be due to mechanical and/or chemical weathering. Evident within rock piles are boulders that completely break up and others that remain intact and durable. The various changes that occur within rock piles affect the slope stability and can facilitate their failure. Detailed weathering processes and their effect on the shear strength of rock piles are explained in the context of this thesis.

3.3 Shear Strength Criteria for Slope Stability Analysis

A failure criterion governing the shear failure of soils was first put forward in 1776 by Coulomb and later modified by Mohr in the form of equation 3.1 and diagrammatically expressed in Figure 3.3. The shear strength on a given surface depends linearly on the normal stress (σ_1, σ_2, and σ_3) acting on that surface (Figure 3.3).

$$\tau = c + \sigma \tan \phi \tag{3.1}$$

Where:

τ = Shear strength

c = Cohesion

σ = Effective normal stress on the failure plane

ϕ = Friction angle

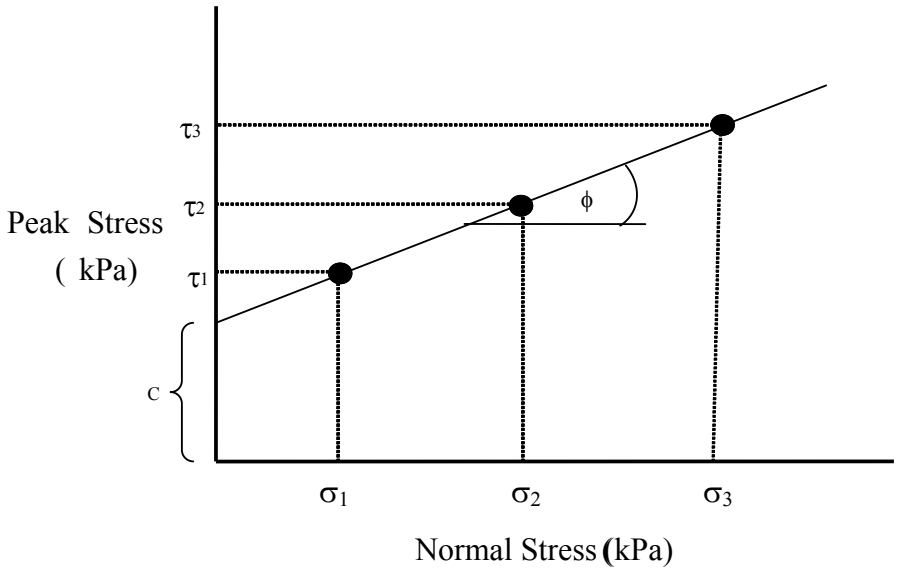

Figure 3.3. Diagrammatic representation of the Mohr-Coulomb shear strength equation

Mohr and Coulomb defined the strength of soils by two parameters: cohesion within the soil and the internal friction angle of the soil particles to resist failure (Holtz and Kovacs, 2003). Cohesion is the adhesive force that exists within the soil and holds the soil particles together. Cohesion is defined by Holtz and Kovacs (2003) as three different categories:

- Apparent cohesion: Apparent cohesion exists due to the presence of pore pressure which holds the soil particles together. The apparent cohesion can be lost when the soil is saturated depending on the type of soil and seismic effect.

- True cohesion: True cohesion (or effective cohesion) exists due to the presence of cementing minerals including clay particles. The effective cohesion is sometimes called the true cohesion.
- Intrinsic cohesion: The intrinsic cohesion of soils is the true cohesion of the soil in which the cohesion exists due to cementation with zero pore pressure.

The angle of internal friction is a measure of the friction existing between the particles of soil. According to many researchers (including Grow et al., 1961 and Mitchell, 1993), these two components (cohesion and friction angle) influence the stability of soils.

3.3.1 Mohr-Coulomb Failure Criteria

Saturated Soils: For saturated soils, it is incorrect to assume that the strength of the soil is governed by the total normal stress (σ) on the shear plane. The application of stress usually results in a temporary increase in the pore-pressure (u). In this situation, effective or intergranular stress (σ') is defined as follows

$$\sigma' = \sigma - u \tag{3.2}$$

and the failure criterion is expressed as a function of effective stress, i.e.

$$\tau = c' + \sigma' \tan \phi' \tag{3.3}$$

The symbols c' and ϕ' indicate that these constants refer to *effective stress* instead of *total stress*

The quantities c and ϕ referred to total stresses and c' and ϕ' referred to effective stresses and depend not only on the type of soil, but also on the saturated conditions of testing or loading in the field. These values should therefore be regarded as empirical constants and not as fundamental soil properties.

Unsaturated Soils: For unsaturated soils, the stress carried by the solid soil expressed in equation 3.1 is modified to equation 3.4. To obtain the cohesion parameters for the same values of matric suction, equations 3.5 and 3.6 as defined by Fredlund and Rahardjo (1993) are mostly used in conditions of unsaturated soils to refine the intrinsic cohesion values.

$$\tau = c + (u_a - u_w)\tan \phi^b + (\sigma - u_a)\tan\phi \quad (3.4)$$

$$c' = c - (u_a - u_w)\tan \phi^b \quad (3.5)$$

$$c'' = c' + (u_a - u_w)\tan \phi^b \quad (3.6)$$

In the above equations τ and σ are shear and normal stresses, u_a and u_w are air and pore water pressures, c and ϕ are cohesion and friction angle, and ϕ^b is the angle that dictates the increase in the cohesion due to the matric suction $(u_a - u_w)$. The matric suction is measured along the shear plane using tensiometers. With u_a equal to zero, and ϕ^b the cohesion c in equation 3.4 can be used to find the cohesion (c′) for zero suction. Equation 3.6 is then used to obtain the cohesion corresponding to a given matric suction (c″). The Questa rock piles are unsaturated and this failure criteria was employed for cohesion analyses.

Dry Soils: For dry granular materials, equation 3.1 is generally simplified to equation 3.7 (Das, 1983; Holtz and Kovacs, 2003; Terzaghi et al., 1996).

$$\tau = \sigma \tan \phi \tag{3.7}$$

Therefore, the shear strength of granular soil is frequently characterized by its internal friction angle (φ).

3.3.2 Curved Failure Criteria

The common criterion used for analyzing failure of geomaterials is the linear Mohr-Coulomb equation as indicated above. On the other hand, some authors report that a nonlinear failure criterion fit their data more closely. Knowing the type of failure criteria will help define the slope stability model to be adopted for analysis. Duncan and Chang (1970) developed a simple, practical procedure by representing the nonlinear, stress-dependent, inelastic stress-strain behavior of soils. By means of this relationship the tangent modulus for soils may be expressed in terms of total stresses in the case of unconsolidated-undrained tests, or effective stress in the case of drained tests. Charles and Watts (1980) developed a Mohr resistance envelope with equation 3.8 which A and b are material constants (Figure 3.4).

$$\tau = A\sigma_n^{\,b} \tag{3.8}$$

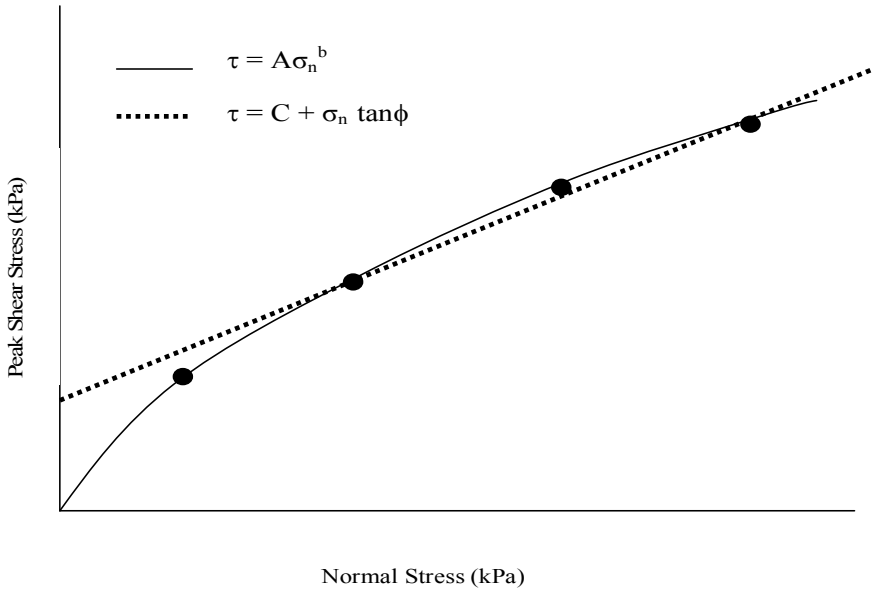

Figure 3.4. Diagrammatic representation of the nonlinear shear strength equation

3.4 Cohesion of Mine Rock Piles

Cohesion can affect the overall stability of mine rock piles. For example, previous studies have identified the influence of microstructures such as cementation on shear strength (El-Sohby et al. 1987; Pereira 1996; Pereira and Fredlund 1999). The existence of cohesion in mine rock piles can be a result of the formation of cementing minerals (e.g. iron oxides, clay minerals, jarosite, and gypsum).

For clay minerals serving as cementing minerals, the individual clay minerals seem to aggregate or flocculate together in submicroscopic fabric units called domains. The domains then group together to form clusters that are large enough to be seen with a visible light microscope. Figure 3.5 is a schematic diagram of the soil microfrabric and macrofabric system proposed by Young and Sheeran (1973) and Pusch (1973) that illustrates different scales are important. The macrostructure, including the stratigraphy of fine-grained soil deposits, has an important influence on soil behavior in engineering

practice. Consequently, in any engineering problem involving stability, settlements, or drainage, the microstructure of the clay particles must be well studied (Holtz and Kovacs, 2003).

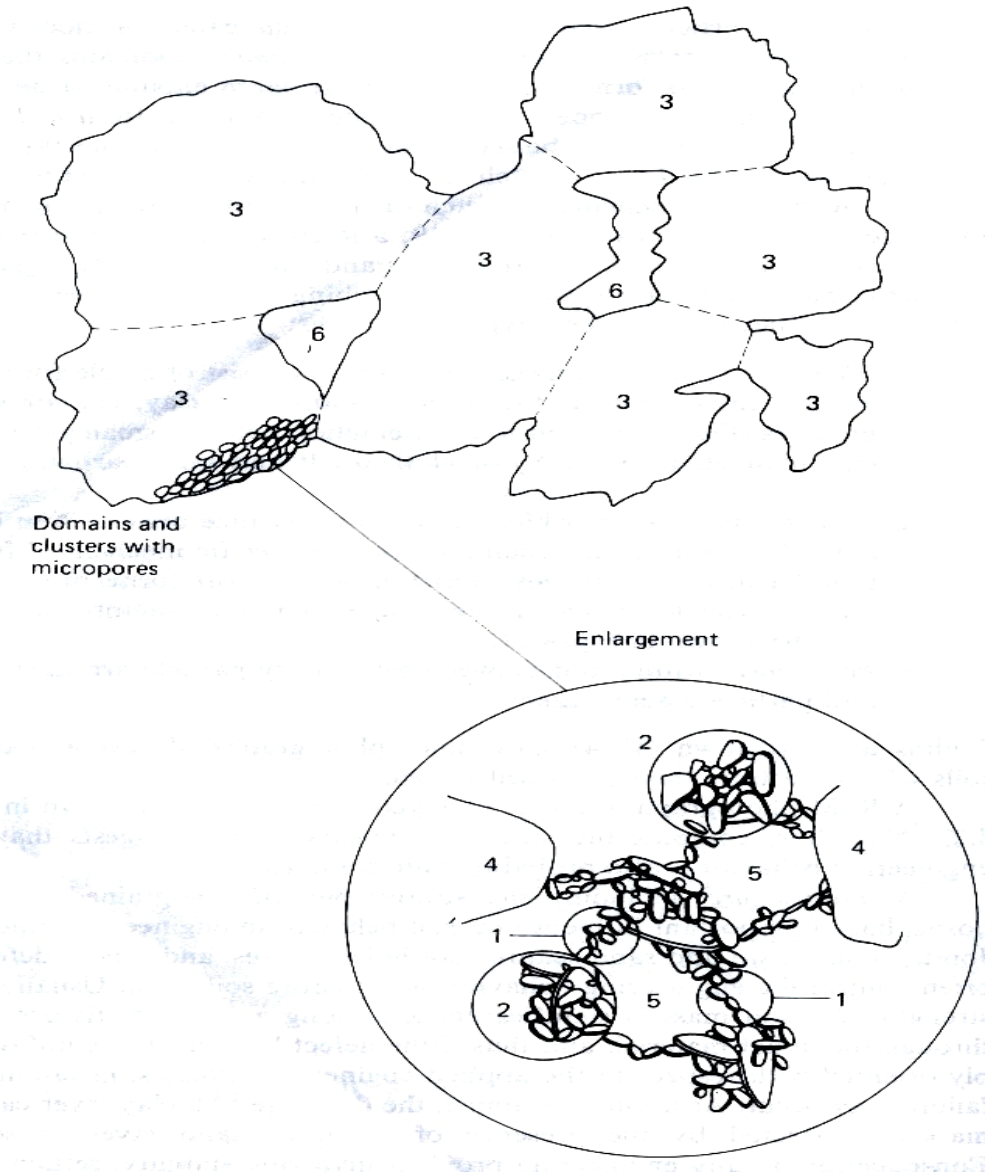

Figure 3.5. Schematic diagram of the soil microfabric and macrfabric systems proposed by Young and Sheeran (1973) and Pusch (1973).

Collins and McGown (1974) suggest a somewhat more elaborated system for describing microfabric features or cohesion existing in natural soils. They propose three types of features:

- Elementary particle arrangements, which consist of a single form of particle interaction at the level of individual clay, silt or sand particles (Figure 3.6a and 3.6b) or interaction between small groups of clay platelets (Figure 3.6c) or clothed silt and sand particles (Figure 3.6d).

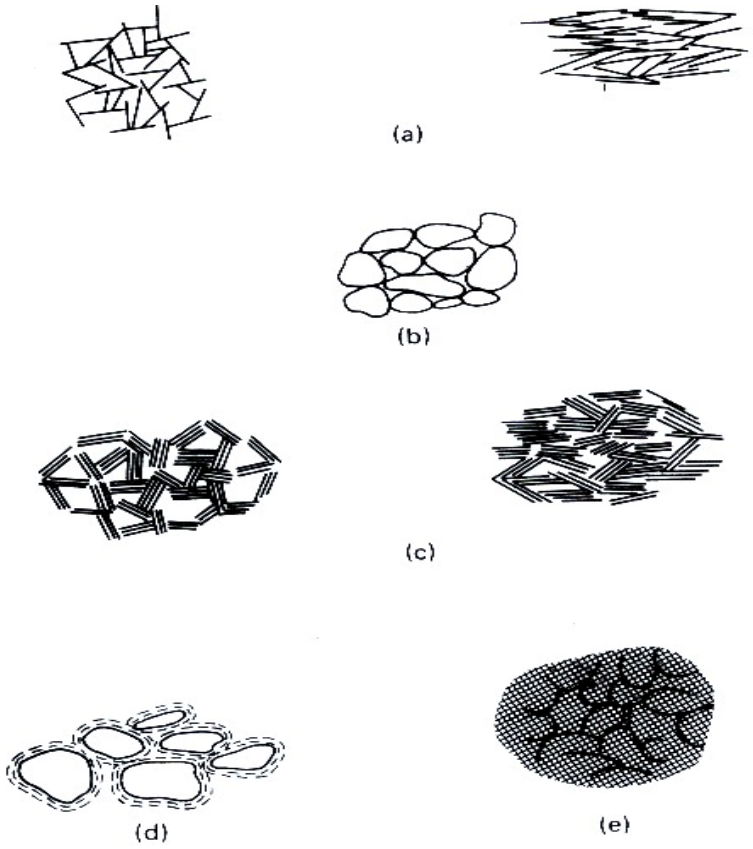

Figure 3.6. Schematic representation of elementary particle arrangements (after Collins and McGown, 1974).

- Particle assemblages, which are units of particle organization having definable physical boundaries and a specific mechanical function. Particle assemblages consist of one or more forms of elementary particle arrangements or smaller particles assemblages, and they are shown in Figure 3.7.
- Pore space within and between elementary particle arrangements and particle assemblages.

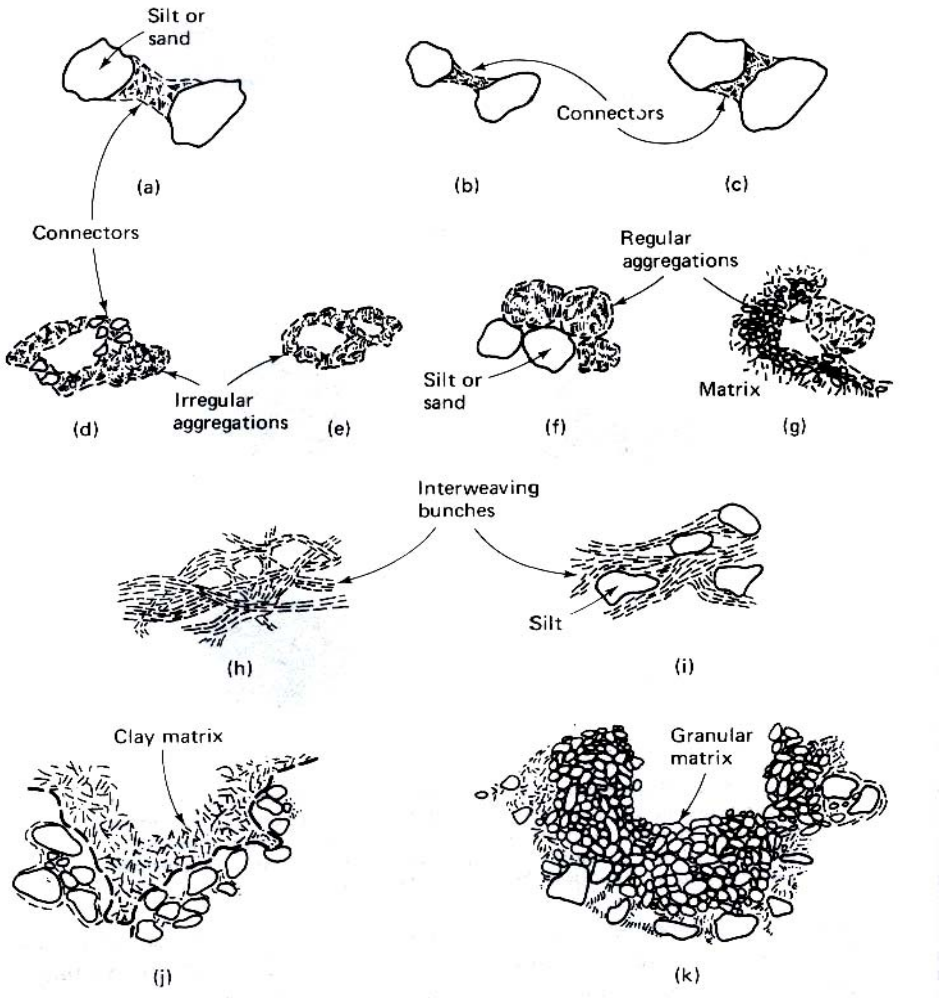

Figure 3.7. Schematic representation of particle assemblages (after Collins and McGown, 1974).

Cohesive soils, to a degree depending on their type, become soft when water is added to them but gain significant tensile and shearing strength in the dry condition. Cohesive soils when dry can be broken into small pieces only by cutting, rasping, grinding or sawing. Classification according to particle size gives less information about their mechanical behavior than the index parameters referring to their consistency and sensitivity to water content. Atterberg limits are used to describe the engineering properties of cohesive soils. In practice the following three consistency limits are used:

- Liquid limit, (ω_L)
- Plastic limit, (ω_p)
- Shrinkage limit, (ω_s)

The water contents based on the three consistency limits relate to particular states of consistency which correspond to qualitative changes in soil behavior. Liquid limit and plastic limit are significant in soil mechanics as they describe the engineering behavior of cohesive soils. If a cohesive soil is mixed with water progressively, it becomes a viscous liquid and loses its shear resistance and cohesion. The water content required to reach this state is called the liquid limit (ω_L). Pa'lossy et al. (1993) indicate that the value of liquid limit ranges between 10 and 20% for fine sands, 15 and 30% for silty sand, from 30 to 40% for silts and from 40 to 150% for clays. These values depend on the particle size distribution of the soil and the mineral composition as well. A cohesive soil with water content below the liquid limit can deform plastically when subjected to pressure. The plastic limit (ω_p) is the water content at which a soil becomes semi-solid. The range of plastic limit is 17 to 20% for silty sand, 20 to 25% for silt and 25 to 50% for clays (Pa'lossy, Scharle and Szalatkay, 1993). The difference between the liquid limit and the

plastic limit is the plasticity index ($I_p = \omega_L - \omega_p$). The plasticity index (I_p) is an important parameter for the identification of soils. Its value can be empirically determined by using equation 3.8 (Pa'lossy et al. 1993):

$$I_p = 0.73(w_L - 20) \tag{3.8}$$

If the soil is gradually dried below the plastic limit, a value of water content is reached below which no further volume changes can occur. The phenomenon of reduction in volume is called shrinkage and the water content where no further volume change occur is called the shrinkage limit. A desiccating soil surface shows a characteristic pattern of shrinkage cracks

3.5 Friction Angle of Mine Rock Piles

Mine rock piles are heterogeneous and are mostly termed well graded soils. Their engineering behaviors are quite different than clays, sand and gravel. Well graded soils contain fractions of several soils groups having different grain sizes. Well graded soils can have high values of friction angle and cohesion because of well distributed grain size and the presence of clay minerals, clay particles, and cementing minerals (Pa'lossy et al. 1993). The internal friction angle is a function of the following characteristics (Hawley, 2001; Holtz and Kovacs, 2003):

- Particle size (friction angle increases with increase in particle size Holtz (1960) and Holtz et al. (1956) while Kirkpatrick (1965) also indicated that frictional angle decreases as the maximum particle size increases)

- Particle shape and roughness of grain surface (friction angle increases with increasing angularity and surface roughness, Cho et al., 2006).
- State of compaction or packing (friction angle increases with increasing density or decreasing void ratio, Bishops, 1966)
- Applied stress level (decreasing friction angle with increasing stress, resulting in a curved strength envelope passing through the origin, Das, 1983).

Holtz (1960) and Holtz et al. (1956) recognized that an increase in the proportion of coarse material in an otherwise fine-grained granular soil can result in an increase in friction angle. The range of internal friction angle values of medium-dense sand is 32^o to 38^o , while typical friction angle values for medium-dense sandy gravel can range from 34^o to 48^o (Das, 1983). Triaxial test results of rock fill material (up to 200 mm in size) for internal friction angles range from 40^o to 50^o, the lower end of the range corresponding to fine-grained material, and the upper end of the range corresponding to coarse-grained material (Leps, 1970).

Cho et al. (2006) investigated the effect of physical abrasion and chemical action on the particle shape. They noted that these processes increase with physical abrasion (alluvial deposit). The particle shape reflects material composition, grain formation and release from the matrix, transportation and deposition environments. Particle shape is characterized by three dimensionless ratios (Barret, 1980; Krumbein, 1941): *sphericity* (eccentricity or platiness), *roundness* (angularity), and *smoothness* (roughness). Figure 3.8 is a visual chart used to specify the sphericity and roundness of particles. Cho et al. (2006) redefine the original chart by Powers (1982) to make it easier to examine the

influence of particle shape on geotechnical properties. The plot in Figure 3.9 shows a negative correlation between critical state internal friction angle and roundness produced by Cho et al. (2006). The open circles are for sand with sphericity > 0.7, and closed circles are for sand with sphericity < 0.7. As roundness varies from 0.1 (very angular) to 1 (well rounded), the internal friction angle decreases from 40^{o} to approximately 28 ^{o}. Holtz and Kovacs (2003) also reported that particles with higher sphericity generally have lower friction angles.

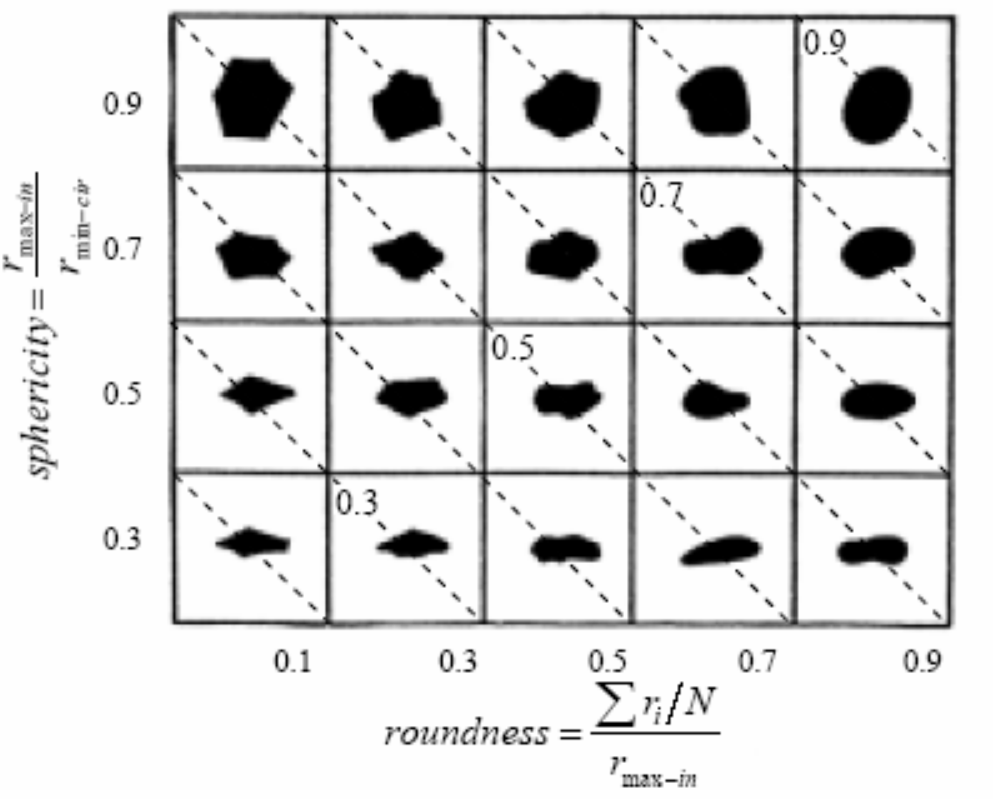

Figure 3.8. Visual chart used to specify the sphericity and roundness of soil particles from Cho et al., (2006)

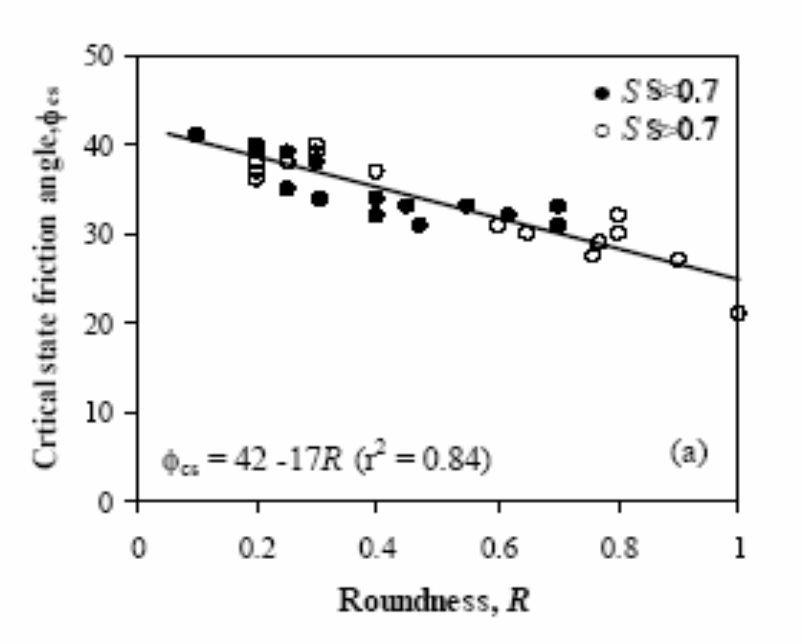

Figure 3.9. The effect of particle shape on critical state internal friction angle for sand (from Cho et al., 2004). Open circles and closed circles are for sand with sphericity higher than 0.7 and sphericity lower than 0.7, respectively.

Grain size distribution has an effect on the internal friction angle that can be observed on samples with the same relative density. Figure 3.10 shows the correlation between the effective friction angles from triaxial compression tests and both relative density and soil classification. Holtz and Kovacs (2003) noted that when two sands have the same relative density, the soil that is better graded (for example SW soil as opposed to SP) has a larger friction angle

With regard to the influence of the void ratio and applied normal stress on friction angles, Das (1983) illustrated that for Ottawa Sand with a void ratio of 0.66, the internal friction angle value decreased from 30^o to 27^o when the normal load was increased from 48 to 766 kPa (Figure 3.11). Similarly, for dense sand the internal friction angle

decreases from 34° to 31° due to an increase in normal stress from 48 to 766 kPa. A reduction of 2 to 4 degrees in friction angle also has been reported when the normal stress was increased during direct in situ shear tests (Hribar et al., 1986; Seedsman et al., 1988).

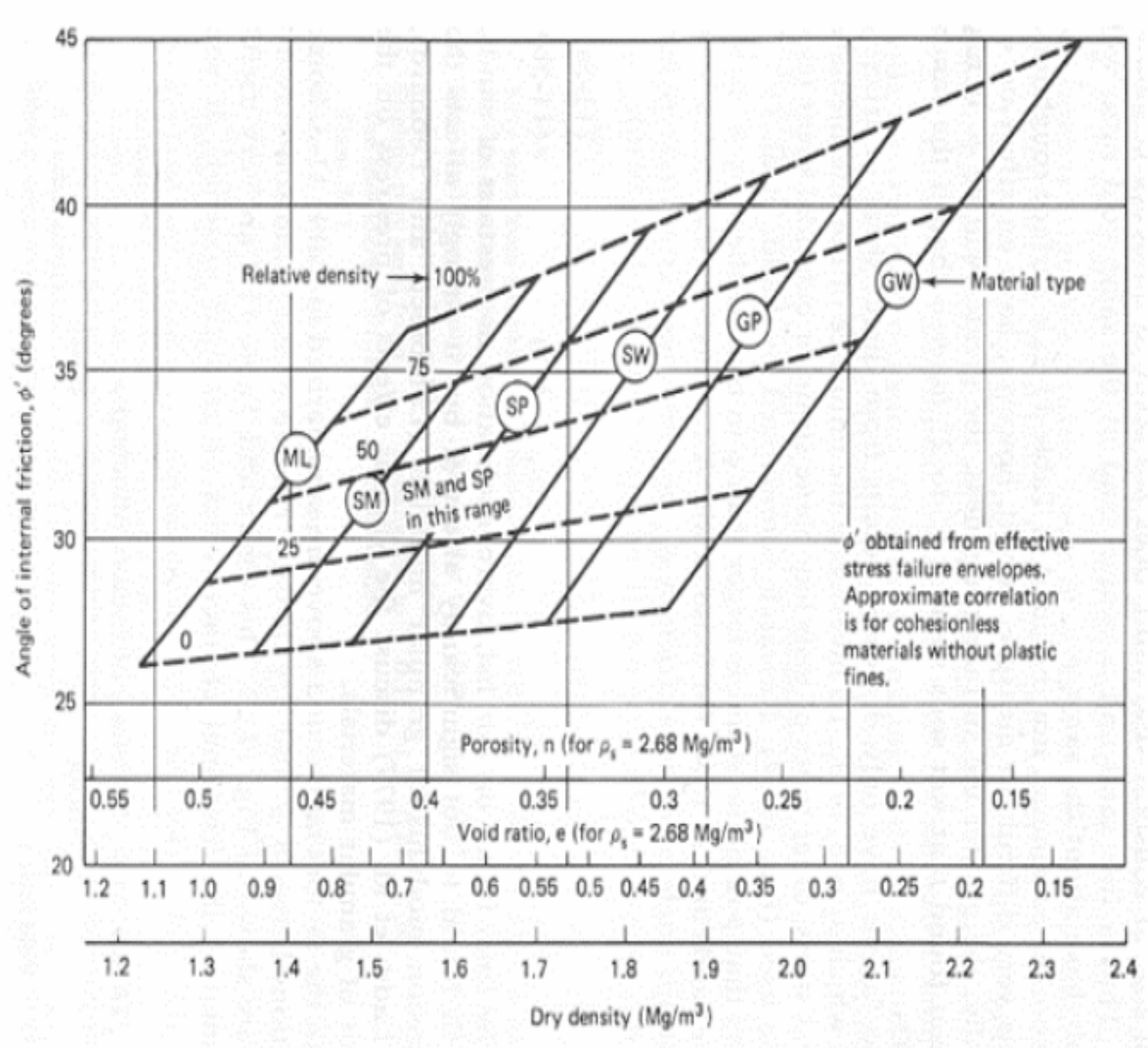

Figure 3.10: Correlations between the effective friction angle and the relative density for different soil types (from Holtz and Kovacs, 2003).

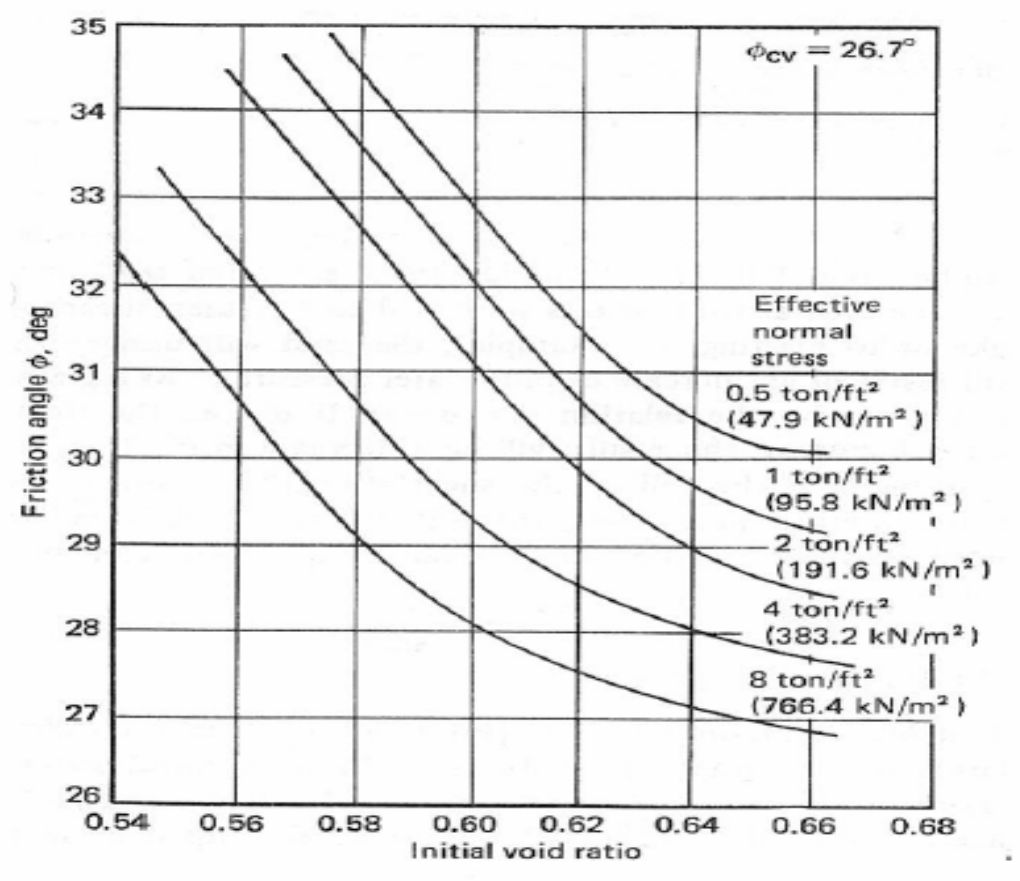

Figure 3.11: The variation of peak internal friction angle with effective normal stress for direct shear tests on standard Ottawa sand (from Das, 1983).

The effects of scalping on friction angle of soils have been evaluated by different authors. Scalping is the process of removing larger particles from soil samples by sieving through a particular sieve number and testing on specimen passing through the sieve. Scalping is performed because the materials tested in the laboratory shear test are small in size compared to in situ particle size and this is not the true representation of the in situ particles. There is a possibility that the test results in the laboratory will not be the true shear strength in situ because of size effect. There can be an overestimation or underestimation of the shear strength even if the test is performed under in situ condition.

Bishop (1948) performed direct shear tests on two types of uniform soil with different particle size. He reported that there is no effect on the shear strength even though two different materials with different particle sizes were used.

Lewis (1956) and Vallerga, et al. (1957) concluded that the friction angle increases with increasing particle sizes. They attributed this to increase in interlocking and also increase in dilatational tendencies of the larger particles.

Leslie (1963), Kirkpatrick (1965), Marsal (1965a), Rowe (1962), Varadarajan et al. (2003) and Koerner (1970) indicated an opposite conclusion that the internal friction angle decreases as the maximum particle size increases.

There is no common agreement on the effect of scalping on shear strength after evaluating the literature work on this topic. Different views are presented with some indicating that internal friction angle decreases with increase in particles size while others have opposite views.

3.6 The Weathering Process in Questa Mine Rock Piles

Weathering is disintegration of rock by physical, chemical, and/or biological processes that result in reductions of grain size, grain shape, changes in cohesion or cementation, and changes in mineralogical and chemical composition (McLemore (2005). There are two general types of weathering that must be examined, physical weathering and chemical weathering.

Physical weathering involves the physical breakup of a rock by mechanical processes. This decrease in grain size results in increased surface area that can lead to greater chemical reactivity and exposure of fresh mineral surfaces. Common processes

that are relevant to the Questa rock piles include: freeze/thaw and related frost-action effects; thermal expansion and contraction of rock; deformation (crushing) of rock fragments due to the weight of overlying rock; abrasion; pressure release on rock by erosion of overlying materials; and growth of plants and living organisms in rock. A special case that is relevant to Questa rock piles is the physical breakup of the rock by the volume change resulting from transformation of anhydrite to gypsum or other crystal growth along fractures. Crystallization of mineral phase also can break up the rock, for example the crystallization of gypsum from anhydrite increase by volume as much as 61% (Yilmaz, (2001).

Chemical weathering encompasses the changes to the texture, structure, and composition of the rock fragments due to geochemical and biogeochemical reactions. Important chemical weathering processes at Questa rock piles include (McLemore, 2005):

1. Oxidation-reduction (redox) reactions, such as the acid-generating oxidation of pyrite, which may be catalyzed by important microbiological interactions
2. Short term acid-base reactions, such as dissolution of carbonates and precipitation of soluble, efflorescent salts that can cement fragments during dry periods but will not provide reliable, long-term cohesion but could provide for site of more stable cementing minerals
3. Precipitation of more stable cements, such as goethite and low to moderate-solubility sulfates and related minerals (e.g., gypsum and jarosite)
4. Acid-base reactions, such as acid hydrolysis and dissolution of alumino-silicate minerals to form new clay minerals

5. Normal soil diagenesis reactions driven largely by atmospheric oxygen and dissolved carbon dioxide where minerals in rock fragments are exposed to air.

A simple weathering index has been proposed to define the degree of weathering within the Questa mine pile. Color, mineralogy and texture are employed as the major factor in this classification. Color is one of the easiest and most obvious characteristics of different intensities of weathering because it reflects differences in mineralogy and texture (Fontes and Carvaalho, 2005). The original igneous rock color reflects the original mineralogy, which is typically related to the presence or absence of mafic and feldspathic minerals. The color of soils weathered from igneous rocks is somewhat dependent upon oxidation of the mafic and feldspathic minerals. Reds, browns and yellows typically reflect the different oxidation states and abundances of iron minerals.

Numerous studies in the literature have used color as an indication of the intensity of weathering. Shum and Lavkulich (1999) used color to estimate iron content and as a weathering indicator. Yokota and Iwamatsu (1999) showed that color shifts towards red with increase in weathering. Yokoyama and Nakashima (2005) showed that color increased towards yellowish-brown with increased weathering as ferrihydrite weathers to goethite. Fontes and Carvaalho (2005) describes various color indices and the relationship to weathering. Martín-Garcia et al. (1999) used a visual degree of weathering (DW; 0-3) based upon reddening, cracks, mineral alterations, compactness and roundness of the clasts. They note a lightening of color, red pigmentation, increase in cracks, decreased compactness and increased roundness with increase in weathering. Martín-Garcia et al. (1999) further showed that weathering profiles in pyrite-bearing rock consist

of a less weathered reduced zone, dissolved zone, and more weathered oxidized zone in areas where the H_2O and O_2 fluxes are in the same direction. If the H_2O and O_2 fluxes are in opposite direction then the oxidized and dissolved zones overlap. Scheinost and Schwertmann (1999) used a colorimeter to determine whether color is useful in identifying goethite, hematite, lepidocrocite, jarosite, maghemite, and feroxyhite but not as useful in identifying ferrihydrite, akaganeite, and Schwertmannite.

The following 5 classes (Table 3.1) describe a simple, descriptive weathering index classification (SWI) for the rock pile material at the Questa mine based on relative intensity of both physical and chemical weathering (modified in part from Little, 1969; Gupta and Rao, 1998; Blowes and Jambor, 1990; V. T. McLemore, written communication):

Table 3.1. Simple weathering index (SWI) for rock pile material at the Questa mine (V. T. McLemore, written communication)

SWI	Name	Description
1	Fresh	Original gray and dark brown to dark gray colors of igneous rocks; little to no unaltered pyrite (if present); calcite, chlorite, and epidote common in some hydrothermally altered samples. Primary igneous textures preserved.
2	Least weathered	Unaltered to slightly altered pyrite; gray and dark brown; very angular to angular rock fragments; presence of chlorite, epidote and calcite, although these minerals not required. Primary igneous textures still partially preserved.
3	Moderately weathered	Pyrite altered (tarnished and oxidized), light brown to dark orange to gray; more clay- and silt-size material; presence of altered chlorite, epidote and calcite, but these minerals not required. Primary igneous textures rarely preserved.
4	Weathered	Pyrite very altered (tarnished, oxidized, and pitted); Fe hydroxides and oxides present; light brown to yellow to orange; no calcite, chlorite, or epidote except possibly within center of rock fragments (but the absence of these minerals does not indicate this index), more clay-size material. Primary igneous textures obscured.
5	Highly weathered	No pyrite remaining; Fe hydroxides and oxides, shades of yellow and red typical; more clay minerals; no calcite,

		chlorite, or epidote (but the absence of these minerals does not indicate this index); angular to subround rock fragments.

Even though the simple weathering index introduced in this study is not a precise tool in evaluating the weathering intensity, it is relatively simple and can be readily used in the field.

3.7 Effect of Weathering on Geotechnical Properties of Mine Rock Pile Materials

The weathering, either physical or chemical, of mine rock piles is an important factor in controlling the slope stability. Some researchers have shown that weathering results in the instability of slopes. For example, Yokota and Iwamatsu (1999) measured the penetrative hardness of weakly welded dacitic to rhyolitic tuff rocks that correlates with their strength as an indicator of rock weathering. Through this technique, they showed that the rock surface had less strength and suffered from more weathering with the consequence of slope instability during heavy rainfall. Furthermore, these researchers claimed that the slope instability continued to occur in the region once the thickness of the weathered zone reaches a specific threshold. Okagbue (1986) studied the landslide in the rock piles in a coal mine area in north central West Virginia. More than 50% of the rock pile material in this mine was made of red shale. The rock pile contained approximately 65% fines. The rock fragments in the rock pile had an averaged slake durability index of 79% which is a medium durability index under Franklin's durability classification (Franklin and Chandra, 1972). This relatively low durability index was used to justify the observed extensive weathering and to rationalize the abundance of fine

material in the rock pile. The high percentage of fine material together with the seasonal high water table was considered as the cause of rock pile instability by Okagbue (1986). Jaboyedoff et al. (2004) studied the effect of weathering on Alpine rock instability. They concluded that the chemical weathering and crushing of rock were the main processes for strength decrease with time that resulted in the instability of the Alpine rock.

Even though weathering of rock fragments in a rock pile can cause particle degradation with the consequence of reduction in the friction angle, it has been reported that in some situations it can increase the cementation of the material at the same time. Lohnes and Demirel (1973) reported the cohesion increase in lateritic soil as the result of weathering. According to these authors, the weathering process included a transformation of feldspars to kaolinite and kaolinite to gibbsite accompanied by formation of iron oxides from iron-rich primary mineral. The cementation was the result of loss of kaolinite, increased enrichment of oxides, dehydration and crystallization of iron oxide minerals into continuous aggregates or networks. Chigira and Oyama (1999) studied the effect of chemical weathering on pyrite-bearing sedimentary rocks. The geotechnical evaluations by these authors showed that sandstone was strengthened because of cementation by iron oxide or hydroxide resulting from oxidation of pyrite, while mudstone was weakened because it had greater clay fractions and larger surface areas than sandstone. Maquaire et al. (2003) in their study of instability conditions of marly hill slopes in South East France concluded that the black marl progressively regained its strength due to increase of the residual friction angle possibly due to alteration of the clay minerals.

3.8 Measurement of Cohesion and Friction Angle

One of the fundamental objectives of soil mechanics is the determination of the strength of soil. Knowledge of strength properties is needed to give proper answers to the flowing questions (Pa'lossy et al., 1993). Some questions to consider include:

- What is the allowable loading or force acting on structures
- What is the stability and bearing capacities of structures embedded in subsoil
- What is the deformation and displacement of loaded soil masses and structures

For an ideal material the total or effective cohesion (c) and internal friction angle (ϕ) are approximately constants that can be determined by carrying out two or more tests with different normal stresses acting on the plane of shear failure. If the shear strength is measured directly (as in the shear box) the shear stress at failure is plotted against the stress normal to the shear plane as in Figure 3.5. The shear box test can be performed in the laboratory or in situ to measure the shear strength parameters.

Even though the direct shear box test is a technique of measuring cohesion and friction angles, there are many in-situ devices like the standard penetrometer device, the vane shear device, etc but these in-situ test devices measure the total strength of the material. In the laboratory, triaxial tests are also common in measuring shear strength of soil and rocks. However, the disadvantages of the laboratory tests must be emphasized. Sampling procedure disturbs the initial stress state in the soil and this effect cannot be eliminated. Lambe et al. (1969) indicated the effect of specimen disturbance by showing that the strains measured during undrained shear strength testing of disturbed samples are

larger than those from undisturbed specimens. Also the initial state of in situ stress is unknown or must be estimated and, therefore, it can be reproduced only approximately in the laboratory prior to investigation. Due to the small size of the specimen in general, the boundary conditions of the laboratory apparatus differ significantly from that in the field and this may cause a substantial difference between measured and real values of strength parameters

3.8.1 Conditions of Direct Shear Tests

The condition of shearing tests for soils is the drained test. For drained test, the samples are consolidated, but the shearing is carried out slowly under conditions of no excess pore pressure generation. The in situ tests performed in this research work use this method as the samples were unsaturated in the field.

Because of the high permeability of sand, consolidation occurs relatively rapidly and is usually completed during the application of the load. Tests on sand are therefore generally carried out under drained conditions. The guiding principle is that the drainage conditions of the test should conform as closely as possible to the conditions under which the soil will be loaded in the field.

3.8.2 Conventional Laboratory Direct Shear Testing

Shear strength, including friction angle and cohesion, can be measured by direct shear tests using a shear box. The shear box consists of two square or circular metal rings (Figure 3.12). The sample is vertically place in the shear box in advance, shearing force is

applied through the upper part of the box by pushing it until the sample fails. Horizontal and vertical displacements as well as applied shearing force are measured. The results may show either hardening or both hardening and softening behavior (Figure 3.13). By performing at least three shear tests and plotting the shear strength vesus normal stress, friction angle and cohesion can be obtained (Pa'lossy et al., 1993). This approach was employed for our laboratory shear strength testing program.

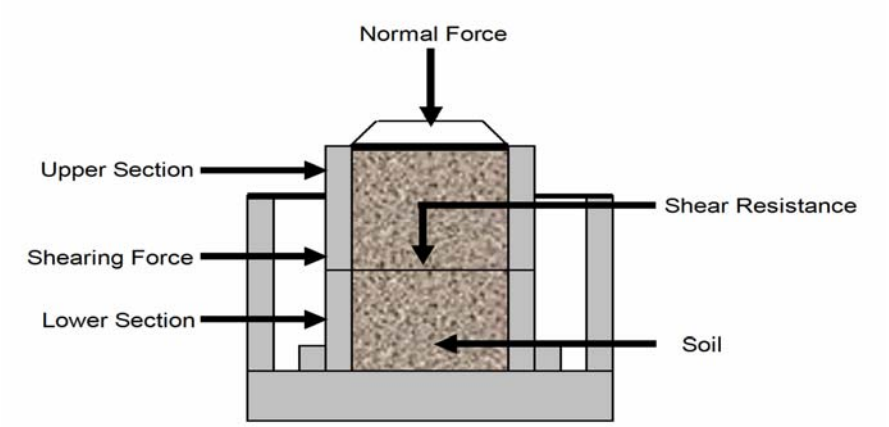

Figure 3. 12. Schematic diagram of a Conventional Laboratory Direct Shear Test Box.

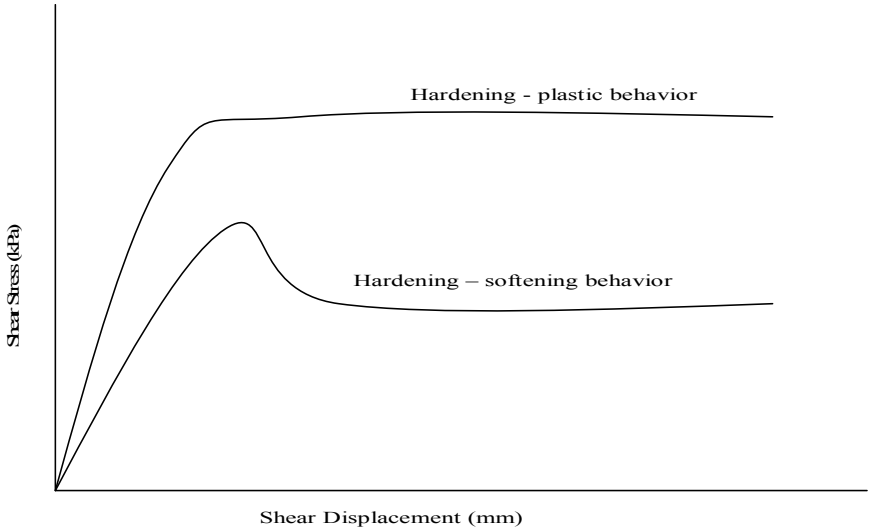

Figure 3.13. Schematic diagram showing the behavior of soil when sheared using direct shear testing method.

3.8.3 In situ Soil Testing Methods and Devices

Geotechnical engineers assess subsurface conditions by accumulating the historic data of the area, the field characterization of the area and determine soil properties through representative sampling and testing. The need for a greater reliability in the evaluation of soils has resulted in the development of new procedures of in-situ soil testing equipment. Soils are rarely homogeneous. Their properties are subjected to significant variation vertically and horizontally. As a result, the mechanical properties determined in the laboratory can differ appreciably from those determined in situ (Klinedist, 1972). Furthermore, it is difficult to obtain a representative sample of certain soils and properly prepare that sample to maintain it's cohesion for laboratory tests due to disturbance. These include soils with a considerable secondary structure such as fissures, joints, slickensides, and those containing particles of rock or shells of appreciable size such as rock piles. It is, therefore, often desirable to test such soils in situ. Although the prime factor favoring the in-situ testing concept is improved accuracy and representativeness, there is a secondary compelling benefit: economics. It is probable that in situ equipment used by experienced operators can produce a greater quantity of reliable data at less cost than conventional sampling and testing methods now generally employed. Before selecting a particular method for our testing, an intensive literature review was made to assess different methods and devices employed to determine the in-situ shear strength parameters.

The in-situ devices evaluated as part of this project can be classified by three general types: 1) shear devices, 2) penetration devices, and 3) pressure meters (see Figure 3.14).

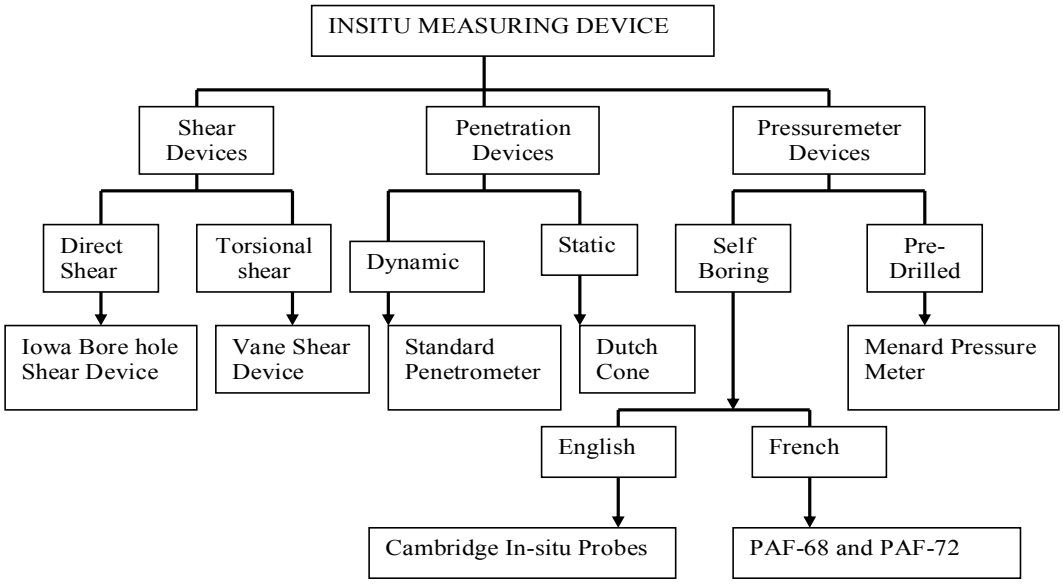

Figure 3.14. A chart of in situ measuring devices (by John, 1980).

The review of in-situ soil testing devices showed that some of the devices do have possibly or even more merit than surface direct shear device since strength variation within stratification of the material can be measured but their limited usage in rock piles due to the large soil particles make it difficult to use for our test. For example Vane Shear Device is physically limited in its strength-measuring capacity, particularly in granular tailings material and rock piles. As with the dynamic and static testing methods, they yield only empirical estimates of the soil strength parameters and may not provide reliable data due to presence of rock fragments in the rock piles.

After evaluation of these devices, efforts were centered only on direct shear devices with further research being carried out to construct our own in situ direct shear device.

3.8.4 History of Development of In situ Direct Shear Devices

In situ direct shear tests performed to obtain more realistic field data are not new in studying landslides, but they have not been widely employed to examine the gravitational stability of rock piles. The invention of in situ direct shear tests for geotechnical engineering began way back in 1904. The earliest recorded use of a large in situ direct shear test box was by Goodrich in 1904 using a 30cm by 30cm shear box (Skempton, 1958). A 76cm by 76cm shear box was used by Frontard in 1914. Common among these tests is that they were performed in cohesionless soils.

Later, Schultze (1957), Hutchinson and Rolfsen (1962) and Mellinger (1966) conducted in situ direct shear tests.

In recent times the in situ direct shear test device has being employed by many consulting engineering organizations in analysis of highway landslides. Other in situ tests were performed by Brand et al. (1983), Endo and Tsurata (1979), Marsland (1971) Tobias (1990), O'Loughlin and Pearce (1976), Wu et al. (1979) and Fakhimi et al. (2004). Fakhimi et al. (2004) conducted in situ shear tests on soil material in a tunnel in Tehran, Iran where the reaction of the normal force was transferred to the tunnel roof.

In situ direct shear tests have some limitations as compared to laboratory testing devices already discussed in the previous section. They are time consuming and expensive. In some cases it is a labor intensive and requires many people to perform the test as compared to other in situ devices that a single person can handle. The major advantage of employing the in situ direct shear test is that the shear box can be designed in any size to accommodate testing larger particle sizes. This advantage was considered

in designing our device for the test program since rock piles have large particles making it difficult to employ some of the existing in situ and laboratory testing devices.

3.8.5 Allowable maximum particle size for direct shear test

There have been a few studies and recommendations that indicate the variability of direct shear testing. One of these recommendations is based on the maximum particle size acceptable for a particular shear box size. For instance, after performing several triaxial tests, Holtz and Gibbs (1956) suggested that the maximum particle size allowable within a particular shear box must be 1/6 of the specimen size. They concluded that the presence of large particles in the specimen causes an increase in strength due to interference between the large particles. Vellerga et al. (1957) concluded that the ratio of the specimen diameter to maximum grain size for uniformly graded soil should be 1/20 and less than 1/6 for well graded soil testing after performing triaxial tests on rock fill dam material. Leslie (1963) concluded the same as Holtz and Gibbs (1956), explaining that the presence of large particles in the sample artificially increases the strength, supporting the suggestion that 1/6 of the specimen size should be the maximum particle size used for shear box tests. The maximum particle size allowable within a particular shear box must be 1/5 of the specimen size (Schultz 1957; and Hriber et al., 19856). These recommendations were considered in selecting the variability of an in situ direct shear test and discussed in Chapter five (5).

4. METHODOLOGY

4.1 Field Test

In-shear strength analysis geotechnical index parameters and properties of the soil and the prevailing pore-pressure conditions can be best obtained by in situ testing. Either intact or disturbed samples can be collected from the field and tested in the laboratory to determine some engineering properties as well. However, the engineer is confronted by the necessity of extracting further information from the mass of soil on which his structure is to rest and should turn to in situ testing. In-situ testing cannot be carried out with the degree of accuracy or under the controlled conditions of laboratory testing. Some information cannot, however, be obtained in any other way than by inspecting the soil mass in situ. Appendix 1 presents specifications of the hydraulic jack used. Appendix 2 presents standard operating procedures for the individual tests performed on the rock pile materials. Appendix 3 presents the field description of the samples tested in-situ and the viability of an in-situ test. Appendix 4 presents plots of all in situ and laboratory direct shear tests results. Appendix 5 presents plots for nonlinear failure criteria for each laboratory direct shear tests. All appendices are on a CD attached to the thesis.

4.1.1 In situ Direct Shear Test Location Selection and Field Geological and Geotechnical Logging of Tested Samples

In-situ test locations were selected based on geologic characteristics (including the SWI), personnel safety factors, and easy accessibility for equipment. It is important to note that the same rock piles can have different degrees of weathering at different spots or location

This indicates that the weathering of the Questa rock pile material is not homogenous and changes from one place to another on the same rock pile. These locations were selected on the basis of different degrees of weathering to help evaluate the effect of weathering on the shear strength of the rock piles and analogs. Four rock piles and two analogs were tested; Middle, Spring Gulch, Sugar Shack South, and Sugar Shack West rock piles and the Pit alteration scar and the Goathill debris flow. Simple description of the analogs and the reason for their testing is in the next section. Each test is identified with a sample number based on the rock pile and analog name and documented. Field geological and geotechnical characterization of samples tested were also documented.

Middle rock piles samples tested in situ and collected for laboratory tests were well graded matrix soils. The samples were mostly ranging in color from yellow brown to brown in nature. Field observation shows that the samples are moist to dry in nature, nonplastic, with angular particles, poorly sorted, and dense in terms of it consistency. Lithology includes andesite, volcaniclastic sediments, quartz-sericite-pyrite (QSP)-altered, rhyolite (Amalia Tuff) and porphyry. Field observations also indicate samples contained pyrite, gypsum, jarosite and hematite.

Spring Gulch rock pile samples tested in situ and collected for laboratory tests were loose soil with grass roots to weathered soils with rock fragments. The samples colors were mostly ranging from dark gray to gray brown in nature. Field observation shows that the samples are moist, nonplastic with some samples medium to high plasticity, angular particles, poorly sorted, and dense in terms of it consistency.

Lithology consists of QSP-, argillic-, propyllitic-altered andesite, porphyry and Amalia Tuff. The samples contain pyrite, gypsum, jarosite and clay in the more weathered zones and chlorite, calcite and pyrite in the least weathered zones. There is a well-cemented zone formed by clay and gypsum.

Sugar Shack South rock piles samples tested in situ and collected for laboratory tests were rocky to loose rocky matrix soils. The samples were mostly light brown to orange brown with some gray. Field observation indicate that the samples are moist, medium to well plastic, angular particles, poorly sorted, and dense to loose in terms of it consistency. Lithology includes QSP- and argillic-andesite, porphyry and Amalia Tuff. The samples consist of pyrite, gypsum, illite and chlorite. Moderate to weak cementation was observed by sight inspection for most of the samples tested in situ.

Sugar Shack West rock piles samples tested in situ and collected for laboratory tests were well graded matrix soils to well graded rocky soils with presence of clay lenses. The samples ranged in color from yellow orange, dark gray, tan gray, dark olive with some yellow to brown. Field observation indicate that the samples are moist dump to dry to in nature, medium plastic to non plastic, angular particles, poorly sorted, and dense in terms of it consistency. Lithology includes QPS-altered andesite, porphyry and Amalia Tuff. The samples contain pyrite, gypsum, chlorite and calcite. There is weak to moderate cementation by sight inspection because of the presence of gypsum.

Description of the analogs: It is a project hypothesis that the alteration scar areas and debris flows could serve as mineralogical and physical proxies or analogs to long-term weathering of the rock piles (Campbell and Lueth, 2008). There is an on-going study to establish the geochemical and geological relationship between the rock piles and

analogs to support this hypothesis. Alteration scars are natural, colorful (red to yellow to orange to brown), unstable landforms that are characterized by steep slopes (greater than 25 degrees), moderate to high pyrite content (typically greater than 1 percent), little or no vegetation, and extensively fractured bedrock (Meyer and Leonardson, 1990).

The Goathill debris flow is formed by sedimentation due to transportation of landslide rock material within the alteration scar by water and gravity. These features were formed thousands to millions of years ago and have been exposed to weathering conditions similar to those affecting the rock piles today and in the future. By characterizing and establishing the geotechnical parameters of these analogs, future changes of geotechnical properties of the rock piles could be predicted. Comparison of the analogs to the rock piles is in Table 4-1.

TABLE 4-1. Comparison of the different weathering environments in the rock piles and analog sites in the Questa area (V.T. McLemore, A. Fakhimi, D. van Zyl, written communication, April 12, 2008). (QSP=quartz- sericite-pyrite). Reported friction angles and cohesion are included to compare materials, not for slope stability analysis.

Feature	Rock Pile	Alteration Scar	Debris Flow
Rock types	Andesite Rhyolite Porphyry Intrusion	Andesite Rhyolite Porphyry Intrusion	Andesite Rhyolite Porphyry Intrusion
Rock type distribution	Mixed	Homogeneous	Mixed
Hydrothermal alteration	Propylitic, argillic, and QSP	Propylitic, argillic, and QSP	Propylitic, argillic and QSP
Paste pH	1.6-8	2-3.2	2-4
Unified soil classification	GP-GC, GC, GP-GM, GW, GW-GC, SP-SC, SC, SW-SC, SM	GP-GC, GP	GP, SP, GP-GC
% fines	0.4-37 Mean 12.4	4-9	1-7
Water transport	Variable with macropores and lower conductivity zones	Advective with some fracture control, no macropores	Advective, no macropores or fractures
Air transport	Higher advective, some diffusive and convective flow	Diffusive flow	Diffusive flow
Water content	0-23%	8-14%	2 – 12%

	Mean 10.0%		
Process of Formation	Truck end dumping on slope	In situ with some mass transport (rock falls, colluvium)	Water assisted transport
Stratigraphy	Man-made interbedded layers and/or fingers parallel to the slope	Inherited, strongly fracture controlled	Water deposited layers, near horizontal
Time	40 years	1.8 million to 300,000 years	Undetermined – 10,000 to 100,000 year scale estimated
Degree of weathering	SWI is 2-4	SWI is 3-5	SWI is 2-4
Depth of weathering	Shallow (<5 m) with weathered zones at the contact between the rock pile and bedrock/colluvium	Shallow (<5 m)	Unknown
Pyrite content	Low to high (0-7%; mean 1.2%)	Moderate to high	Moderate to high
Dry density kg/m^3	1200 – 2500 Mean 1700	1800 – 2500	1500 – 2000
Particle shape	Angular to subangular	Angular to subangular	Subangular to subrounded
Liquid Limit			
Plasticity Index	0-33.6 Mean 21.1	Nonplastic to plastic	Nonplastic to plastic
Degree of chemical cementation	Low to moderate (sulfates, Fe ox)	Moderate to high (sulfates, Fe ox)	Moderate to high (sulfates, Fe ox)
Average peak friction angle (degree), 2-inch shear box (air dried)	40.9	40.3	43.2
Average cohesion (kPa), in-situ shear tests	9.6	16.6	38.8

The Pit alteration scar samples tested in situ and collected for laboratory tests were well graded soils to well graded rocky soils. The samples mostly ranged in color from yellow brown to brown. Field observation indicate that the samples are dry, highly to medium plastic, subangular to angular particles in shape, poorly to moderately sorted, and dense to loose in terms of it consistency. Lithologies include QSP-altered andesite, porphyry and Amalia Tuff. Field observation also indicates samples contain fluorite, gypsum, illite and jarosite. Well to moderate cementation exists due to clay and gypsum.

The Goathill debris flow samples tested and collected for laboratory tests were well graded soils. The samples ranged in color from tan to light brown. Field observation indicate that the samples are dry, nonplastic, subangular to angular particles shape, poorly sorted, and loose to dense in terms of it consistency. Lithologies include QSP-altered andesite, porphyry and Amalia Tuff. Field observation also indicates samples contain no calcite, chlorite and epidote.

Samples of disturbed rock pile material and analogs (soil including rocks and soil particles) were collected from the shear plane for various laboratory tests. Samples were collected along the shear plane for geological and geotechnical characterization. The collected samples consisted of a mixture of rock fragments ranging in size from boulders 0.5 m) to >1 mm in diameter within a fine-grained soil matrix. Most rock fragments are hydrothermally altered before mining occurred; some are oxidized and weathered since emplacement in the rock pile (Figure 4.1 and 4.2). Figure 4.1 and 4.2 are two samples collected with different degree of weathering. Degree of weathering was determined using the simple weathering index, color changes, the presence or absence of pyrite, gypsum, jarosite, and iron oxides, and presence or absence of tarnished or oxidized pyrite crystals. Weathered samples exhibit replacement of pyrite by iron oxides (Figure. 4.2) or rims of iron oxides surrounding pyrite and typically little or no calcite or chlorite. Least weathered samples contain relatively unaltered crystals of pyrite, calcite, chlorite, and muscovite (Figure. 4.1).

Approximately 5 gallons of solid material were collected from each test location for geotechnical analysis. Samples also were collected in tins for gravimetric moisture content. The gravimetric samples were kept in coolers to retain their moisture until the

tests were performed. The samples were labeled with respect to the location of the individual in situ test. Description of samples accepted as viable in situ direct shear tests based on recommendation of maximum particle size allowable in direct shear test are presented in Table 4.2. Descriptions of all samples tested are presented in Appendix 3.

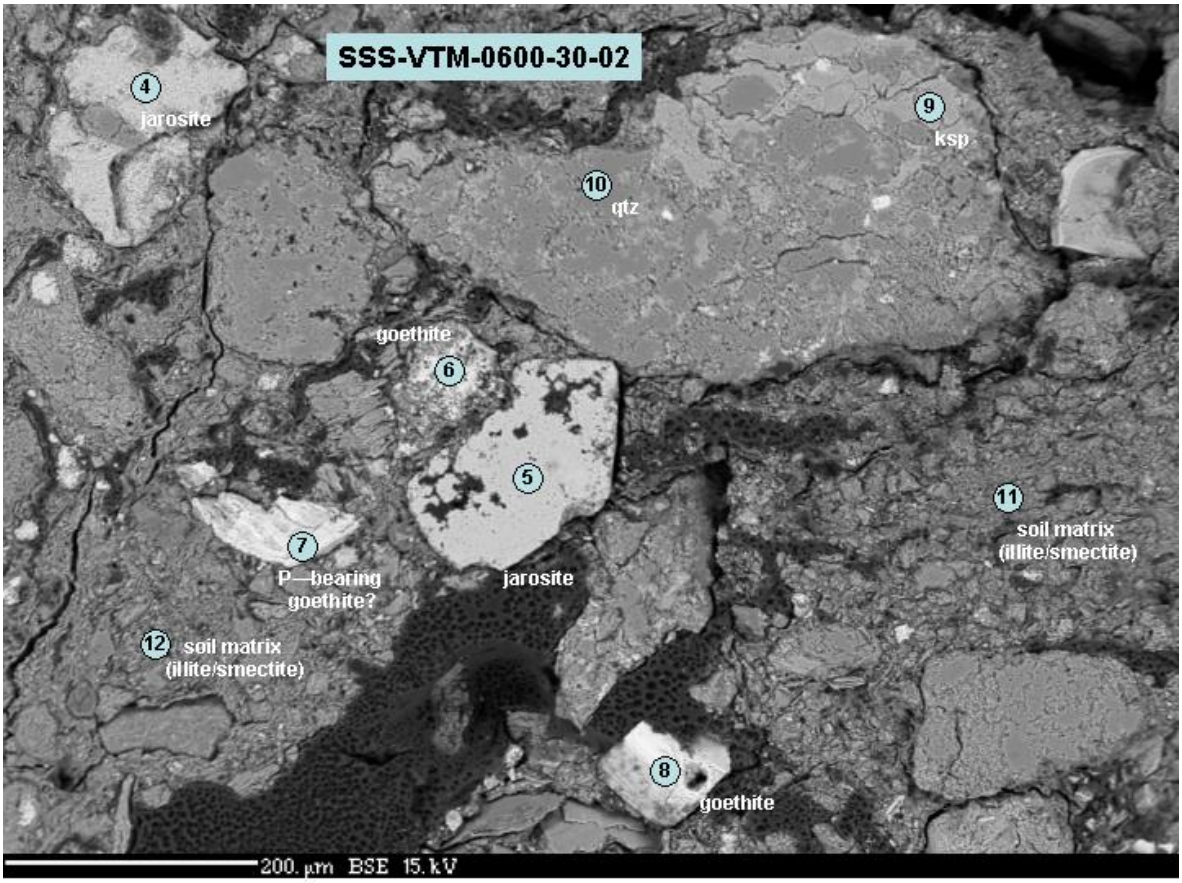

Figure 4.1. Backscattered electron microprobe image of least weathered (SWI=2) large siliceous andesite rock fragments, quartz, jarosite, and goethite in clay-rich matrix (sample SSS-VTM-0600-02 from in situ test id SSS-VTM-0600-1 in Table 4.2). There is minor cementation by clay and gypsum of the rock and mineral fragments. Pyrite grains (bright white cubes and euhedral crystals) are relatively fresh.

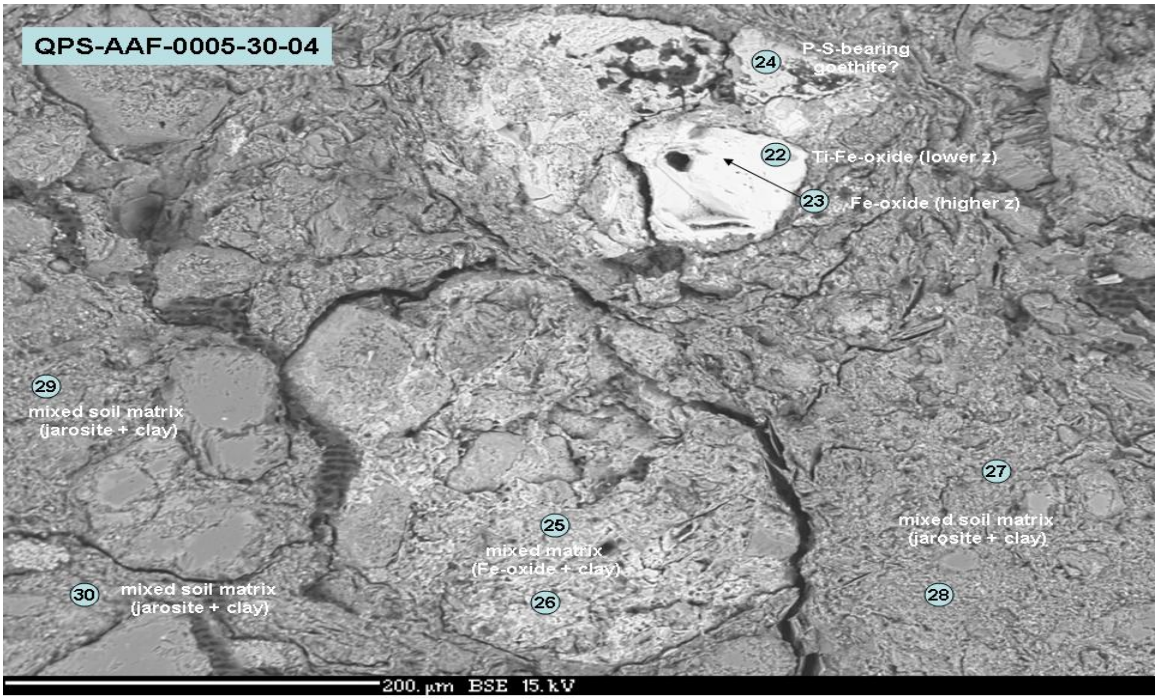

Figure 4.2. Backscattered electron microprobe image of weathered (SWI=4), hydrothermally altered rhyolite rock fragments cemented by jarosite, iron oxide, and clay minerals (sample QPS-AAF-0005-30-03 from in situ test id QPS-AAF-0001-3 in Table 4.2). Relict pyrite (point 22) has been oxidized to iron oxides.

Table 4.2. Lithology and texture of rock pile material at the in situ test locations (written communication by Virginia McLemore, 2008).

Test id	Sample id	SWI	Lithology	Original magmatic texture	Hydrothermal alteration and intensity	Indications of Weathering
MID-VTM-0001-1	MID-VTM-0002	4	100% andesite, trace intrusion	textures visible, moderate feldspar replacement	QSP: 40%	Iron oxide present, skeletal feldspar crystals, rounded pyrite grains
MIN-AAF-0001-1	MIN-AAF-0001	4	98% intrusive, 2% rhyolite tuff	texture still visible but slightly overprinted by hydrothermal texture	QSP: 50%	Iron oxide present
MIN-AAF-0012-1	MIN-AAF-0013	4	100% andesite, trace intrusion	texture visible, moderate-heavy feldspar replacement	QSP: 55%	Iron oxide present, skeletal feldspar crystals
QPS-AAF-0001-3	QPS-AAF-0005	4	100% andesite, trace intrusion	texture visible, limited feldspar replacement	QSP: 25% Propyllitic: 5%	Iron oxide present, authigenic gypsum present, skeletal feldspar crystals

QPS-VTM-0001-1	QPS-VTM-0001	5	100% andesite	texture visible, moderate-heavy feldspar replacement	QSP: 55% Propyllitic: 1%	Iron oxide present, authigenic gypsum present
SPR-AAF-0001-1	SPR-AAF-0001	2	100% andesite	textures visible	Propyllitic: 25%	Iron oxide present, authigenic gypsum present
SPR-AAF-0001-2	SPR-AAF-0003	2	100% andesite	texture visible, moderate feldspar replacement	QSP: 45% Propyllitic: 3%	Iron oxide present, authigenic gypsum present, skeletal feldspar crystals
SPR-VTM-0012-1	SPR-VTM-0012	4	99% andesite, 1% intrusion	texture visible, moderate feldspar deterioration	QSP: 45%	Iron oxide present, skeletal feldspar crystals
SPR-VTM-0012-2	SPR-VTM-0014	4	100% rhyolite tuff	texture slightly visible, heavy overprinting	QSP: 60%	Iron oxide present
SPR-VTM-0012-3	SPR-VTM-0017	4	100% rhyolite tuff	texture slightly visible, heavy overprinting	QSP: 50%	Iron oxide present
SPR-VTM-0019-1	SPR-VTM-0019	4	100% rhyolite tuff	texture slightly visible, heavy overprinting	QSP: 50%	Iron oxide present
SPR-VTM-0019-2	SPR-VTM-0021	4	100% rhyolite tuff	texture visible, moderate hydrothermal overprinting	QSP: 55%	Iron oxide present
SSS-VTM-0600-1	SSS-VTM-0600		80 % andesite, 20% intrusion	hydrothermal overprinting	QSP	Iron oxide present
SSS-AAF-0001-1	SSS-AAF-0001	3	100% andesite, trace rhyolite tuff	textures visible	QSP: 10% Propyllitic: 20%	Iron oxide present, authigenic gypsum present
SSS-AAF-0005-1	SSS-AAF-0005	3	100% andesite, trace intrusion	texture visible, moderate feldspar replacement	QSP: 40%	Iron oxide present, authigenic gypsum present
SSS-AAF-0009-1	SSS-AAF-0009	3	100% andesite	texture visible, moderate feldspar replacement	QSP: 35%	Iron oxide present, trace authigenic gypsum
SSW-AAF-0005-1	SSW-AAF-0005	4	95% andesite, 5% rhyolite tuff, trace intrusion	texture slightly visible, heavy overprinting	QSP: 60% Propyllitic: 2%	Iron oxide present, authigenic gypsum present
SSW-AAF-0007-1	SSW-AAF-0007	4	andesite	hydrothermal overprinting	QSP	iron oxides present
SSW-AAF-0004-1	SSW-AAF-1009	3	98% andesite, 2% intrusion	texture visible, moderate feldspar replacement	QSP: 40%	Iron oxide present, authigenic gypsum present, skeletal feldspar crystals
SSW-VTM-0600-1	SSW-VTM-0600	4	andesite	hydrothermal overprinting	QSP	iron oxides present

SSW-VTM-0600-2	SSW-VTM-0001	4	100% rhyolite tuff	texture slightly visible, heavy overprinting	QSP: 60%	Iron oxide present
SSW-VTM-0600-3	SSW-VTM-0004	4	99% andesite, 1% rhyolite tuff	texture not visible, heavy overprinting	QSP: 75%	Iron oxide present, authigenic gypsum present
SSW-AAF-0026-1	SSW-VTM-0027	3	100% andesite, trace rhyolite tuff, trace intrusion	texture visible, slight feldspar replacement	QSP: 30% Propyllitic: 2%	Iron oxide present, authigenic gypsum present, skeletal feldspar crystals, rounded pyrite grains
SSW-AAF-0030-1	SSW-VTM-0030	3	100% andesite	texture visible	Propyllitic: 17%	Iron oxide present, authigenic gypsum present, presence of tarnished pyrite

4.1.2. Design of In situ Direct Shear Test Device and Test Procedure

A modified in-situ shear test apparatus was designed at New Mexico Tech and fabricated by Questa mine engineers. The apparatus consists of a 30 cm or 60 cm square metal shear box, a metal top plate, a fabricated roller plate, normal and shear dial gages with wooden supports, and two hydraulic jacks. Unlike conventional laboratory shear and in situ shear test apparatuses that consist of two boxes that move relative to each other, the in situ shear box designed for this project is made of only one box. This innovation allows for easier and faster site preparation. Further details about this box, its accessories, and the procedures employed to obtain an undisturbed rock pile block can be found in Fakhimi et al (2007).

A standard operating procedure (SOP 82; Appendix 2) was written and implemented in the field. All in situ tests were performed at depths of 1 to 4 m below the original rock pile surfaces. To keep the rock-pile material intact while preparing the site for the shear strength test, a technique introduced by Coker and Flores (2000) was used.

The procedures employed to obtain an undisturbed rock pile block similar to what was used by Coker and Flores (2000) described in Fakhimi et al (2007). The shear box is then carefully placed over the block. Any gaps between the shear box walls and the soil block are filled with coarse sand or excavated rock-pile material to maintain full contact between the soil block and the shear box. Next, the top metal plate is placed on top of the soil block and leveled. Either dead weight or a hydraulic cylinder (Figure 4.3) is used to apply the normal load. When using a high normal load, the roller plate is placed on the top plate and the normal hydraulic cylinder is situated such that its reaction is transferred to the bucket of an excavator (Fakhimi et al., 2007).

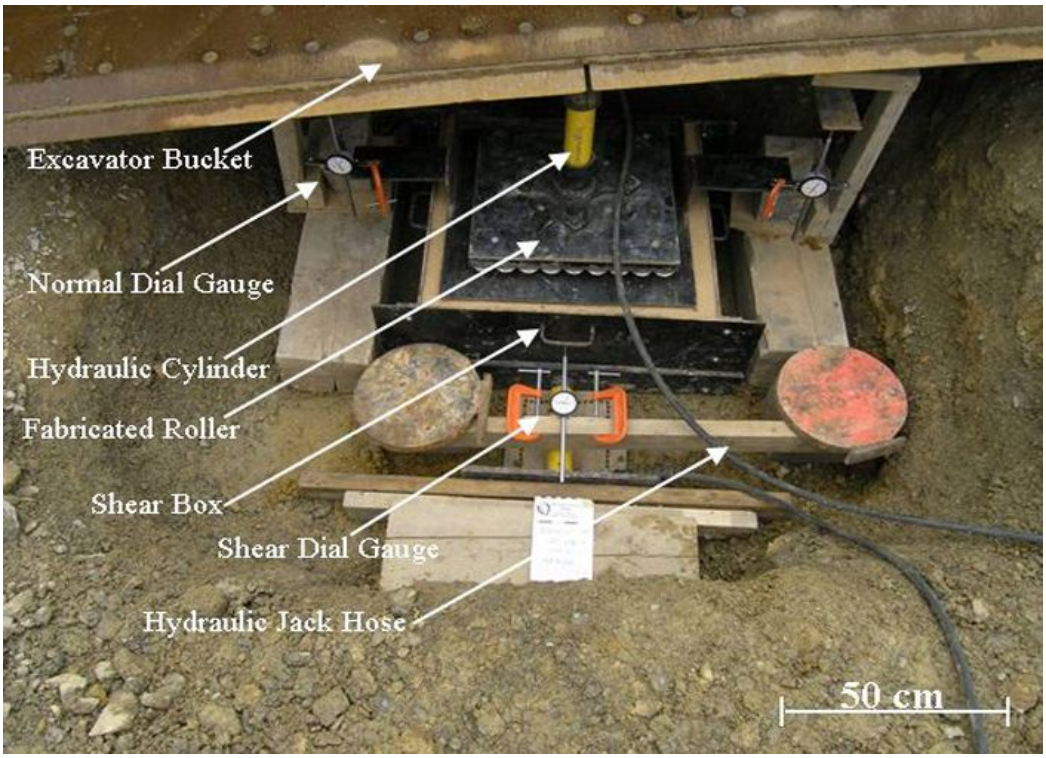

Figure 4.3. Set-up of in situ test using the bucket of an excavator to support the hydraulic jack.

One dial gage was used to measure shear displacement, while two normal dial gages attached to the lateral sides of the top platen were used to measure normal displacement of the shear block. The shear load is gradually increased. The hydraulic jack loads and dial gages are read after each 0.51 mm (20/1000 inch) of shear displacement. The average shear displacement rate was approximately 0.025 mm/s. Each in situ shear test was normally continued for a shear displacement of 7.5 cm. Each in situ shear test takes approximately 3 hours to excavate and set up and about 1 hour to run. A team of 4-6 people is required to perform a test. Detailed specification of hydraulic jack used for the test is presented in Appendix 1.

The applied normal stress for the in situ tests ranges from 15 to 75 kPa. This range of normal stresses was lower than the overburden pressure to prevent consolidation of rock pile samples.

Measurements of matric suction and soil temperature were taken at the shear plane following the appropriate standard operating procedures. Representative samples were sent to the laboratory for Atterberg limits, specific gravity, and disturbed laboratory direct-shear tests, plus moisture content, particle size, mineralogical, chemical, and petrographic analyses. After each in situ shear test, the shear plane was inspected for the maximum particle size and was photographed. Particle size analyses were performed in the laboratory on the rock-pile samples that were collected from the in situ tests locations. The samples were classified based on the Unified Classification System (UCS).

4.1.3 Matric Suction

Soil suction is defined as the negative pressure by which water is retained in the pores of a sample of soil when the sample is free from external stress. The pressure deficiency (below atmospheric pressure) also can exist in soil subjected to certain stress regimes associated with particular loading conditions.

A typical relationship between moisture content and soil suction is that as the moisture content decreases, soil suction increases and can become very large as the soil dries out.

To measure the in situ matric suction of the Questa rock piles, a "Quick Draw" moisture probe and standard tensinometers (Soil moisture Equipment Corp., 2000) were used (Figure 4.4). The instruments are soaked in a bucket of water to ensure that the porous cups were fully saturated before using it.

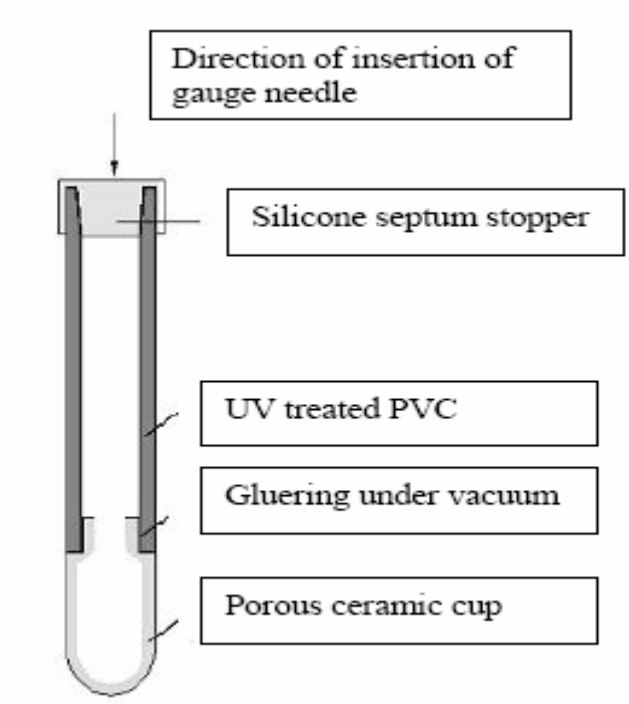

Figure 4.4. Standard Tensinometer instrument diagram (Shannon, 2007).

A tensinometer is filled with deionised water making sure there are no bubbles in the top section of the tensometer. A hole about 5 cm(2 in) daimeter is constructed using a hammer and a metal rod in the vicinity of shear plane similar to the diameter of the tensinometer. The size of the hole is able to accommodate the tensinometer and still be in contact with the soil. The tensinometers is placed within the hole and twisted to make sure the tensinometers is well in contact with the soil (Figure 4.5).

The tensinometer is left in place for some time (about 5 min) to be in equilibrium with the soil. The meter is placed on top of the tensinometer to measure the matric suction in kPa (Figure 4.5). If the tensinometer is placed perpendicular to the shear plane (vertically), the measured suction must be corrected considering the height of the tensinometer.

Figure 4.5. Tensinometer meter set up for reading the pore pressure

4.1.4 Sand Replacement Density Test

This test method is the modification of the ASTM D1556 sand-cone method for determining in-place density or unit weight of soils. There are several methods of measuring the bulk density Examples of technique to determine the wet density include: the sand-replacement method which is a modification of the cone replacement method, and the nuclear emissions method. For our research work, the sand-replacement method was employed. This method is suitable for all soils including coarse-grained soils such as the rock pile material at the Questa mine.

The standard test method for determining the wet density using sand replacement method was performed in accordance with the standard operating procedure (SOP 70) which is presented in Appendix 2.

4.2 Laboratory Tests

Like other construction materials, rock pile material possesses mechanical properties such as strength, and permeability. Quantifying these properties is important to predict how soil will behave under stresses. Some of these properties can be determined in situ as already discussed in the previous section. The quantification of some of these mechanical properties can be determined in the laboratory using standardized laboratory test procedures. For our research work, standard operating procedures (SOP) were written and documented for each test (Appendix 2). The procedures described are in accordance with American Society for Testing and Material (ASTM) standards.

4.2.1 Measurement of water Content

The standard test method for laboratory determination of water (moisture) content of soil was performed in accordance with ASTM D2216. The standard operating procedure (SOP 40) for the test is presented in Appendix 2. Water content measurement is primarily used for performing weight-volume calculation in soils. Moisture also is a measure of the shrink-swell and strength characteristics of cohesive soils.

4.2.2 Specific Gravity Test

Specific gravity of soil solids (G_s) is the mass density of the mineral solids in soil normalized relative to the mass density of water, which also can be viewed as the mass of a given volume of soil solid normalized relative to the mass of an equivalent volume of water. Specific gravity is typically expressed using three significant figures. Published values indicate that the specific gravity of sand is 2.65 because this is the specific gravity of quartz. Since the mineralogy of clay is more variable, G_s for clay is variable, and is often assumed to be somewhere between 2.70 and 2.80 depending on the mineralogy (Holtz et al., 2003).

The standard test method for laboratory determination of specific gravity of soil was performed in accordance with ASTM D2216. The standard operating procedure (SOP 75) for the test is presented in Appendix 2.

4.2.3 Particle Size Analysis

Particle size analysis is required to understand the hydrological and structural properties of the rock pile, which is used in modeling the seepage and stability of the rock piles. This Standard Operation Procedure (SOP 33-Appendix 2) is based on ASTM D422-63. This method covers the quantitative determination of the distribution of particle size in soils.

Two general methods are considered for particle size analysis for air-dried samples. One condition is used when the fine particles in the sample do not clog the sieve openings. In this case, the distribution of particle sizes larger than 75 μm (retained on the No. 200 sieve) is determined by sieving, while the distribution of particle sizes smaller than 75 μm is determined by a sedimentation process using a hydrometer to secure the necessary data. Another condition is used when the fine particles clog the sieve openings. In this case, the sample is divided into two portions. One portion contains only particles retained on the No. 10 sieve (2 mm or 0.132 in) that its distribution is determined by sieving, while the other portion contains only particles passing the No. 10 sieve that its distribution is determined by sedimentation process (Hydrometer) and sieving. For this purpose, sedimentation process is performed for 100 g particles passing No. 10 in order to obtain the distribution of fine particles (finer than No. 200 sieve), and then, after taking final hydrometer reading, the suspension is transferred to a No. 200 sieve (0.075 mm or 0.0029 in) and washed with tap water until the wash water is clear. Then the material retained on the No. 200 sieve is transferred to a container and dried in an oven. Finally, in order to obtain the distribution of particles passing No. 10 sieve and retained on No. 200 sieve, sieve analysis of the oven-dried material remained on No. 200 sieve is made.

Mchanical Particle Size Analyses

The air-dried sample is split using the sample splitter to obtain the representative sample for particle size analysis. The size of the sample shall depend on the diameter of the largest particles in the sample. The total sample weight is recorded, and the top sieve is selected based on the weight of the sample as the one with openings that are slightly larger than the diameter of the largest particle in the sample. The series of sieves are arranged so that they have decreasing opening size from the top to the bottom of the stack. The sieve stack is placed in the shaking machine for at least 10 minutes or until additional shaking does not produce appreciable changes in the amounts of material on each sieve screen. Finally, the sieve stack is removed from the machine, and the weight of retained soil particles on each sieve is recorded on the data sheet

Hydrometer Analyses

The sample is placed in a 250 ml beaker, and distilled or demineralized water is added until the sample is submerged, then 15 ml of the dispersing agent (antiflocuant) is added at this time. The sample is allowed to soak overnight or until all soil lumps have disintegrated. At the end of the soaking period, the sample is dispersed further by transferring the complete sample to the dispersion cup. Any residue from the beaker is washed with distilled or demineralized water. Distilled water is added if the cup is less than half full. The cup is placed in dispersing machine to disperse the suspension for 1 to 10 minutes. The solution is transferred to the sedimentation cylinder and distilled water is added to the 1000 ml mark. The suspension is shaken vigorously for a few seconds. At the end of the 1 minute shaking period, the cylinder is set on a stable surface and the time

is noted. The hydrometer is immersed slowly into the liquid for each reading. Hydrometer readings are taken after 1 and 2 minutes have elapsed from the time the cylinder was placed on the table. As soon as each reading is taken, the hydrometer is removed from the suspension carefully. Since during the first two readings, errors are likely to happen, these first reading steps are repeated to make sure that the same values are obtained. Then the sample is shaken again to proceed to the next steps. At the end of the second 2 minutes and after each subsequent hydrometer reading, a thermometer is placed in the suspension and the temperature is recorded. After reading at 1 minute and 2 minutes, hydrometer readings are recorded at the following time intervals: 4, 15, 30, 60, 120, 240, 960, 1440 minutes. Distribution of particle sizes smaller than 75 μm was determined by a sedimentation process with a hydrometer. The same procedure was also adopted for the second method by performing sedimentation test on samples passing the number 10 sieve (2mm or 0.132 in).

4.2.4 Atterberg Limit Test

The liquid limit (LL) and plastic limit (PL) tests give information regarding the effect of water content (w) on the mechanical properties of soil. The effect of water content on volume change and soil consistency is addressed by performing the ASTM D4318 Atterberg standard test. The steps for performing the test are described out in SOP 54 (included in Appendix 2). The results of the test are used to classify soil plasticity in accordance with ASTM D2487.

4.2.5 Conventional Direct Shear Laboratory Test

For our laboratory shear testing on the air-dried samples collected from the in situ test sites, a 2-inch shear box was used. The tests were performed on rock-pile materials collected from the in situ direct shear test shear planes from each location of in situ direct shear tests. This is to perform the conventional laboratory direct shear test on the same material as tested in situ so that a good comparison can be made between the two methods. The in situ rock pile material is sieved using the No. 6 sieve (3.8 mm or 0.2 in) and material passing the sieve is used for the laboratory direct shear test. Each sample's dry density was calculated from the sand replacement method. The dry density ranged from 1.4 to 2.7 g/cm^3 (87.4 to 169.0 pcf) with a standard deviation of 0.3 g/cm^3 (18.7 pcf). The wet density ranged from 1.5 to 2.9 g/cm^3 (93.6 pcf to 181 pcf) with a standard deviation of 0.3 g/cm^3 (18.7 pcf). These high values of density may be due to compaction of the rock piles with time after their placement. The sample to be tested is divided into four portions and weighed within the range of 100-105 g (0.22 – 0.23 lb) (Figure 4.6).

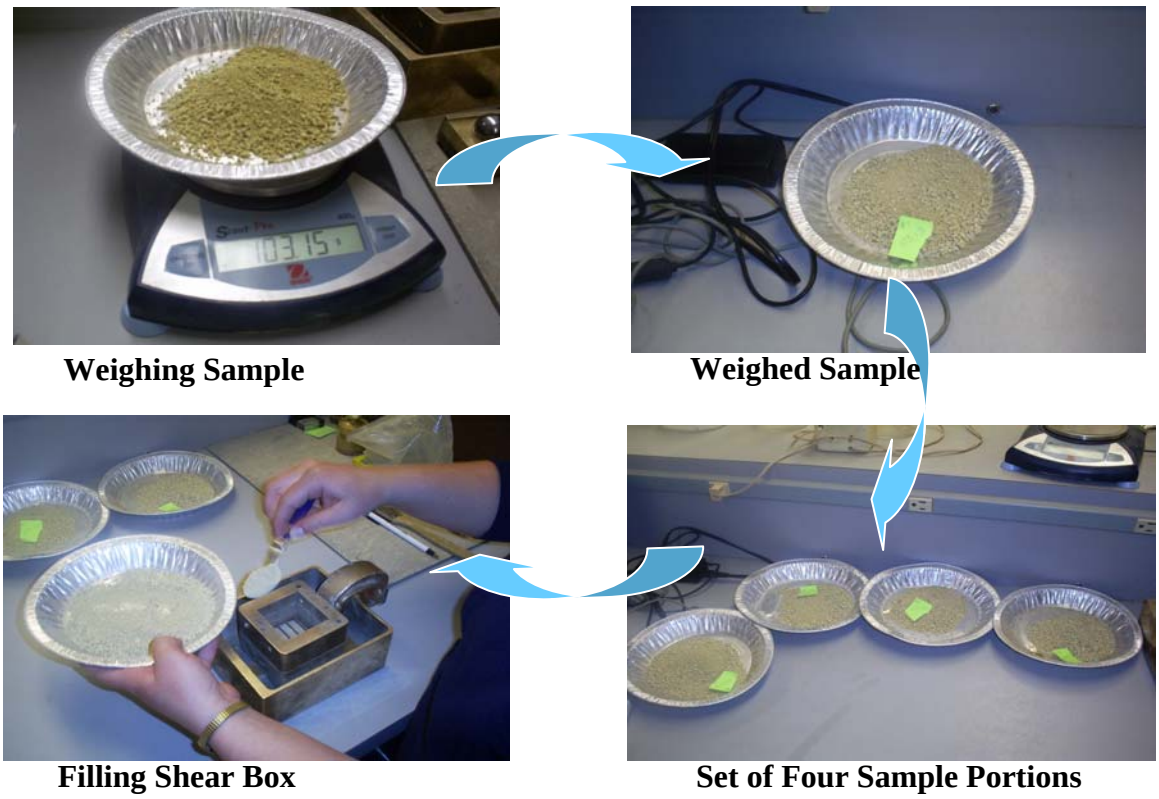

Figure 4.6. Systematic steps for preparation of sample for direct shear test, including dividing the sample into four equal portions.

To achieve the dry densities similar to what was measured in the field for each sample, the material was added to the laboratory direct shear test sample chamber in several stages and hand compacted (Figure 4.7). The vertical load is held constant during the test without compensation for the change in area of the shear plane.

Figure 4.7. Compaction of specimen to achieve the same dry density as measured in situ.

The normal stress varied between 20 kPa and 800 kPa in the shear tests. A shear displacement rate of 0.00833 mm per second (3.333 X 10^{-2} in per second) was used to perform the shear test. Peak and residual shear strengths were determined from the plot of shear stress versus shear displacement. The maximum horizontal (shear) displacement for the laboratory direct shear tests was 12 mm (0.5 in).

5. RESULTS

The results of in situ and laboratory tests are presented in summary tables in this chapter. Statistics were created by using a statistics program (SigmaStat 3.1) to report the range of values and their standard deviations. Specific histogram plots were made for the rock piles and analogs to identify differences in their characteristics. Charts based on the results with discussions are presented in the next chapter. All plots of in-situ direct shear and laboratory direct shear results are presented in Appendix 4.

5.1 In situ Tests Results

In-situ tests were performed to measure in situ parameters for four rock piles and two analogs. These parameters are cohesion, friction angle, wet density, gravimetric water content, and matric suction.

5.1.1 In situ Cohesion

In-situ measurement of cohesion was made at the Questa mine during 2006 and 2007. Detailed methodology is presented in chapter four. A total of 52 in situ direct shear tests were performed. The range of normal stresses in the in situ shear tests was 19 to 67 kPa. These ranges of normal stresses were used to simulate the shallow depth of the in situ direct shear test. The overburden stress of the rock pile to test location was also considered in the selection of the range of normal stresses. The laboratory friction angles

with low normal stresses (20 to 120 kPa) were used together with the Mohr-Coulomb failure envelope in order to obtain the cohesion for each location.

Based on recommendations of the allowable maximum particle size in direct shear test presented in Chapter 3, only the results of in situ tests where the maximum particle size was less than 1/5 the width of the shear box was used as presented in the SOP (see Appendix 2 and 3). Using this criterion, only 24 in situ shear test results remained for the statistical analysis; the remaining 28 tests were not acceptable. The cohesion values reported are corrected with their corresponding in situ matric suctions to obtain the intrinsic cohesion of the rock pile material. To calculate the intrinsic cohesion parameters for the same zero matric suction, Eqs. 3.3, 3.4 and 3.5 were used (Fredlund and Rahardjo, 1993).

The range of values of cohesion for the 52 samples is 0 to 46.1 kPa and intrinsic cohesion ranges from 0 to 37.7 kPa. Results for the 24 accepted tests range from 0 to 46.1 kPa with intrinsic cohesion ranging from 0 to 37.3 kPa. Table 5.1 and 5.2 are the summary results for the 24 accepted tests.

Figure 5.1 shows a histogram distribution plot of cohesion to differentiate the results obtained for the analogs and the rock piles. Figure 5.1a and 5.1b also shows a histogram distribution plot for the accepted twenty four (24) tests, comparing the cohesion of the rock piles with the analogs, respectively. It is easy to see that the cohesion of the analogs is higher than that of the rock piles.

Table 5.1. Descriptive statistics of cohesion for the twenty-four in situ direct shear tests with no particles larger than 1/5 the width of the shear box.

Field Measured Cohesion (kPa) - Particle size less than 1/5 the width of the size of shear box							
Samples Location	**Maximum**	**Minimum**	**Mean**	**Median**	**Standard Deviation**	**Coffe. Of Variation (%)**	**Number of Samples**
Middle Rock Pile	0.5	0.5	0.5	0.5	0	0	1
Sugar Shack West	25.9	0.3	11.9	12.7	8.4	70.4	8
Spring Gulch Rock Pile	16.8	0	9.8	12.7	6.1	62.2	7
Sugar Shack South	17.2	1.8	7.0	4.4	7.2	102.8	4
Pit Alteration Scar	23.9	9.4	16.7	16.7	10.3	61.7	2
Debris Flow	46.1	31.4	38.8	38.8	10.4	26.8	2

Table 5.2. Descriptive statistics of intrinsic cohesion for the twenty-four in situ direct shear tests with no particles larger than 1/5 the width of the shear box.

Intrinsic Cohesion (kPa) - Particle size less than 1/5 the width of the size of shear box							
Samples Location	**Maximum**	**Minimum**	**Mean**	**Median**	**Standard Deviation**	**Coffe. Of Variation (%)**	**Number of Samples**
Middle Rock Pile	0.5	0.5	0.5	0.5	0	0	1
Sugar Shack West	25.6	0	10.8	12.14	9.3	86.1	7
Spring Gulch Rock Pile	16.3	0	8.8	10.36	5.8	66.0	7
Sugar Shack South	14.8	1.5	6.2	4.24	6.1	98.4	4
Pit Alteration Scar	23.9	6.5	15.2	15.18	12.3	80.9	2
Debris Flow	37.3	34.7	31.0	30.98	8.9	28.7	2

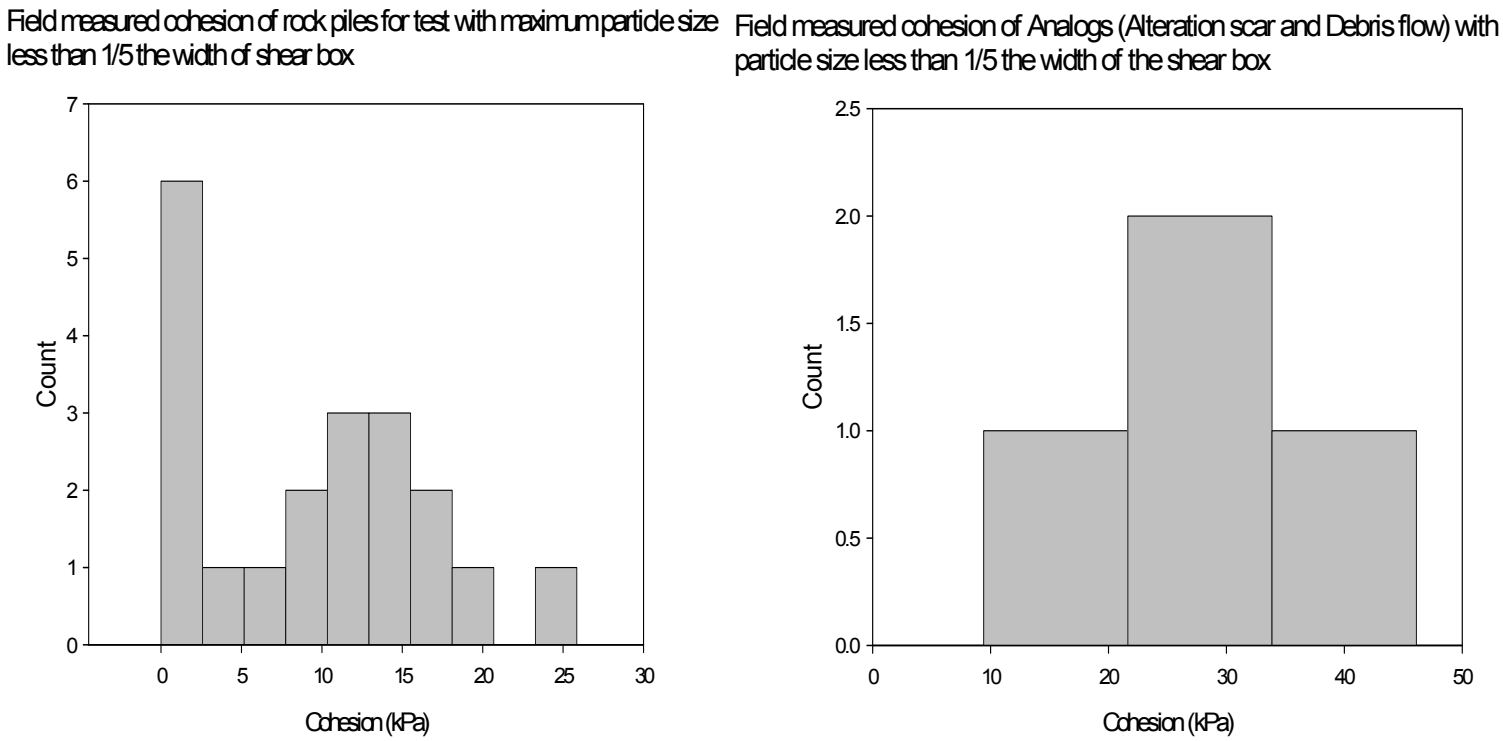

(a) (b)

Figure 5.1. Histogram distributions of cohesion data of Questa material

5.1.2 In situ Friction Angle

Figures 5.2, 5.3, and 5.4 shows a typical result of three in situ shear tests conducted on Sugar Shack West rock pile using normal stresses of 18.0, 27.8, and 58.7 KPa. All plots of in situ shear tests results for high normal load are presented in Appendix 4. Figure 5.2 shows the shear stress plotted versus the shear displacement. As expected, the shear stress corresponding to a fixed normal stress increases initially until it reaches the peak strength, which then reduces gradually toward its residual strength.

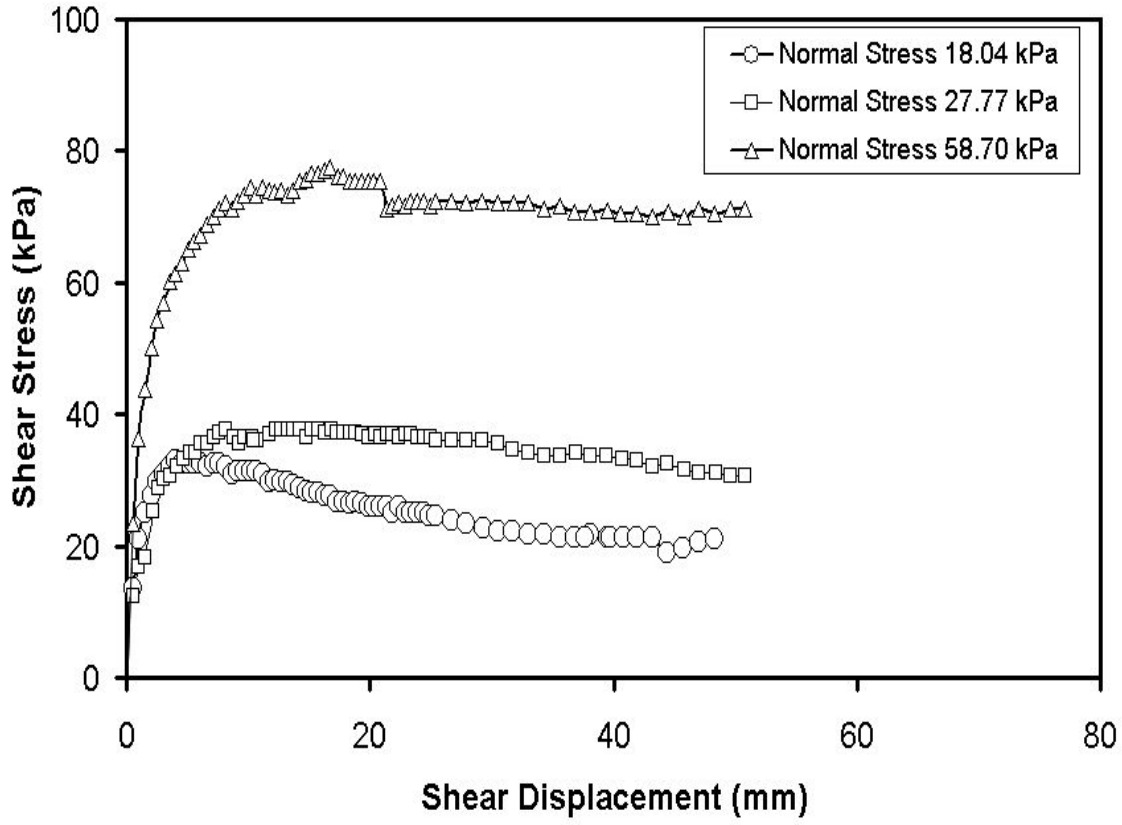

Figure 5.2. A plot of shear stress vs shear displacement of a set of in situ tests on Sugar Shack West rock pile.

A plot of normal displacements against shear displacement is used to identify the dilatation or contraction behavior of the material during the test. Positive displacements indicate dilation of the material (Figure 5.3). Note that two curves for each test is shown in Figure 5.3 as the normal displacements are measured at lateral sides of the top plate using two dial gages.

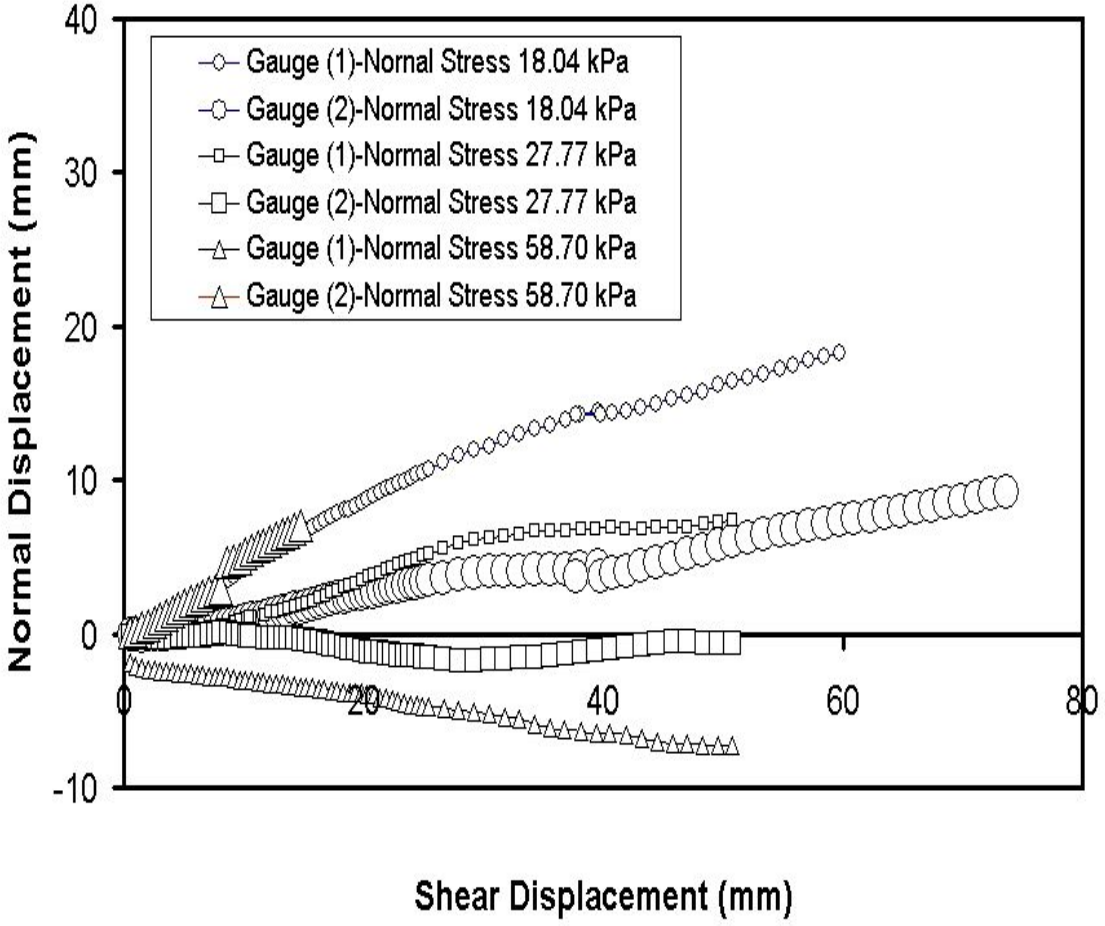

Figure 5.3. A plot of normal displacement vs shear displacement of an in situ test

Figure 5.4 illustrates the Mohr-Coulomb failure envelope for the three tests conducted on the rock pile material. The figure indicates a friction angle of 48º.

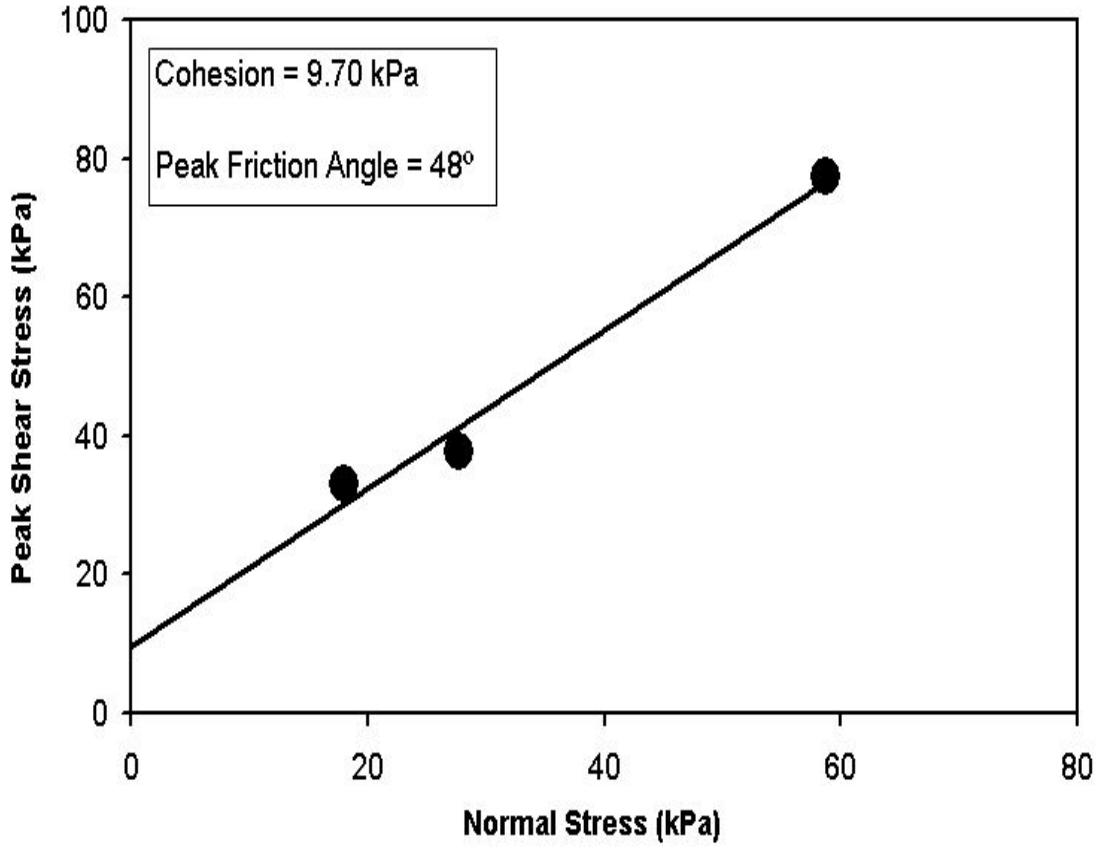

Figure 5.4. Mohr-Coulomb plot for in situ test to determine friction angle Sugar Shack West rock pile.

After eliminating the tests which exceeded the recommended maximum particle size, only two valid friction angles were left (Table 5.3). The Mohr-Coulomb plots for the two valid friction angles are shown in Figure 5.4 and 5.5.

Table 5.3 Friction angles of in situ direct shear tests with no particles larger than 1/5 the width of the shear box.

Sample Location	Friction Angle (^{o})	Number of Points used to Calculate the friction angle
Middle Rock Piles	n/a	n/a
Sugar Shack West	48.7	3
Spring Gulch Rock Pile	49.6	4
Sugar Shack South	n/a	n/a
Pit Alteration Scar	n/a	n/a
Debris Flow	n/a	n/a

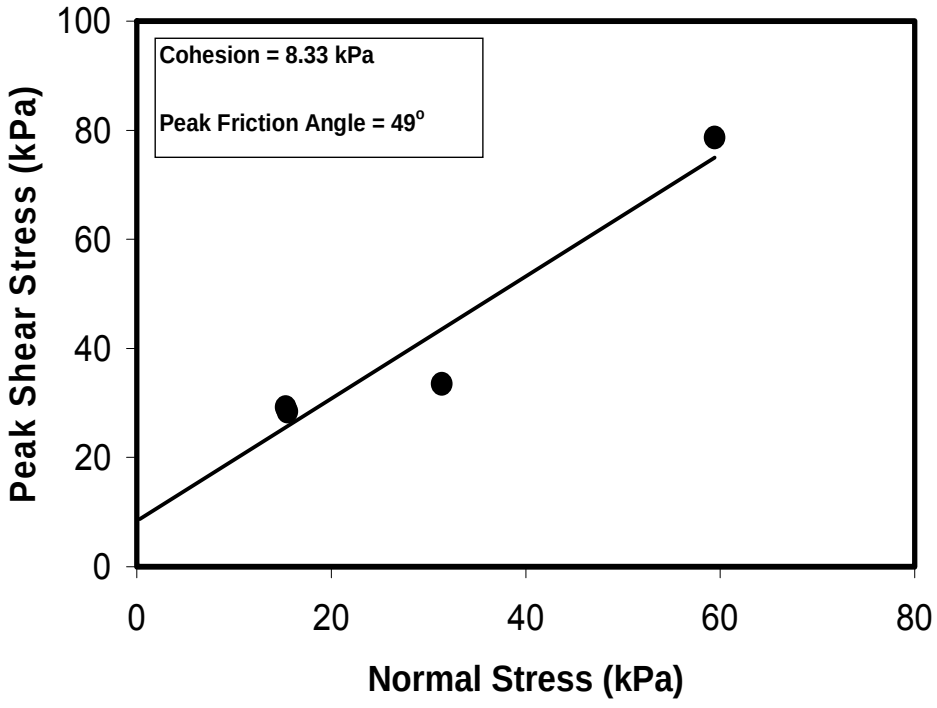

Figure 5.5. Mohr-Coulomb plot for in situ test to determine friction angle on Spring Gulch Rock Piles.

5.1.3 Densities

Measurements of wet density were also made in situ at the Questa mine. A total of forty-seven (47) bulk density measurements were conducted on the same four (4) rock piles (Middle rock pile, Spring Gulch rock pile, Sugar Shack South rock pile and Sugar Shack West rock pile) and two (2) analogs (one (1) pit alteration scar and one (1) debris flow). The wet density is used to calculate the normal load due to the weight of block on the shear plane in the in situ direct shear test. Table 5.4 is the summary of density results. The average density for all samples ranges from 2010 to 2600 kg/m^3. This range of wet density results is comparable to that obtained by Gutierrez (2006) as presented in chapter 2. Gutierrez (2006) reported results for the mean bulk density of Goathill North rock pile using nuclear gage, sand replacement and water replacement tests ranging from 1160 to 2430 kg/m^3 with an average of 1800 kg/m^3 and standard deviation of 180 kg/m^3. The measured wet densities are similar to what is reported by Shannon (2006).

Table 5.4 Descriptive statistics of in situ wet density for the fifty-two in situ direct shear tests from four rock piles and two analogs

Wet Density (kg/m^3)							
Samples Location	**Maximum**	**Minimum**	**Mean**	**Median**	**Standard Deviation**	**Coffe. Of Variation (%)**	**Number of Samples**
Middle Rock Pile	2960	2240	2600	2600	510	20	2
Sugar Shack West	2700	1490	2150	2190	330	15	15
Spring Gulch Rock Pile	2690	1550	2010	2010	340	17	10
Sugar Shack South	2330	1910	2100	2100	140	7	7
Pit Alteration Scar	2160	1710	2010	2090	170	8	8
Debris Flow	2600	1800	2120	2030	300	14	5

The dry densities for the samples were calculated by subtracting water content from the mass of soil collected from the sand replacement test to obtain the dry mass of soil and dividing the dry mass of the soil by the volume of the hole made for the sand replacement test. These calculated dry density values were used in the conventional laboratory direct shear tests to simulate field conditions. The range of dry densities calculated is 1400 to 2680 kg/m^3. URS Corporation (2003) indicated their range of calculated dry density as 1500 to 2300 kg/m^3. Norwest's (2005) study of the stability of the front rock piles at Questa reported dry densities ranging from 1520 to 1890 kg/m^3. Gutierrez (2006) reported a range of dry densities of 1700 to 1800 kg/m^3 after performing direct shear tests on the Goathill North rock pile samples. Table 5.5 is the statistical summary table of calculated dry densities.

Table 5.5 Descriptive statistics of in situ dry densities for the fifty-two in situ direct shear tests locations from four rock piles and two analogs

Dry Density (kg/m^3)							
Samples Location	**Maximum**	**Minimum**	**Mean**	**Median**	**Standard Deviation**	**Coffe. Of Variation (%)**	**Number of Samples**
Middle Rock Pile	2680	1960	2220	2120	320	14	4
Sugar Shack West	2400	1400	1920	1870	270	14	17
Spring Gulch Rock Pile	2160	1430	1760	1750	240	14	10
Sugar Shack South	2090	1680	1890	1890	120	6	8
Pit Alteration Scar	1960	1510	1800	1870	160	8	8
Debris Flow	2460	1710	2020	1940	280	14	5

5.1.4 Water Content

Water content is one of the numerous measurements considered in geotechnical analysis. A build up of pore pressure due to the presence of water causes a reduction in shear strength and subsequently leads to failure under saturated condition. This condition is not observed within the Questa rock piles.

A total of forty-six (46) samples were analyzed to determine the range of the water content. The water content for all samples ranges from 5.0 to 11.7 %. Robertson GeoConsultants (2000), URS Corporation (2003), Norwest Corporation (2004, 2005), and Gutierrez (2006) reported similar ranges of water content for Questa rock piles as presented in Chapter 2. Table 5.6 is a summary of water content for the samples tested for this thesis research. Figure 5.6a and 5.6b are histogram distribution plots of the near-surface moisture content results for the rock piles and analogs, respectively.

Table 5.6. Descriptive statistics of in situ water content for the fifty-two in situ direct shear test locations including four rock piles and two analogs.

Water Content (%)							
Samples Location	**Maximum**	**Minimum**	**Mean**	**Median**	**Standard Deviation**	**Coffe. Of Variation (%)**	**Number of Samples**
Middle Rock Pile	10.3	5.6	8.0	8.0	3.3	41.3	2
Sugar Shack West	11.8	4.8	7.7	7.5	2.4	31.2	15
Spring Gulch Rock Pile	12.2	6.6	8.7	8.6	1.6	18.4	8
Sugar Shack South	15.1	4.7	10.4	10.3	3.3	31.7	8
Pit Alteration Scar	14.9	9.0	11.7	11.7	2.0	17.0	8
Debris Flow	7.8	2.0	5.0	5.4	2.1	42.0	5

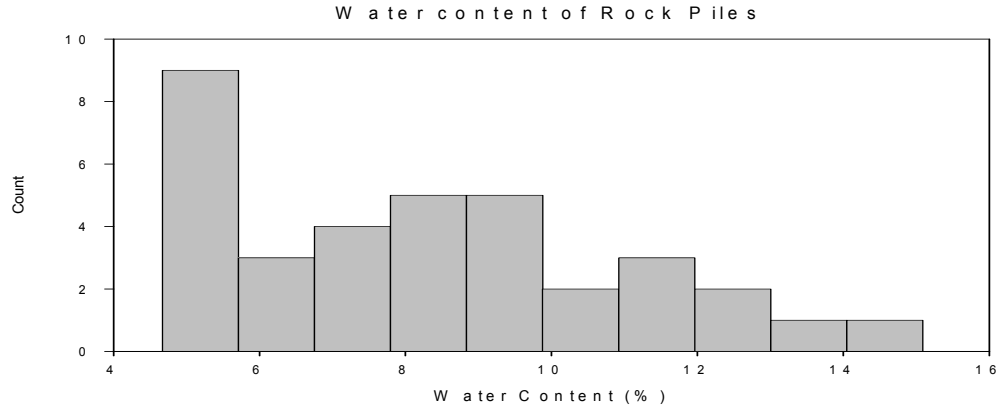

(a)

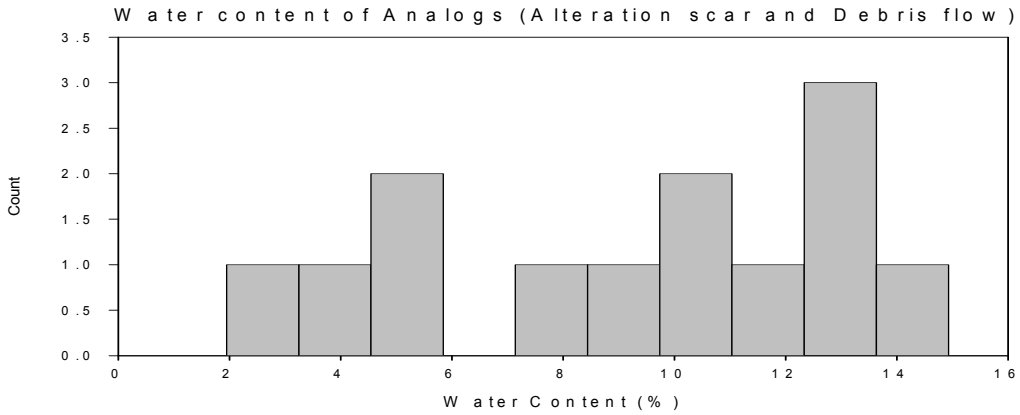

(b)

Figure 5.6. Histogram distribution of water content data of rock pile and analogs

5.1.5 Matric Suction

Pore water pressure measurements were made on each shear plane during the in situ shear tests. Determination of the pore pressure was necessary to identify the influence of water pressure on cohesion. Large values of matric suction measured were associated with large values of cohesion related to debris flow. Matric suction measurements range between 0 to 45 kPa. Shannon (2006) reported similar values of

matric suction by conducting series of tensinometers tests on the Goathill north rock pile. The highest value of matric suction is associated with the debris flow. Note that high values of cohesion were measured in the debris flow locations as well. Table 5.7 is a summary of the matric suction measurements.

Table 5.7. Descriptive statistics of in situ matric suction for the fifty-two in situ direct shear tests from four rock piles and two analogs

Matric Suction (kPa)							
Samples Location	**Maximum**	**Minimum**	**Mean**	**Median**	**Standard Deviation**	**Coffe. Of Variation (%)**	**Number of Samples**
Middle Rock Pile	2.0	0.5	1.3	1.3	1.1	84.6	2
Sugar Shack West	30.0	0.0	7.1	3.0	8.9	125.4	14
Spring Gulch Rock Pile	10.0	0.0	3.6	2.5	3.6	100.0	10
Sugar Shack South	9.0	0.0	2.3	1.0	3.5	152.0	7
Pit Alteration Scar	13.0	0.0	6.5	8.0	5.9	90.8	8
Debris Flow	45.0	24.0	30.2	26.0	8.7	28.8	5

5.2 Laboratory Test Results

Laboratory tests were conducted to measure the index and shear strength parameters of the Questa rock pile materials. The laboratory tests included a conventional direct shear test, Atterberg limit tests, and particles size analyses using mechanical sieving and hydrometer tests. All results were statistically analyzed and plotted on histograms to identify any variation in results between in situ tests and the laboratory tests and between the rock piles and the analogs. Statistical results were also compared with published data on the Questa rock pile material.

5.2.1 Conventional Laboratory Direct Shear Tests

A two-inch diameter sequare direct shear box was used to perform shear tests on air-dried specimens collected from in situ test locations. A total of four hundred and eight (408) direct shear tests were performed in the laboratory with two different ranges of applied normal load conditions (High normal load and low normal load). Four points were used to generate Mohr Coulomb plots for determining friction angle.

High normal stresses of 150 to 650 kPa were applied to simulate the deeper depths of the rock piles. The corresponding peak and ultimate friction angles were calculated and statistically analyzed. Figures 5.7, 5.8, and 5.9 show typical results of the tests on Sugar Shack South rock pile material using high normal loads. All plot of shear tests results using high normal loads are presented in Appendix 4. Figure 5.7 shows the shear stress plotted versus the shear displacement. As expected, the shear stress corresponding to a fixed normal stress increases initially until it reaches the peak strength, which then reduces gradually towards its residual strength.

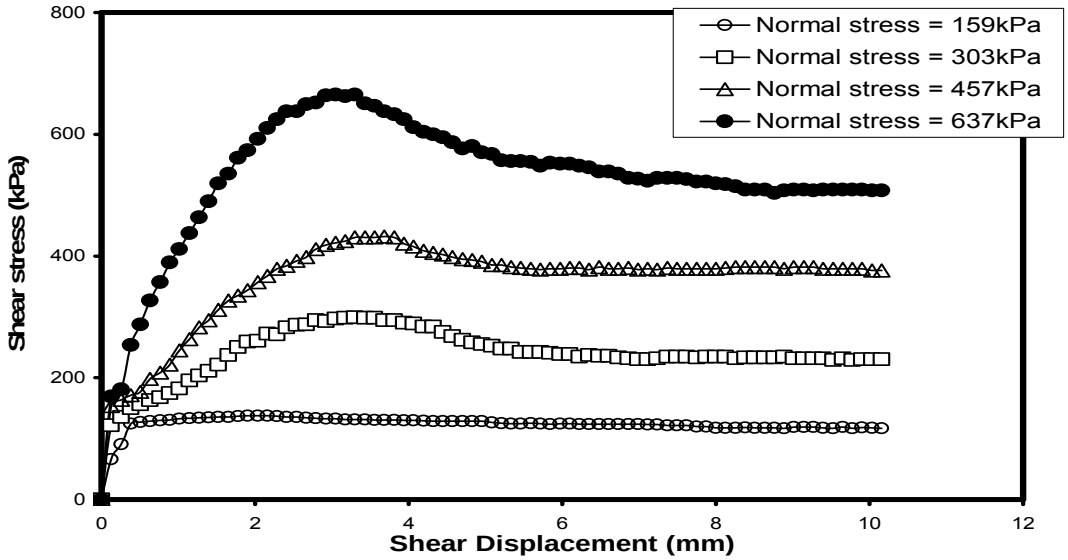

Figure 5.7. A plot of shear stress vs shear displacement of laboratory shear tests using high normal stresses for sample SSS-AAAF-0001 of Sugar Shack South

A plot of normal displacements against shear displacement is used to identify the dilatation or contraction behavior of the material during the test. Positive displacements indicate dilation of the material (Figure 5.8). As expected, as the applied normal stress increases, the material shows more contraction during the shear test.

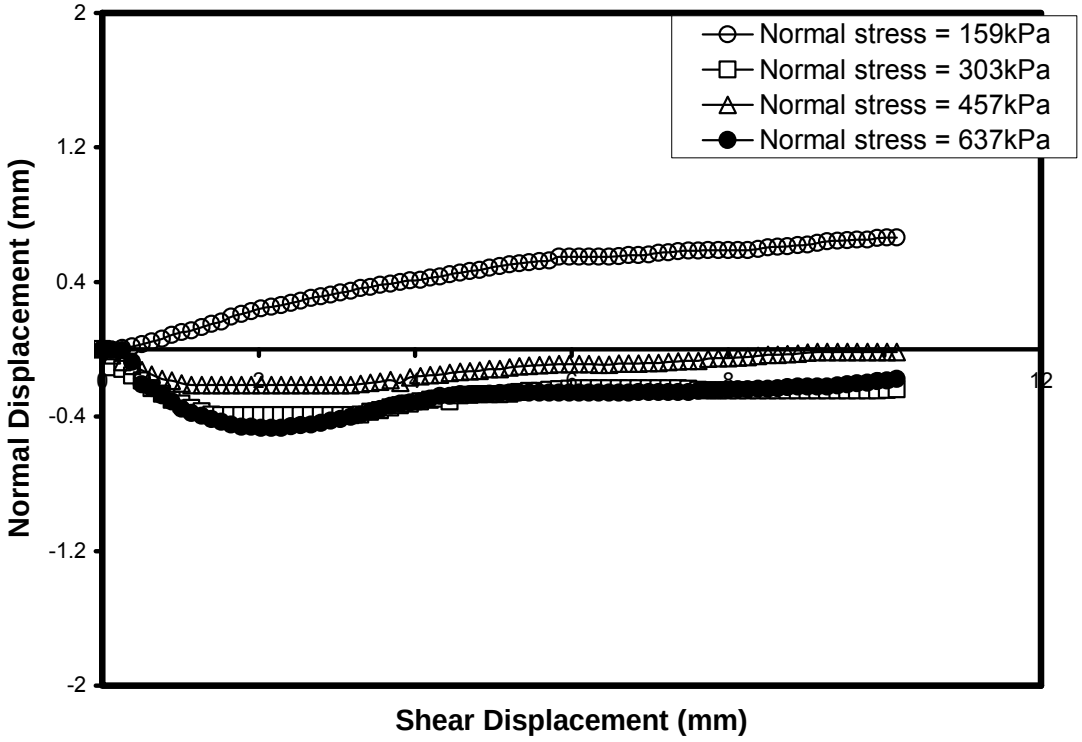

Figure 5.8. A plot of normal displacement vs shear displacement of an laboratory direct shear test (high normal load) for sample SSS-AAAF-0001 of Sugar Shack South

Figure 5.9 illustrates the Mohr-Coulomb failure envelope for the four tests conducted on the rock pile material. The figure indicates a peak friction angle of 45º and a post peak friction angle of 39º.

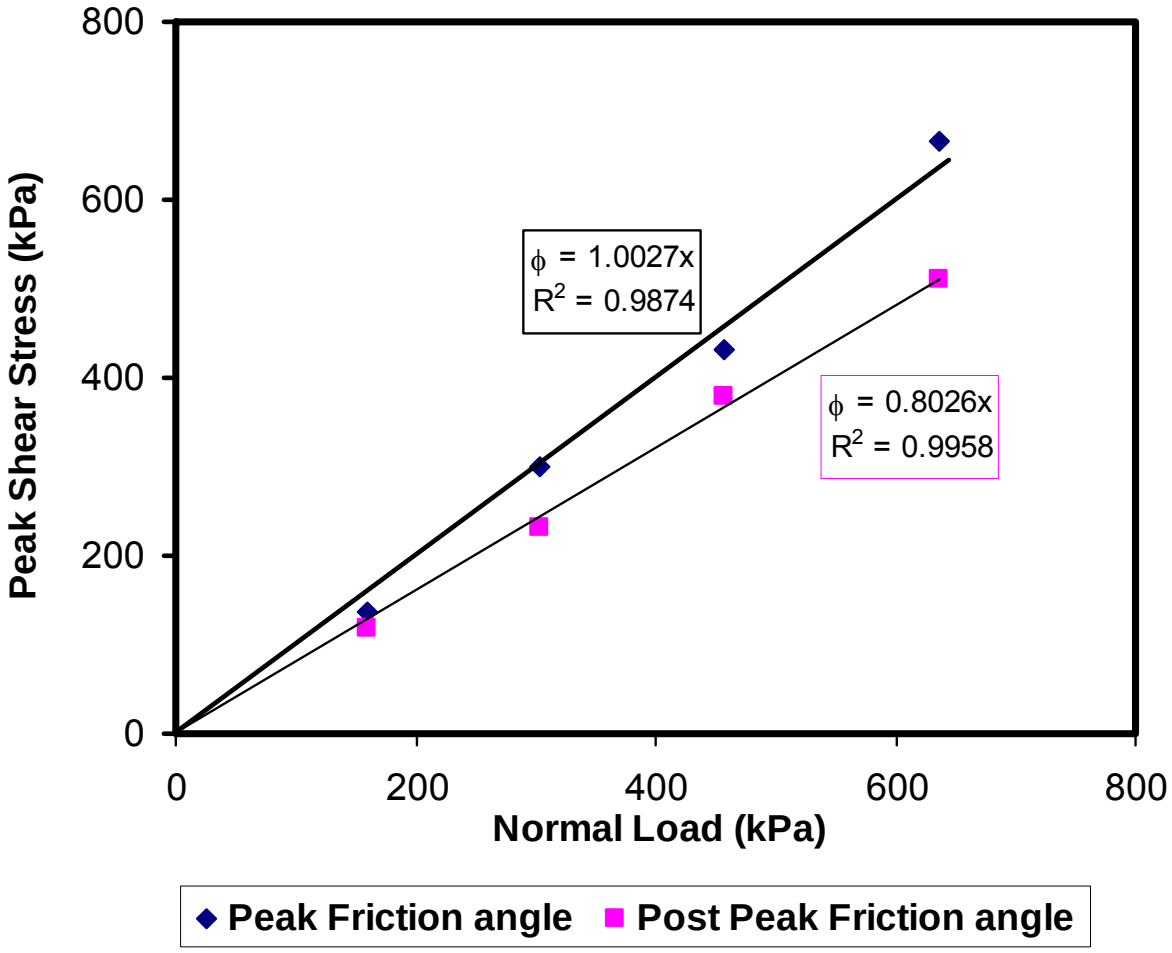

Figure 5.9. Mohr-Coulomb plot for high normal load laboratory direct shear test to determine friction angle (high normal load) for sample SSS-AAAF-0001 of Sugar Shack South

High normal stress peak friction angles ranged from 38° to 51°. The high normal stress post peak friction angles ranged from 35° to 41°. Tables 5.8 and 5.9 are the summary tables for the high normal load peak friction angles and the corresponding ultimate friction angles, respectively.

Table 5.8. Descriptive statistics of high normal load peak fiction angle for the fifty-two in situ direct shear test locations including four rock piles and two analogs

(High Normal Load-150 to 650 kPa) Laboratory Peak Friction Angle (^{o})							
Samples Location	**Maximum**	**Minimum**	**Mean**	**Median**	**Standard Deviation**	**Coeff. Of Variation (%)**	**Number of Samples**
Middle Rock Pile	44.4	38.8	41.3	41.0	2.8	6.8	4
Sugar Shack West	48.3	37.6	44.2	44.2	2.5	5.7	17
Spring Gulch Rock Pile	46.6	37.6	41.0	39.8	3.3	8.0	10
Sugar Shack South	47.8	41.8	44.5	44.5	1.9	4.3	8
Pit Alteration Scar	45.2	38.9	42.3	42.6	2.8	6.7	8
Debris Flow	50.5	42.4	46.0	42.2	3.4	7.4	5

Table 5.9. Descriptive statistics of high normal load post peak fiction angle for the fifty-two in situ direct shear test locations including four rock piles and two analogs.

(High Normal Load-150 to 650 kPa) Laboratory Post Peak Friction Angle (^{o})							
Samples Location	**Maximum**	**Minimum**	**Mean**	**Median**	**Standard Deviation**	**Coeff. Of Variation (%)**	**Number of Samples**
Middle Rock Pile	38.97	37.39	38.01	37.83	0.76	2.0	4
Sugar Shack West	41.22	36.18	38.53	38.57	1.34	3.5	17
Spring Gulch Rock Pile	38.97	35.00	37.09	37.33	1.35	3.6	10
Sugar Shack South	39.68	36.59	38.39	38.69	1.18	3.1	8
Pit Alteration Scar	38.66	35.66	37.63	37.82	1.04	2.8	8
Debris Flow	40.32	35.95	36.99	36.33	1.87	5.1	5

Direct shear tests with low normal stresses ranging from 20–120 kPa were conducted as well to simulate the stress condition at shallow depths of the rock piles. Note that the friction angles obtained from laboratory shear tests with low normal stresses should be comparable to the in situ friction angles as the range of the applied normal stresses are in close agreement.

Figures 5.10, 5.11, and 5.12 show typical results of shear tests on Sugar Shack South rock pile material at low normal stresses. All plots of low normal load laboratory direct shear test (20-120 kPa) results are presented in Appendix 4. Figure 5.10 shows the shear stress plotted versus the shear displacement. As expected, the shear stress corresponding to a fixed normal stress increases initially until it reaches the peak strength, which then reduces gradually towards its residual strength.

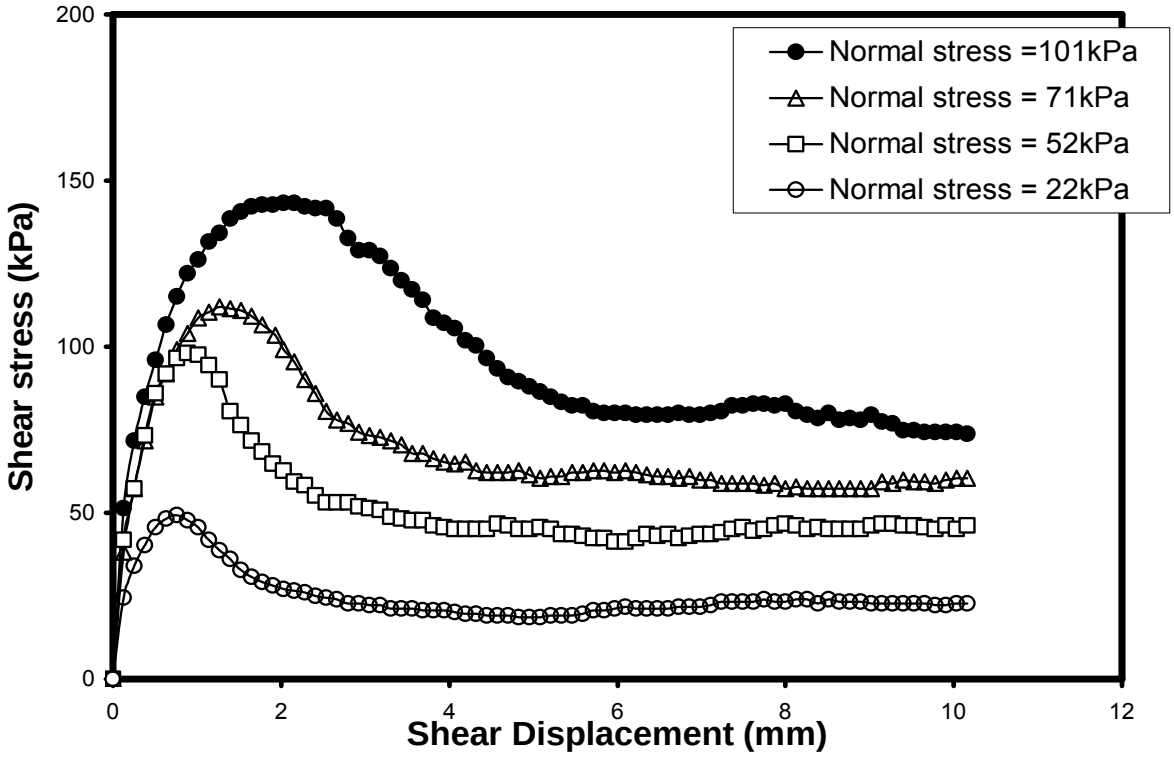

Figure 5.10. A plot of shear stress vs shear displacement of an in laboratory shear test (low normal load) for sample SSS-AAAF-0001 of Sugar Shack South

A plot of normal displacements against shear displacement is used to identify the dilation or contraction behavior of the material during the test. Positive displacements indicate dilation of the material (Figure 5.11).

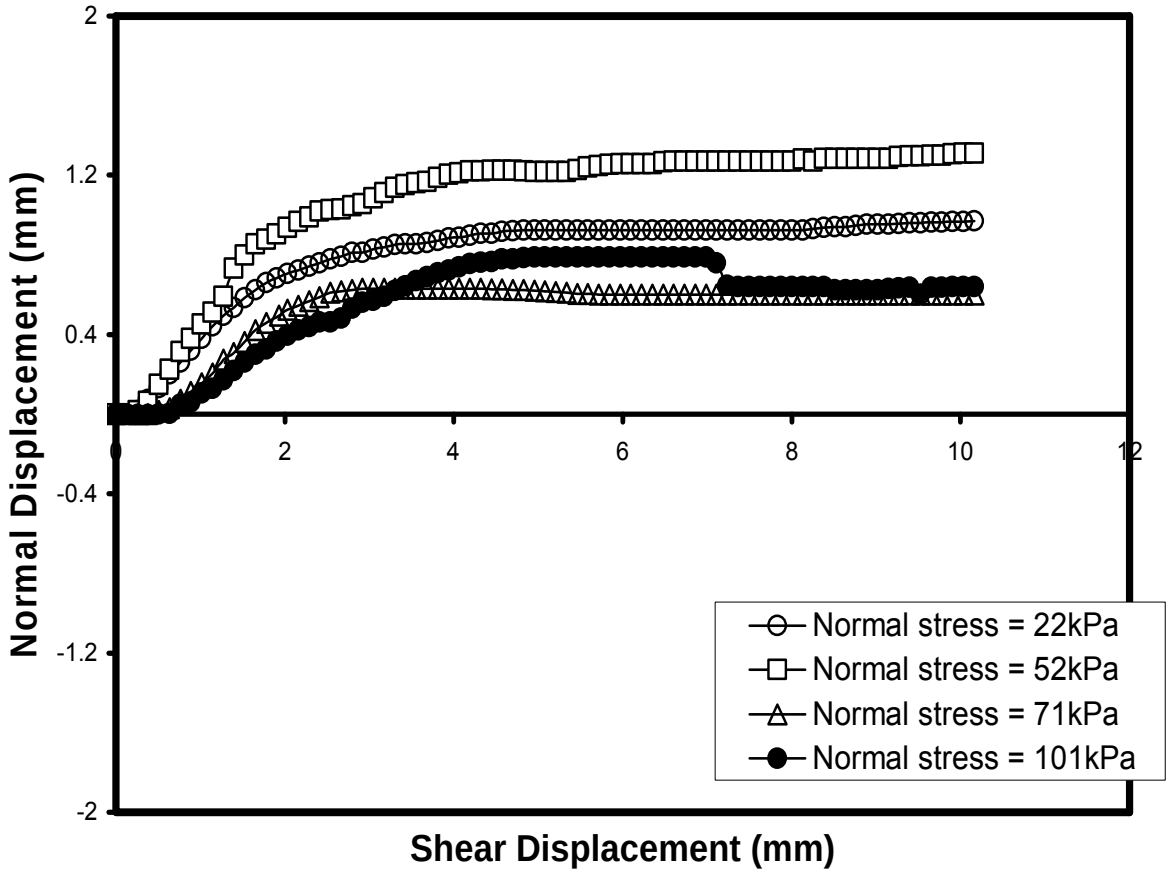

Figure 5.11. A plot of normal displacement vs shear displacement of laboratory shear tests using low normal stresses for sample SSS-AAAF-0001 of Sugar Shack South

Figure 5.12 illustrates the Mohr-Coulomb failure envelope for the three tests conducted on the rock pile material. The figure indicates a friction angle of 49º and apparent cohesion of 30 kPa for this material. The measured apparent cohesion is due to some existing moisture after air-drying the samples that causes induced suction. Note also that due to the reduction of normal load, there has been an increase in the friction angle (compare figures 5.9 and 5.12).

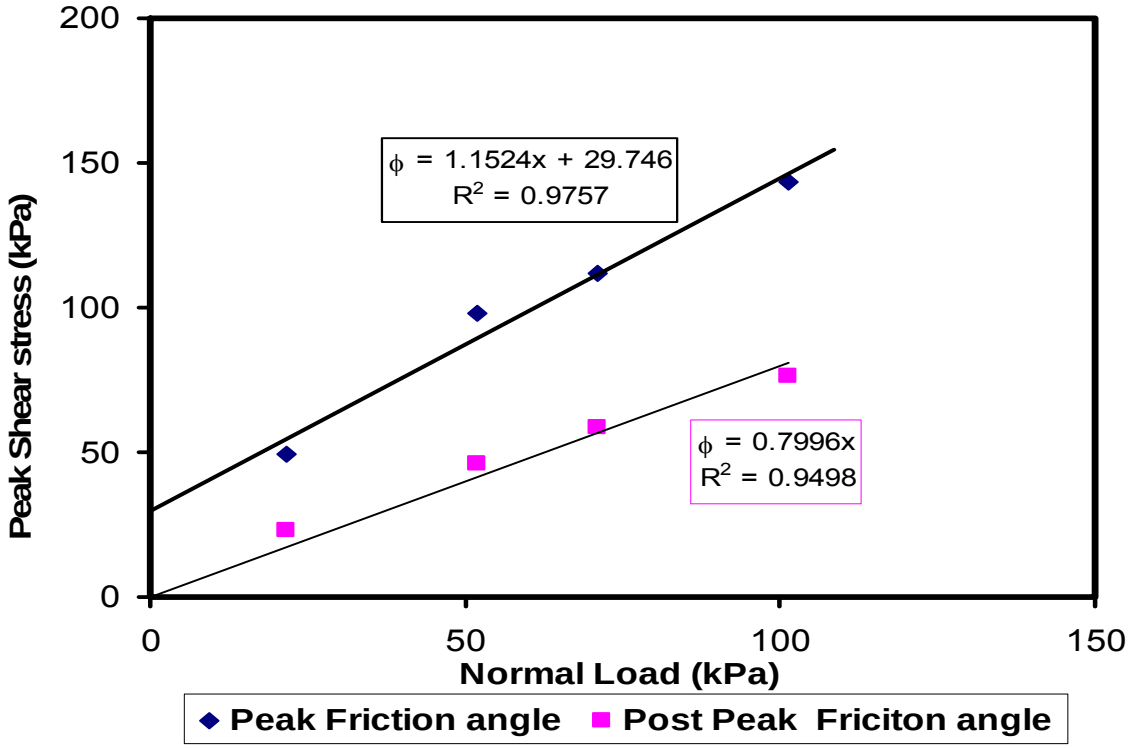

Figure 5.12. Mohr-Coulomb plot for low normal load for laboratory direct shear test to determine friction angle (low normal load) for sample SSS-AAAF-0001 of Sugar Shack South

The laboratory peak friction angles corresponding to the low normal stresses range from 38° to 56°. The corresponding ultimate friction angles range from 31° to 46°. The summary of the low normal load laboratory test statistical data is presented in Tables 5.10 and 5.11. Figures 5.13a and 5.13b show the histogram distribution of high normal load laboratory friction angles for rock piles and analogs, respectively. Figures 5.13c and 5.13d show the histogram distribution of low normal load laboratory friction angles for rock piles and analogs. Note that the cohesion values for in-situ shear tests were calculated using the Mohr-Coulomb failure envelope and friction angles that where obtained from laboratory shear tests with low normal stresses as the same range of normal stresses was used in the field.

Table 5.10 Descriptive statistics of low normal load peak fiction angle for the fifty-two in situ direct shear tests from four rock piles and two analogs

(Low Normal Load-20 to 120 kPa) Laboratory Peak Friction Angle (°)							
Samples Location	**Maximum**	**Minimum**	**Mean**	**Median**	**Standard Deviation**	**Coffe. Of Variation (%)**	**Number of Samples**
Middle Rock Pile	52.0	38.0	48.1	51.1	6.7	13.9	4
Sugar Shack West	56.0	43.0	49.2	48.2	3.8	7.7	17
Spring Gulch Rock Pile	50.2	42.3	46.7	47.3	2.9	6.2	10
Sugar Shack South	54.1	45.3	49.8	49.7	3.0	6.0	8
Pit Alteration Scar	51.1	42.0	47.2	47.5	3.2	6.7	8
Debris Flow	54.5	47.0	49.9	48.0	3.7	7.4	5

Table 5.11 Descriptive statistics of low normal load post peak fiction angle for the fifty-two in situ direct shear tests from four rock piles and two analogs.

(Low Normal Load-20 to 120 kPa) Laboratory Post Peak Friction Angle (°)							
Samples Location	**Maximum**	**Minimum**	**Mean**	**Median**	**Standard Deviation**	**Coffe. Of Variation (%)**	**Number of Samples**
Middle Rock Pile	43.3	38.8	41.4	41.7	2.3	5.6	4
Sugar Shack West	44.6	40.1	41.7	41.7	1.5	3.6	17
Spring Gulch Rock Pile	44.2	36.7	40.5	40.9	2.2	5.4	10
Sugar Shack South	44.6	38.0	40.7	41.0	2.2	5.4	8
Pit Alteration Scar	45.6	31.0	41.3	41.9	4.5	10.9	8
Debris Flow	43.0	41.2	42.1	42.1	0.8	1.9	5

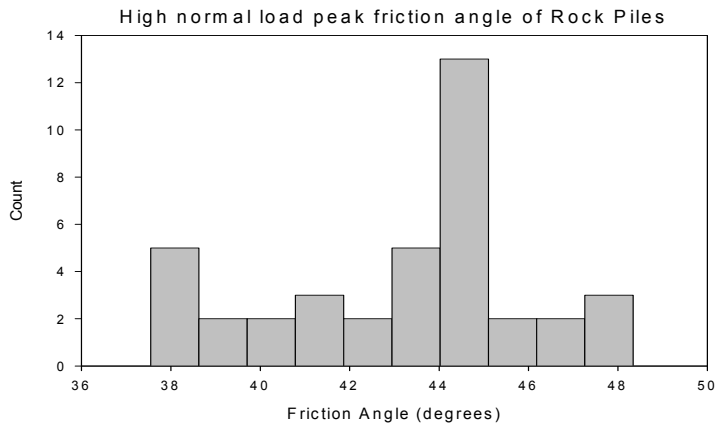

(a)

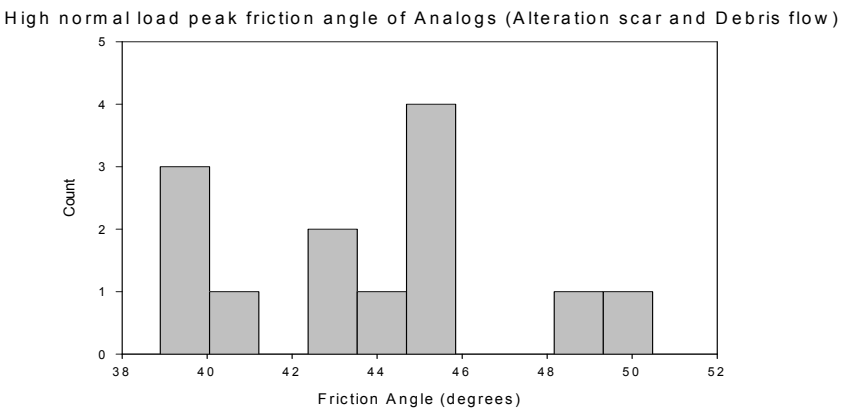

(b)

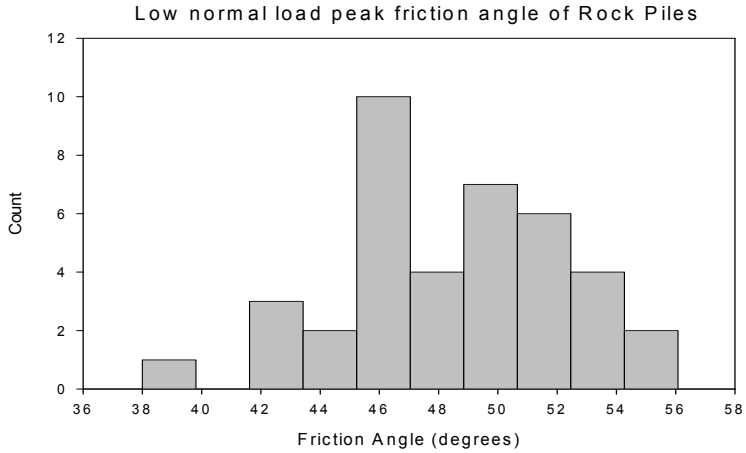

(c)

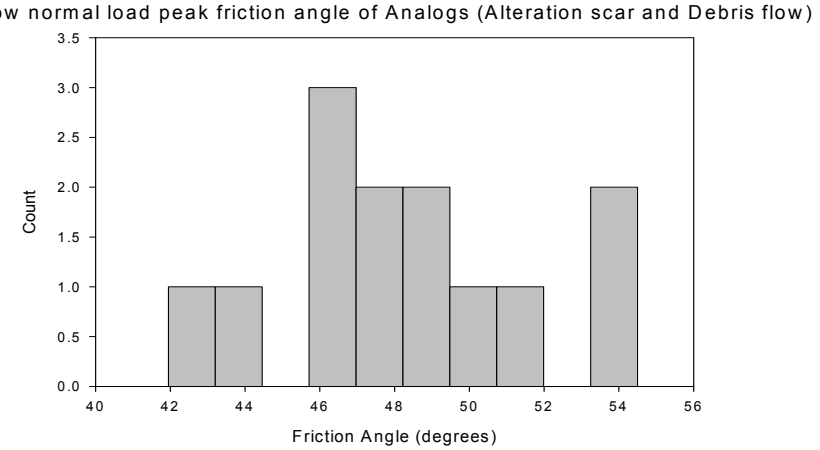

(d)

Figure 5.13. Histogram distribution of peak friction angles of rock piles and analogs.

Histogram plots clearly show that as expected as the normal stress increases the friction angle reduces.

Peak friction angle measurements have been made in other studies of the Questa rock piles as presented in chapter 2. Robertson GeoConsultants (2000) indicates a peak friction angle range of 41^o to 47^o. URS Corporation (2003) indicates a range of peak friction angle of 33^o to 49^o. Gutierrez (2006) performed laboratory direct shear tests on Goathill North rock pile samples reported a similar range of peak friction angle of 40^o to 47^o. These ranges of measured peak friction angles are similar to those reported in this thesis.

5.2.3 Atterberg Limits Results

Atterberg limits were obtained for the rock pile samples by performing the Atterberg limit tests. The liquid limits for the samples collected at the in situ shear tests locations range from 20 to 39 %. The plastic limits range from 13 to 31%. The plasticity indices of the samples range from 0 to 16%. Tables 5.12, 5.13 and 5.14 are summary results for the liquid limit, plastic limit, and plasticity index, respectively.

Table 5.12 Descriptive statistics of liquid limit tests collected from in situ shear tests locations including four rock piles and two analogs.

Liquid Limit (%)							
Samples Location	**Maximum**	**Minimum**	**Mean**	**Median**	**Standard Deviation**	**Coeff. Of Variation (%)**	**Number of Samples**
Middle Rock Pile	32	28	30	31	2	6	4
Sugar Shack West	39	25	31	30	5	2	17
Spring Gulch Rock Pile	26	20	24	22	3	1	10
Sugar Shack South	36	27	32	32	4	1	8
Pit Alteration Scar	36	28	33	35	3	9	8
Debris Flow	30	22	25	23	4	2	5

Table 5.13. Descriptive statistics of in situ plastic limits for the fifty-two in situ direct shear tests from four rock piles and two analogs

Plastic Limit (%)							
Samples Location	**Maximum**	**Minimum**	**Mean**	**Median**	**Standard Deviation**	**Coeff. Of Variation (%)**	**Number of Samples**
Middle Rock Pile	26	21	22	21	3	14	4
Sugar Shack West	26	14	22	23	3	14	17
Spring Gulch Rock Pile	26	13	19	17	5	26	10
Sugar Shack South	32	18	25	27	5	20	8
Pit Alteration Scar	24	17	21	22	3	14	8
Debris Flow	19	16	18	18	1	6	5

Table 5.14. Descriptive statistics of in situ plasticity index for the fifty-two in situ direct shear tests from four rock piles and two analogs

Plasticity Index							
Samples Location	**Maximum**	**Minimum**	**Mean**	**Median**	**Standard Deviation**	**Coeff. Of Variation (%)**	**Number of Samples**
Middle Rock Pile	11	2	8	10	4	50	4
Sugar Shack West	15	2	9	8	4	56	8
Spring Gulch Rock Pile	10	0	4	4	3	75	10
Sugar Shack South	11	7	9	9	1.	11	8
Pit Alteration Scar	19	5	12	12	5	42	8
Debris Flow	14	4	7	5	6	86	5

Figure 5.14 a and 5.14 b show the histogram distribution of liquid limit for rock piles and analogs respectively. Figure 5.14 c and 5.14 d show the histogram distribution of plastic limit for rock piles and analogs, respectively.

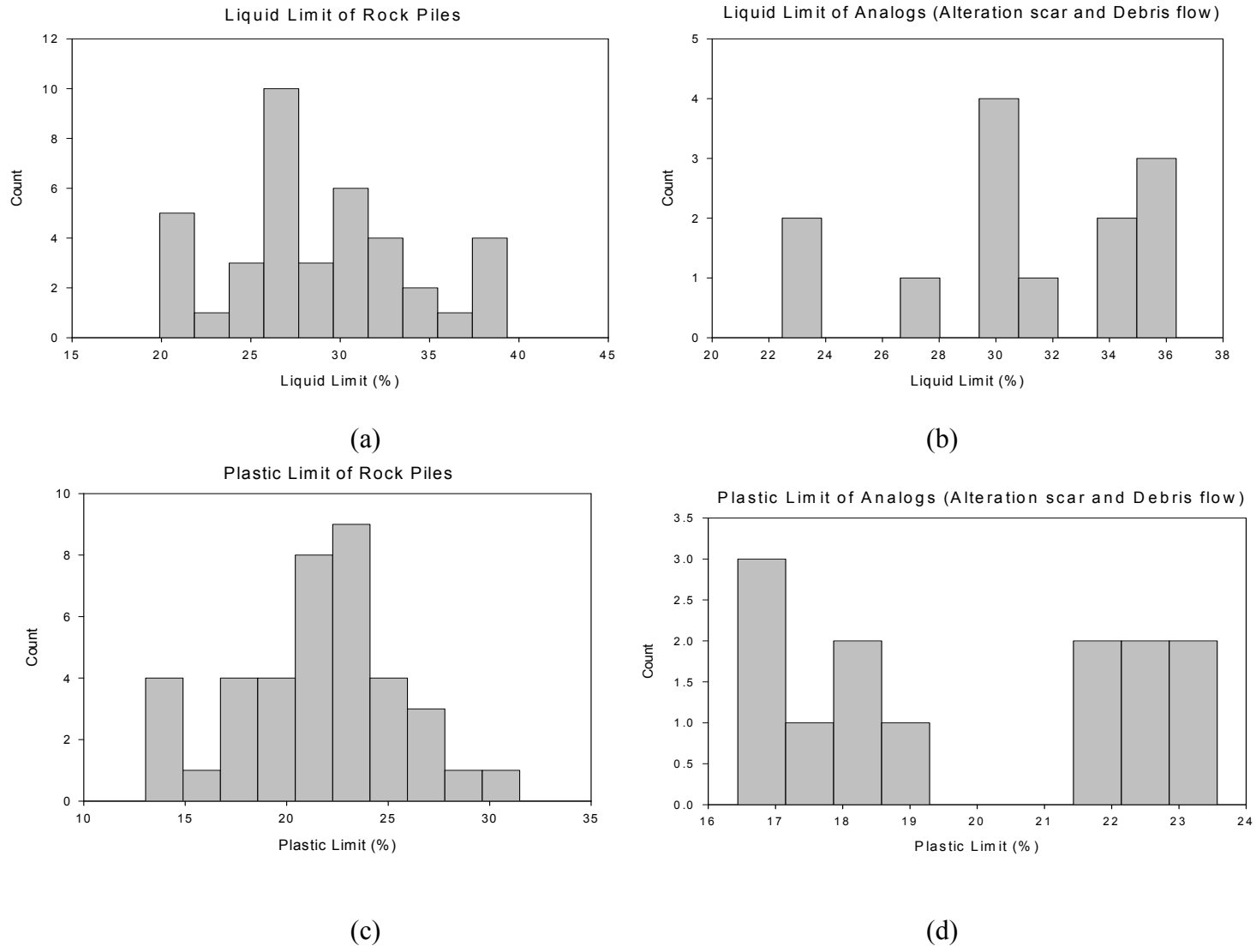

Figure 5.14. Histogram distribution of consistency limit data of rock piles and analogs

5.2.4 Particle Size Analysis

The tested soils range from a poorly graded gravel with some clay content (GP-GC) to a poorly graded sand with some clay content (SP-SC) based on the Unified Soil Classification System. The gravel content ranges from 80 to 33 % while the sand content ranges from 66 to 16 %. The fines (the percentage of particles passing the No. 200 sieve) range from 13 to 0 %. The summary of grain size distribution results is presented in Tables 5.15, 5.16, and 5.17.

Table 5.15. Descriptive statistics of in situ % gravel for the fifty-two in situ direct shear tests locations including four rock piles and two analogs.

Gravel (%)							
Samples Location	**Maxim-um**	**Minimum**	**Mean**	**Median**	**Standard Deviation**	**Coeff. Of Variation (%)**	**Number of Samples**
Middle Rock Pile	54	33	43	43	11	27	4
Sugar Shack West	71	38	56	58	10	18	17
Spring Gulch Rock Pile	70	43	56	55	9	16	10
Sugar Shack South	74	45	61	63	9	14	8
Pit Alteration Scar	71	52	62	63	7	12	8
Debris Flow	80	46	64	65	14	22	5

Table 5.16. Descriptive statistics of in situ % sand for the fifty-two in situ direct shear tests from four rock piles and two analogs

Sand (%)							
Samples Location	**Maximum**	**Minimum**	**Mean**	**Median**	**Standard Deviation**	**Coeff. Of Variation (%)**	**Number of Samples**
Middle Rock Pile	66	45	56	56	12	5.80	4
Sugar Shack West	61	28	41	40	9	2.22	8
Spring Gulch Rock Pile	55	24	38	38	9	2.84	10
Sugar Shack South	53	20	36	36	10	3.55	8
Pit Alteration Scar	45	22	32	29	9	3.26	17
Debris Flow	54	16	33	35	16	7.07	5

Table 5.17. Descriptive statistics of in situ % fines for the fifty-two in situ direct shear tests from four rock piles and two analogs

Fine (%)							
Samples Location	**Maximum**	**Minimum**	**Mean**	**Median**	**Standard Deviation**	**Coeff. Of Variation (%)**	**Number of Samples**
Middle Rock Pile	2	0	1	1	1	0.42	4
Sugar Shack West	14	0	3	1	5	1.12	8
Spring Gulch Rock Pile	9	1	6	6	3	0.81	10
Sugar Shack South	7	1	3	2	2	0.75	8
Pit Alteration Scar	9	2	6	7	2	0.85	8
Debris Flow	6	0	2	1	3	1.11	5

Figures 5.15 a and 5.15 b show a histogram distribution plot for percent fine of the rock piles and analogs, respectively

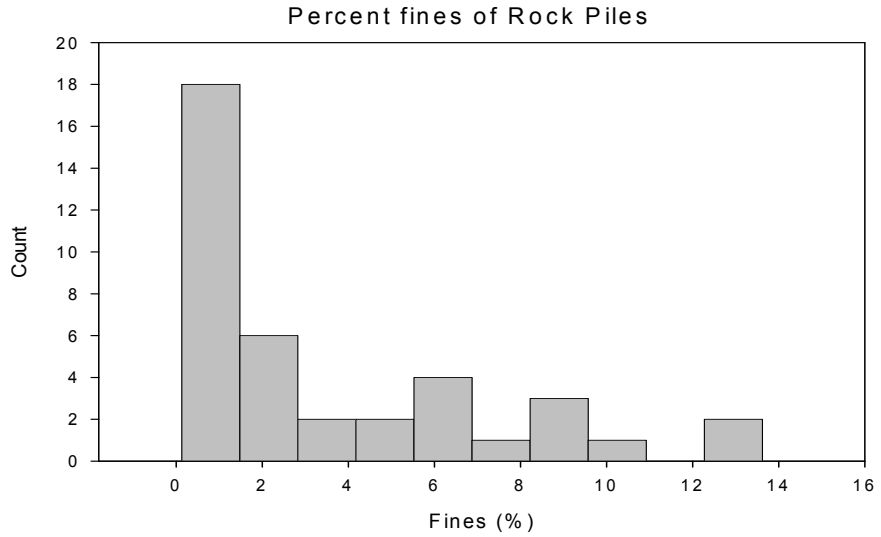

(a)

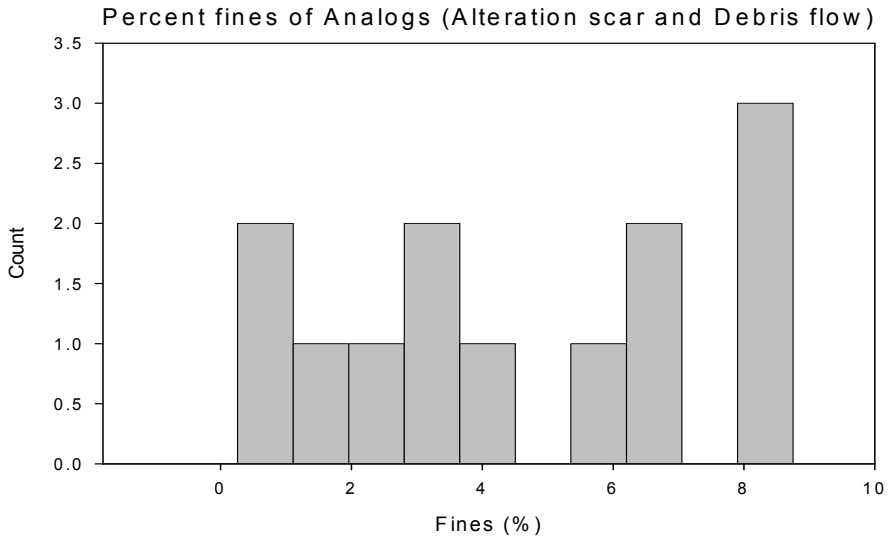

(b)

Figure 5.15. Histogram distribution of % fines data of rock piles and analogs.

Robertson GeoConsultants (2000), URS Corporation (2003), Norwest Corporation (2004, 2005), and Gutierrez (2006) reported similar ranges of percent gravel, sand and fine in their publications after studying Questa rock piles. Figure 5.16 shows the

gradation curves of the rock-pile materials and literature (Li ,1999; Savci and Williamson, 2002; Stormont and Farfan, 2005). Note that the gradation curves from the in situ tests locations fall approximately within the literature range.

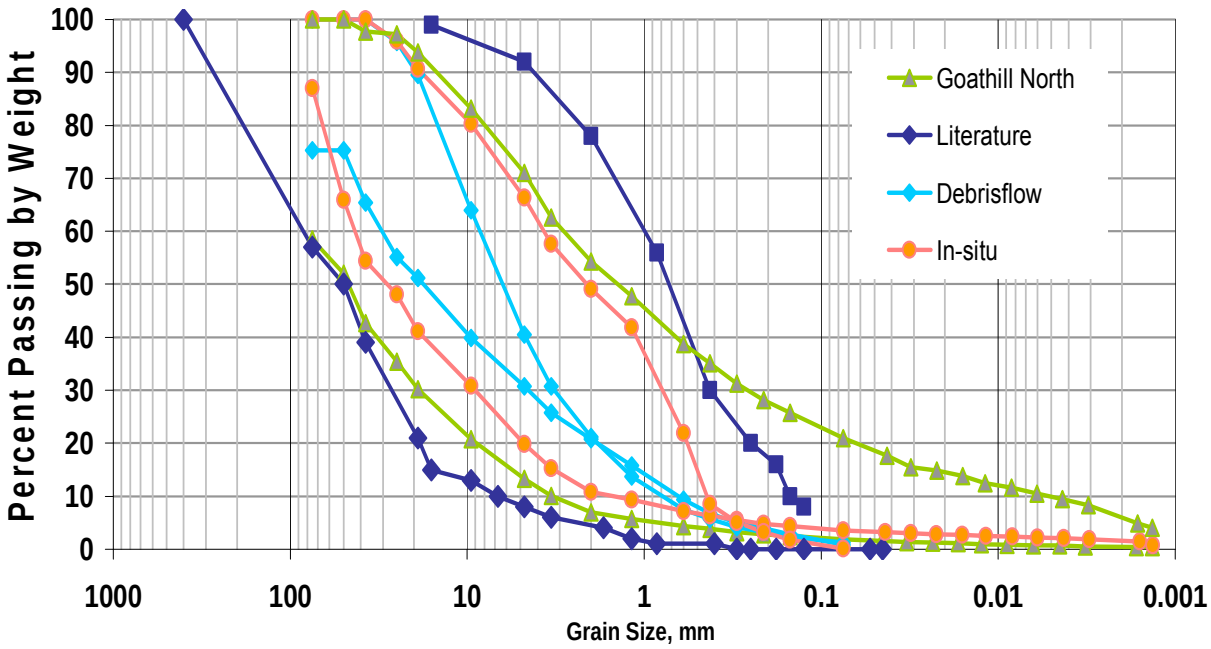

Figure 5.16. Ranges of gradation curves of the rock pile materials collected from the locations where in situ shear tests were conducted and those reported in the literature.

5.2.5 Specific Gravity

Specific gravity measurements were performed on all samples collected from the in situ direct shear test sites. The material used for the test was first passed through the No. 4 sieve. Each sample was between 100 to 110 grams according to ASTM and

standard operating procedure. The measured specific gravity was between 2.89 to 2.70 for the samples tested. Table 5.18 is a summary of the specific gravity results analyzed statistically. Specific gravity measurements have been made in other studies of the Questa rock piles. Robertson GeoConsultants (2000) indicated a range in specific gravity between 2.44 and 3.04. URS Corporation (2003) indicated a range of 2.34 and 3.04 and an average of 2.81 for the rock pile material. The Norwest Front Rock Pile Report (Norwest, 2005) indicated a range in specific gravity between 2.1 and 2.7 and an average of 2.59 for rock piles material and a range between 2.10 and 2.63 with an average of 2.49 for the alteration scar material. Figures 5.17 a and 5.17 b show a histogram distribution plot for specific gravity of the rock piles and analogs respectively.

Table 5.18. Descriptive statistics of in situ specific gravity for the fifty-two in situ direct shear tests from four rock piles and two analogs

Specific Gravity							
Samples Location	**Maximum**	**Minimum**	**Mean**	**Median**	**Standard Deviation**	**Standard Error**	**Number of Samples**
Middle Rock Pile	2.83	2.70	2.74	2.73	0.05	0.02	5
Sugar Shack West	2.85	2.70	2.78	2.79	0.06	0.01	17
Spring Gulch Rock Pile	2.79	2.70	2.74	2.75	0.03	0.01	10
Sugar Shack South	2.89	2.75	2.82	2.82	0.05	0.02	8
Pit Alteration Scar	2.84	2.70	2.76	2.75	0.06	0.02	8
Debris Flow	2.74	2.70	2.71	2.70	0.02	0.01	5

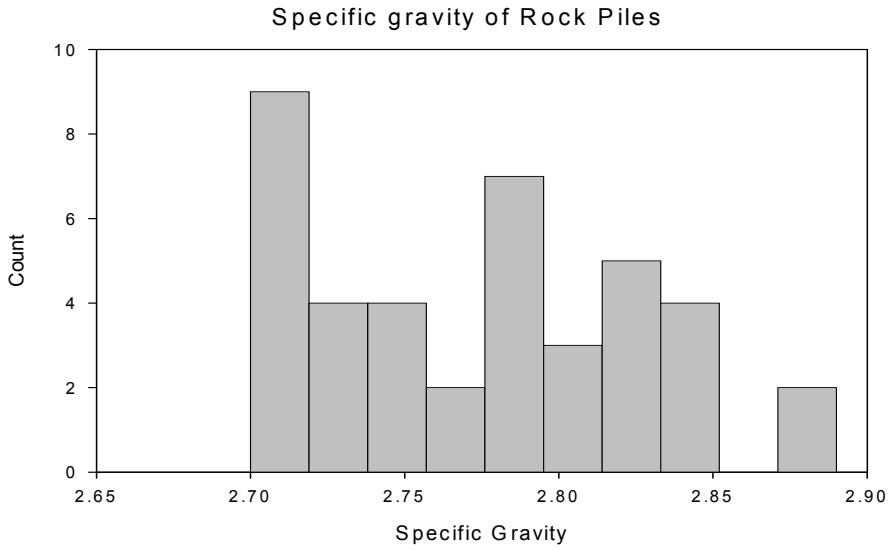

(a)

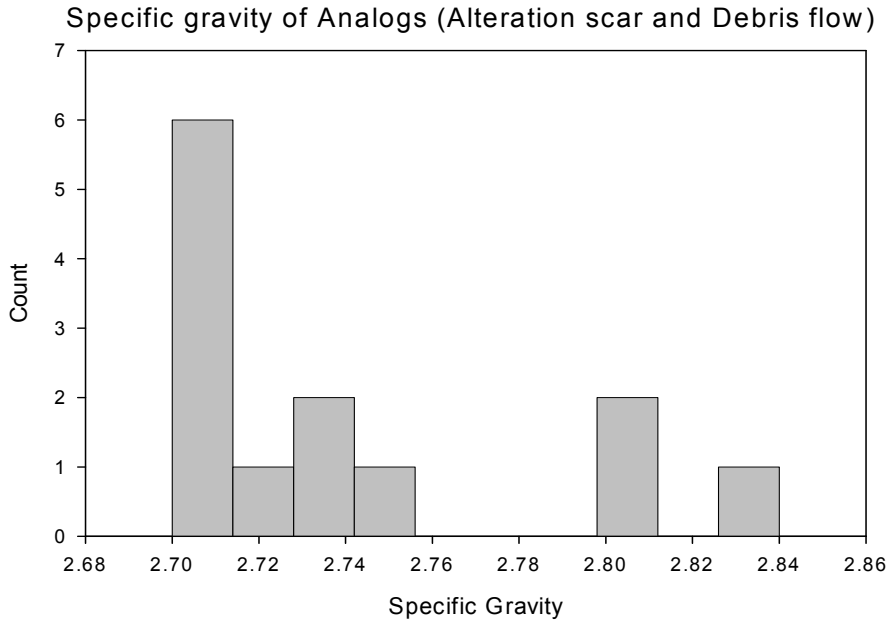

(b)

Figure 5.17. Histogram distribution of specific gravity data of rock piles and analogs

6. DISCUSSION

6.1 Introduction

The results obtained for in situ and laboratory tests will be discussed in this section. Comparison of results with literature is presented. The effect of weathering, index parameters, mineralogy and chemistry of the rock piles and analogs materials on cohesion is investigated.

6.2 Comparison of in situ and laboratory results with previous studies and literature

The natural analogs have been subjected to weathering for a much longer time compared to the rock piles (Campbell and Lueth, 2008). Nevertheless, histogram plot analysis of the rock piles and the analogs indicate not much of a difference in some of their geotechnical properties. Note that some variation exists between the cohesion values of rock piles and analogs; the cohesion values evaluated for the analogs are higher as compared with those for the rock piles.

The overall geotechnical results of this research work are comparable with published values. Williams (2000) reported that mine rock piles with side slopes are formed at the angle of repose in the range of 35º to 40º. He also noted that waste rock friction angle ranges between 40º to 50º after studying a number of mine rock piles in Australia. The measured peak friction angles of this study fall within this range. The rock materials at Questa are volcanic igneous rocks, which do not weather as fast as coal-bearing sedimentary formations.

Williams (2000) indicated that the density of mine rock piles ranges from 1.6 to 2.2 t/m^3 depending on whether the material has undergone compaction or not. The rock piles and analogs in question have been subjected to gravitational compaction and the generation of some fines filling the voids accounting for the high measured densities. The measured densities are similar to the range reported by Williams (2000). He also reported that the natural water content of mine rock piles typically ranges from 3% to 7%. The measured water content of the four Questa rock piles and natural analogs ranges from 1% to 15%. Rock pile index properties and shear strength parameters from around the world are summarized in Tables 6.1 and 6.2. These rock pile data do not include those of this study, but give the range of other measured data from around the world and can be compared with our measured parameters. All measured parameters for our rock piles and analogs falls with the range reported in Tables 6.1 and 6.2.

Table 6.1. Rock pile geotechnical properties around the world (V. T. McLemore written communication 12/08/2007)

Mine	Mine rock material	USCS soil group	Paste pH	Dry Density g/cc	Specific gravity	LL	PL	PI	Porosity %	Moisture Content %	References
Tyrone, NM (heap leach)	Porphyry, granite	GC, GW-GC, SC	2.07-4.27	2.64-2.78		28-40	15-18	8-23			Earley et al. (2003)
Davis mine, Mass.	Schist, quartzite			2.65					35-55		Adams et al. (2007)
Heath Steele, New Bruswick	Greenschist metamorphic rocks			2.35							Nolan, Davis and Assoc., Lmt. (1991)
Stratmat, New Bruswick	Greenschist metamorphic rocks		4.1-9.4	2.64-3.25					26.4		Li (1999)
Ajo, Arizona	Volcanic rocks, monzonite			1.61-2.06						0.5-7	Savci and Williamson (2002)
Bonner, CO		GP-GM		1.65 (in situ)						6-10	Stormont and Farfan (2005)
Golden Sunlight, Montana	Latite and diameter breccia pipe	SW, GP, GW	2.3-6.1	1.5-2.1	2.63-2.78				22.1-33.5	4-39	Herasymuik (1996), Azam et al. (2006)
Central Pit, Turkey	Sedimentary rocks	GC				35	24	11			Kasmer and Ulusay (2006)

Lignite Creek, Alaska	Sedimentary rocks	SM		1.5		19-20	15-18	2-4			Kroeger et al. (1991)
Aberfan, England	Sedimentary rocks			1.60-1.94	2.1						Lucia (1981)
Equity			3.54-7.05								Saretzky (1998)
Kidston, Australia					2.65				40		Bews et al. (1997)
Midnight (South Spoils)					2.75-2.84	19-52		1-29			URS Corp. (2003)
Lichtenberg pit, Germany				2.1	2.75				24		Hockley et al. (2003)
Yorkshire coal mine	Coarse discard			1.5-1.9	2.04-2.63	23-44	16-25			8-13.6	Bell (1996)
Brancepath coal mine	Coarse discard			1.06-1.68	1.81-2.54	23-42	Non-35			5.3-11.9	Bell (1996)
Wharncliffe coal mine	Coarse discard			1.39-1.91	2.16-2.61	25-46	14-21			6-13	Bell (1996)
Bogdanka coal mine, Lubelskie, Poland	5 yrs old 7 yrs old 8 yrs old			1.95 1.69 1.75						11-14 15-19 21	Filipowicz and Borys (2005)

Table 6.2. Distribution of particle size of rock piles around the world (V. T. McLemore written communication 12/08/2007)

Mine	% Cobbles	% Gravel	% Sand	% Fines	% Silt	% Sand	Reference
Stratmat, New Brunswick	10	70	20	0			Li (1999)
Ajo, Arizona	5	67	20	8	7	1	Savci and Williamson (2002)
Aitik, Sweden Cu	6	45	34	15			URS Corp. (2003)
Midnight, Washington U		50-65	21-43	11-29			URS Corp. (2003)
Bonner, Colorado		70	21	10	8	2	Stormont and Farfan (2005)
Kidston, Australia Au	30	37	30	3			URS Corp. (2003)
Morenci, Arizona		50-56	30-34	10-20			URS Corp. (2003)
Lichtenberg pit, Germany		5.6	52.6	41.8	16.5	25.3	Hockley et al. (2003)

6.3 Correlation between Index parameters and Shear Strength Parameters

The main purpose for performing in situ direct shear tests was to measure the rock-pile cohesion in order to investigate the intensity of cementation between particles. In this section the correlation between cohesion of rock pile materials with index parameters are investigated. The index parameters investigated are water content, dry

density, liquid limit, plastic limit, plasticity index, percent gravel, percent sand, percent fine and matric suction. Pearson correlation of the data obtained using the WinSTAT program indicates that there is no strong linear correlation between index parameters and cohesion. Table 6.3 shows the results of the Pearson correlation analysis using WinSTAT indicating the correlation between two parameters (Fig. 6.1-6.5).

Table 6.3. Pearson correlation results for index parameters analysis.

		Water Content (%)	**Dry Density (kg/m3)**	**Matric Suction (kPa)**	**Liquid Limit (%)**	**Plastic Limit (%)**	**Plasticity Index (%)**	**% of Gravel**	**% of Sand**	**% of Fines**
Cohesion (kPa)	**Linear Correlation (R2)**	-0.21	-0.20	***0.62***	0.03	-0.17	0.24	0.30	-0.21	-0.23
	Number of samples	22	24	23	24	24	24	24	24	24

6.3.1 Correlation of Plasticity Index with Cohesion

The influence of plasticity index on the cohesion was investigated and is shown in Figure. 6.1 which suggests no significant correlation between cohesion and plasticity index.

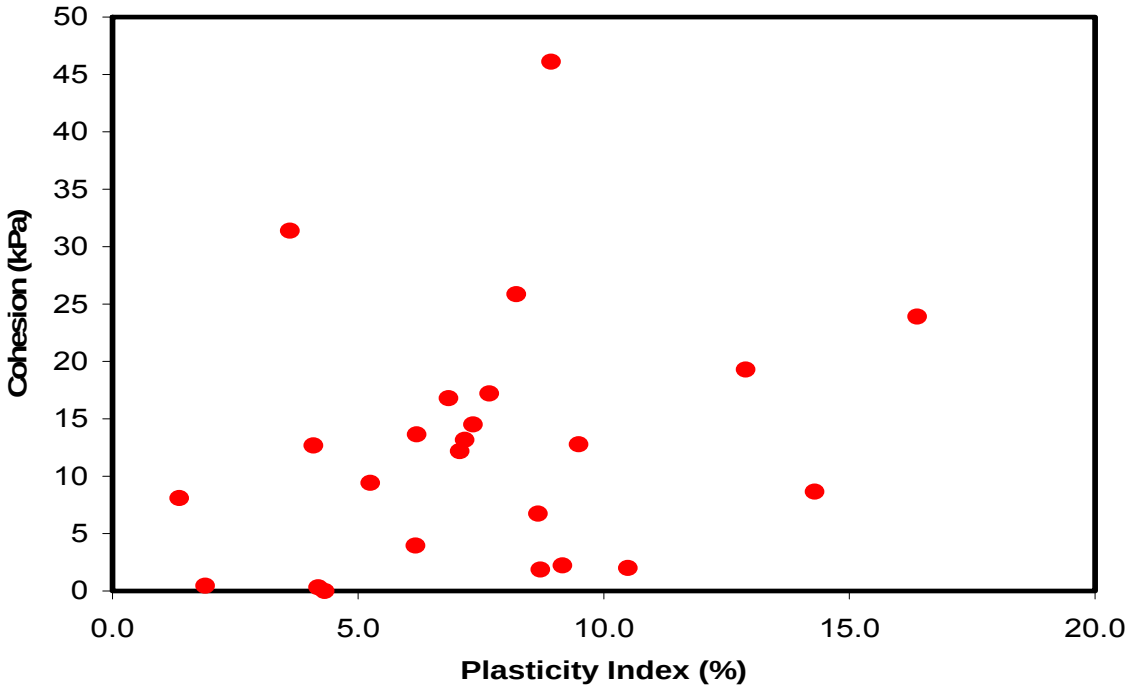

Figure 6.1. Correlation between cohesion and plasticity index.

6.3.2 Correlation of Dry Density with Cohesion

Figure 6.2 shows a plot of cohesion with dry density. There is no correlation between dry density and cohesion. This indicates that the cohesion measured in the field is not a result of gravitational compaction of the material alone. In general, gravitational compaction of materials can have some influence on the cohesion but other controlling factors are involved as well. Note also that the in-situ tests were conducted at shallow depths within the rock piles where the compaction effects are minimal.

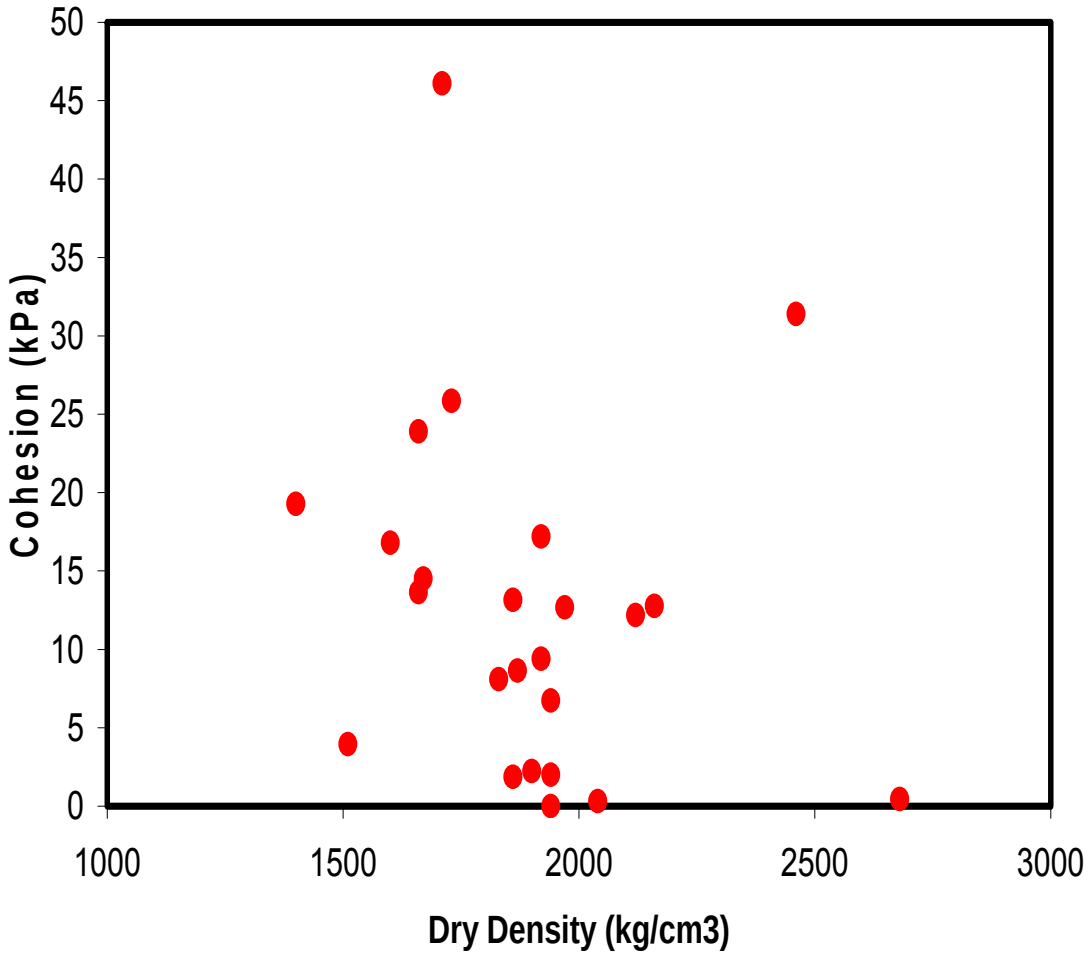

Figure 6.2. Correlation of cohesion with dry density.

6.3.3 Correlation of Percent fines with Cohesion

The influence of percent fines on the cohesion was investigated and is shown in Figure 6.3, which suggests little correlation between cohesion and percent fines. The lower cohesion values tend to correlate with higher %fines, but some samples with lower cohesion also have low %fines.

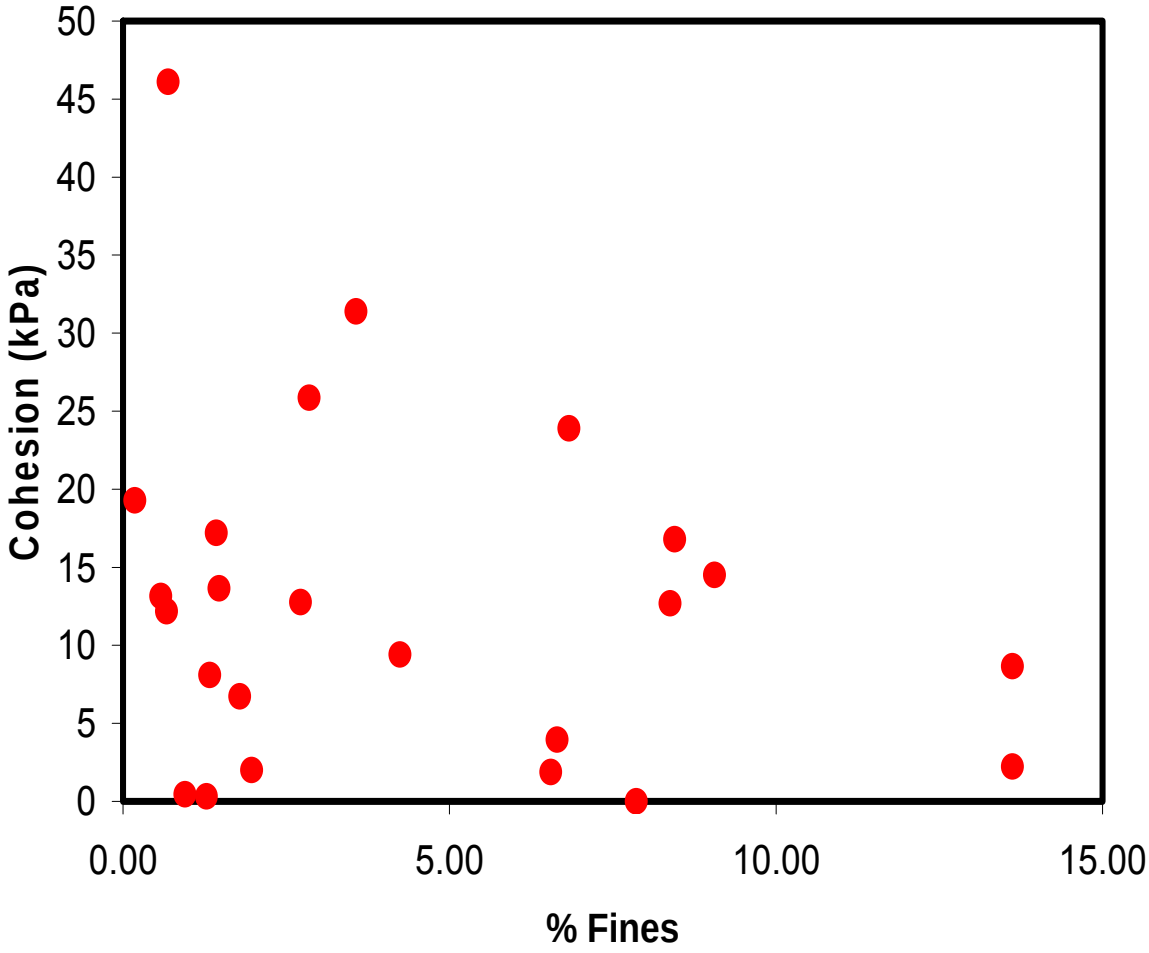

Figure 6.3. Correlation of cohesion with percent fines.

6.3.4 Correlation of Cohesion with Matric Suction and Water Content

To see the correlation between the measured cohesion and matric suction, a plot of the two parameters was generated (Figure 6.4).

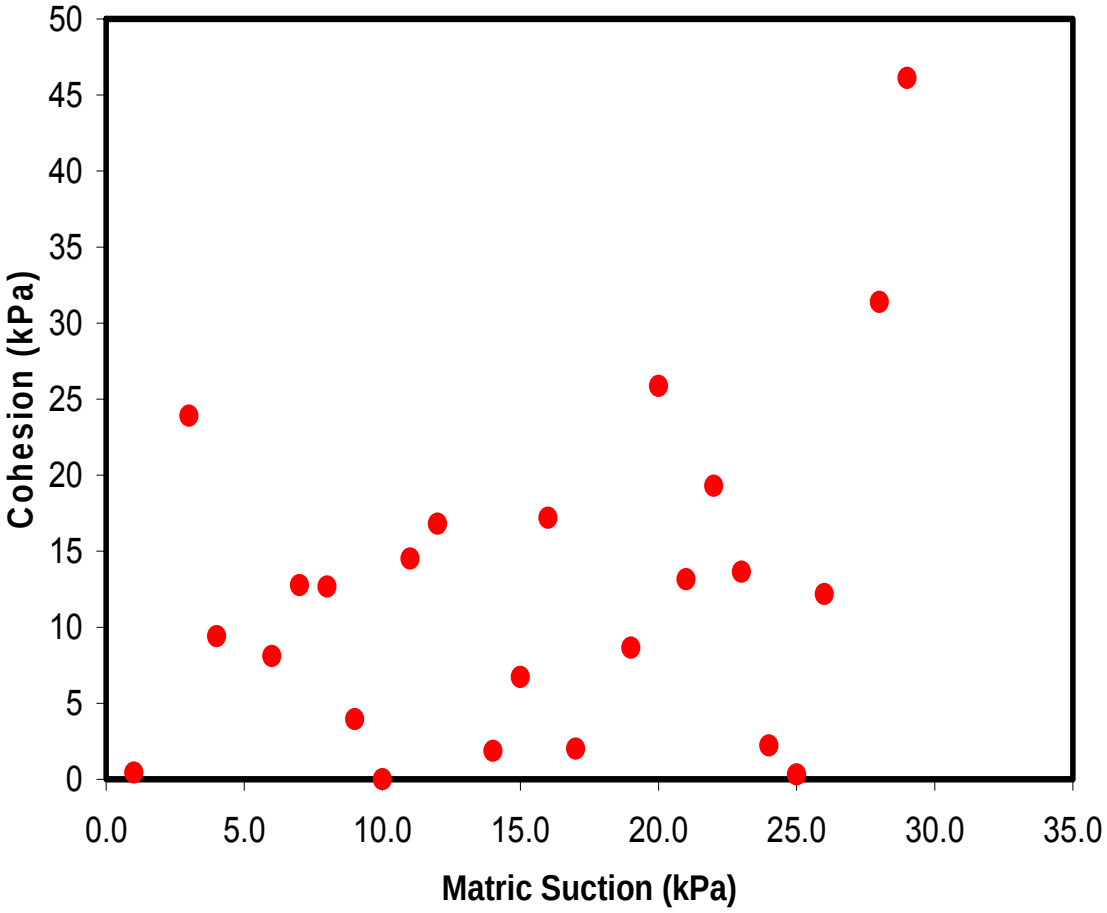

Figure 6.4. Correlation of cohesion with matric suction

Figure 6.4 shows a weak positive correlation between cohesion and matric suction. This can indicate that the measured cohesion is only partly due to the existing negative pore water pressure within the rock pile and analog samples. Figure 6.5 shows a plot of cohesion vs. water content. This plot shows a slight negative correlation between cohesion and water content that is consistent with the plot in Fig. 6.4.

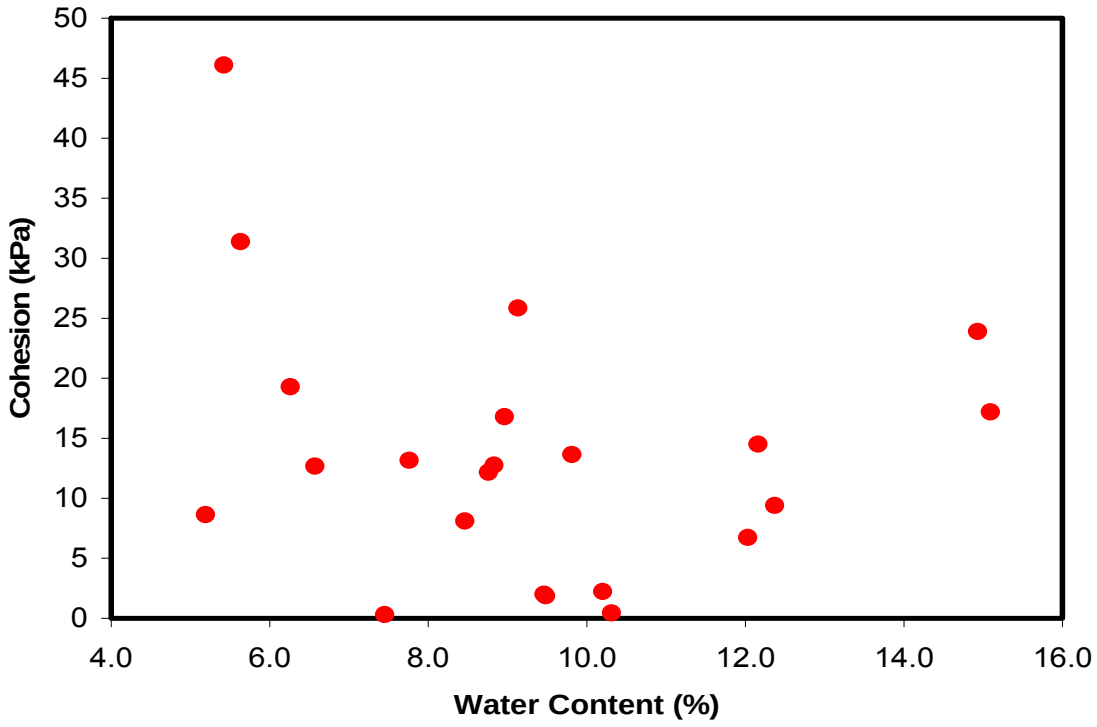

Figure 6.5. Correlation of cohesion with water content

6.4 Effect of Mineralogy on Shear Strength Parameters

Coduto (2001) indicates that cementation by cementing agents, electrostatic and electromagnetic attraction hold soil particles together, and adhesion that occurs in overconsolidated clays are the prime indicators of existing cohesion. Cementing agents that exists within Questa rock piles and analogs are gypsum, jarosite, iron oxides, and pre-existing clay minerals. The effect of pre-existing clay minerals on cohesion is investigated. These existing clays are hydrothermal clays and are not weathered clays (K. Donahue, written communication, September 2007). The analyses were performed for only those in situ direct shear tests locations where the largest particle size in the soil block was smaller than one-fifth of the width of the shear box. Pearson correlation of the

data obtained using WinSTAT program indicates that there is no to weak linear correlation between specific minerals and cohesion. Table 6.4 shows the results of the statistical analysis using WinSTAT indicating the correlation between two parameters (Fig. 6.6-6.13). Table 6.4 shows Pearson correlation results for mineralogical analysis. Pearson correlation of the data obtained using WinSTAT program between cohesion and chemistry indicates that there is weak to no linear correlation between specific elements and cohesion. Table 6.5 shows the results of the statistical analysis using WinSTAT indicating the weak to no linear correlation existing between two parameters. Detail results of mineralogy and chemistry are presented in Appendix 3.

Table 6.4 Pearson correlation results for mineralogy analysis.

		Quartz	**K-spar/orthoclase**	**Plagioclase**	**illite**	**Chlorite**	**Smectite**	**Kaolinte**	**Epidote**
Cohesion (kPa)	**Linear Correlation (R2)**	0.15	-0.09	-0.08	-0.14	-0.47	0.06	0.30	-0.51
	Number of Variables	23	23	17	23	13	23	23	9
		Pyrite	**Calcite**	**Gypsum**	**Detrit Gypsum**	**Auth Gypsum**	**Zircon**	**Fluorite**	**Jarosite**
Cohesion (kPa)	**Linear Correlation (R2)**	-0.24	-0.12	0.03	-0.12	-0.42	0.19	-0.99	0.10
	Number of Variables	23	23	9	9	11	21	3	20
		Fe oxide	**Rutile**	**Apatite**	**Pyrite+Calcite+Epidote**	**Gyp+Jarosite+Fe oxide**	**Gypsum+ Jarosite**		
Cohesion (kPa)	**Linear Correlation (R2)**	-0.13	-0.03	-0.259	-0.23	-0.05	-0.01		
	Number of Variables	23	23	18	24	24	24		

Table 6.5 Pearson correlation results for chemical analysis.

		SiO2	TiO2	Al2O3	Fe2O3T	FeOT	MnO	MgO		
Cohesion (kPa)	Linear Correlation (R2)	0.05	0.01	-0.07	-0.06	-0.06	-0.26	-0.093		
	Number of Variables	24	24	24	24	24	24	24		
	Cohesion (kPa)	CaO	Na2O	K2O	P2O5	S	SO4	C	LOI	
Cohesion (kPa)	Linear Correlation (R2)	-0.13	-0.03	0.03	0.01	-0.49	0.05	0.43	0.07	
	Number of Variables	24	24	24	24	23	23	23	24	

Note that Gutierrez (2006) reported that there is little or no correlation between friction angle and mineralogical changes on the Questa rock pile after studying the Goathill north rock pile. However, Gutierrez (2006) and Gutierrez et al. (2008) did show a correlation between friction angle and chemical weathering indices based upon the whole rock geochemistry, similar to that reported in Table 6.5. These chemical weathering indices were not used in this report.

6.4.1 Correlation of percent gypsum with Cohesion

Figure 6.6 shows little correlation between cohesion and percent gypsum . Low cohesion values correspond with low gypsum values but not all low cohesion values correspond with low gypsum values which supports the observation that cohesion existing within the rock piles and analogs, is not controlled by only one mineral. Figure 6.7 show no correlation between sulfate and cohesion.

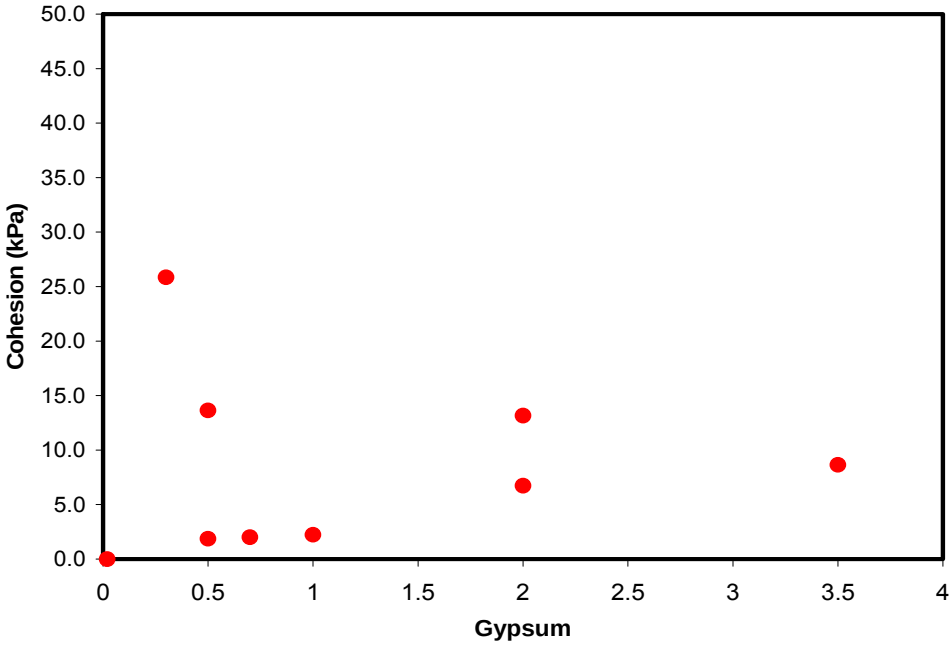

Figure 6.6. Correlation of cohesion with percent gypsum.

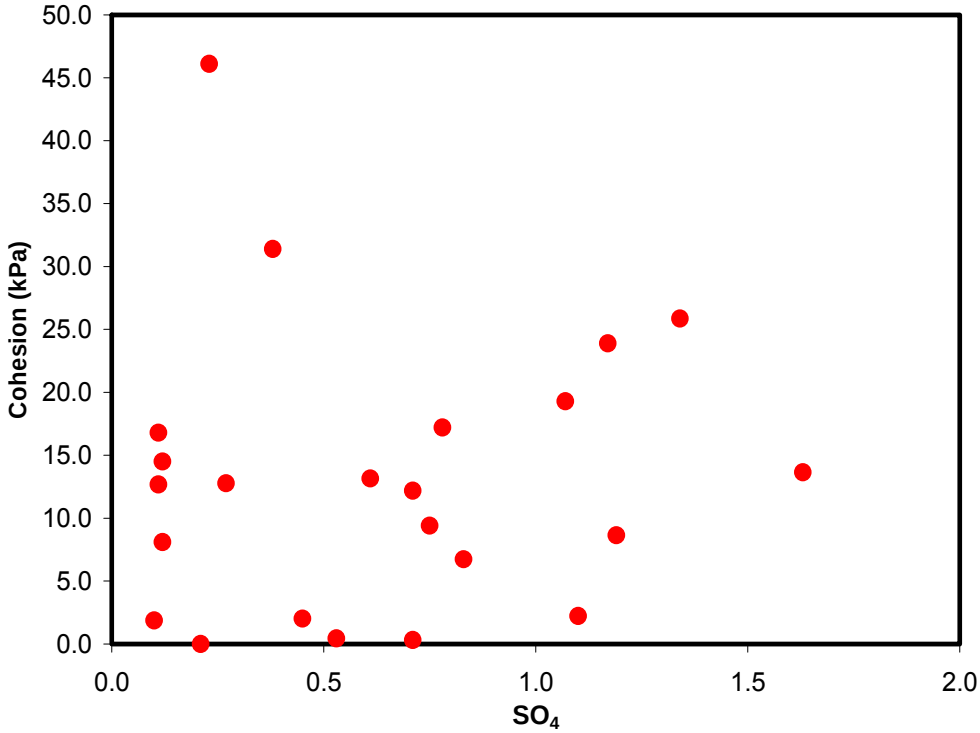

Figure 6.7. Correlation of cohesion with SO4.

6.4.2 Correlation of percent Authigenic gypsum with Cohesion

Figure 6.8 shows little correlation between cohesion and percent Authigenic gypsum, which also supports the observation that cohesion existing within the rock piles and analogs is not controlled by only one mineral. Authigenic gypsum is the gypsum formed after the placement of the rock piles due to oxidation of the pyrite minerals.

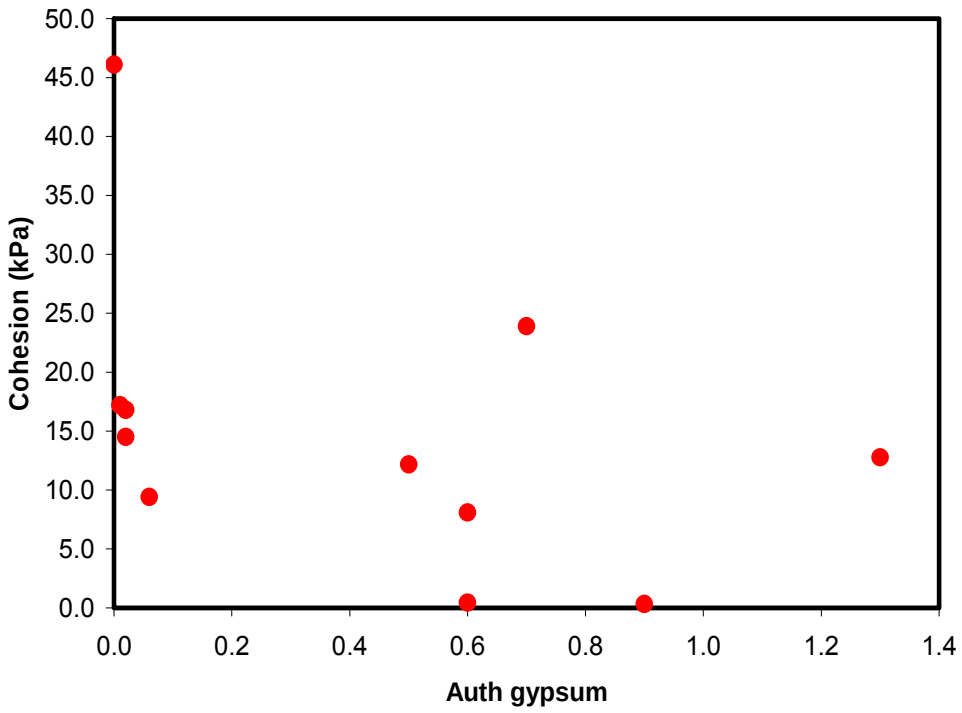

Figure 6.8. Correlation of cohesion with percent Authigenic gypsum.

6.4.3 Correlation of percent pyrite with Cohesion

Figure 6.9 shows little correlation between cohesion and percent pyrite, which supports the observation that the cohesion existing within the rock piles and analogs is not only a factor of oxidation of pyrite to form cementing agents within the rock piles and

analogs. Figure 6.10 show no correlation between sulfur and cohesion which support the observation made between cohesion and pyrite.

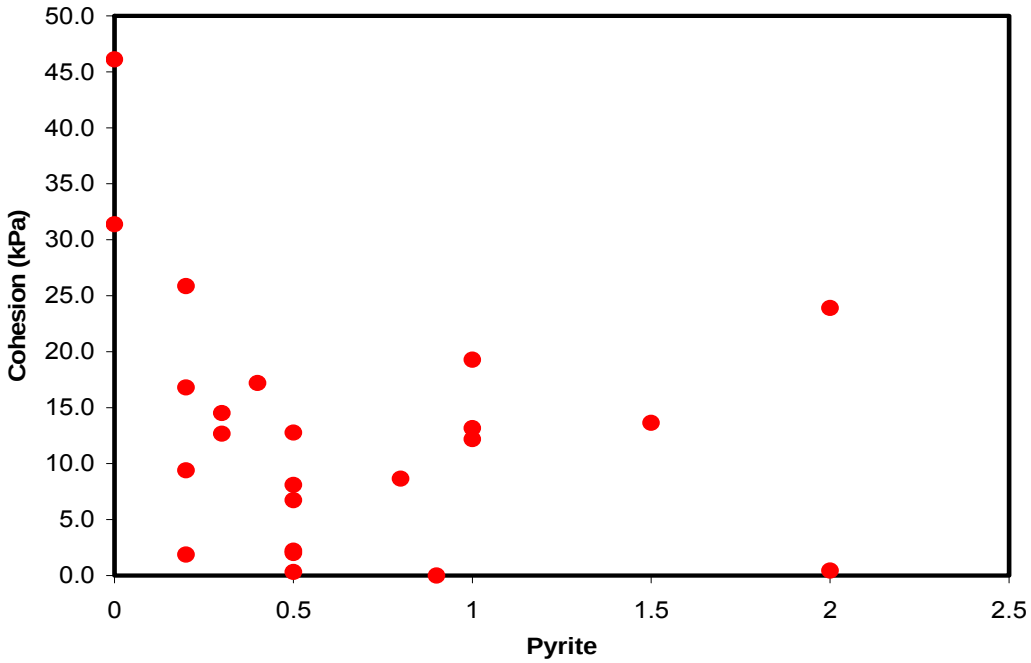

Figure 6.9. Correlation of cohesion with percent pyrite.

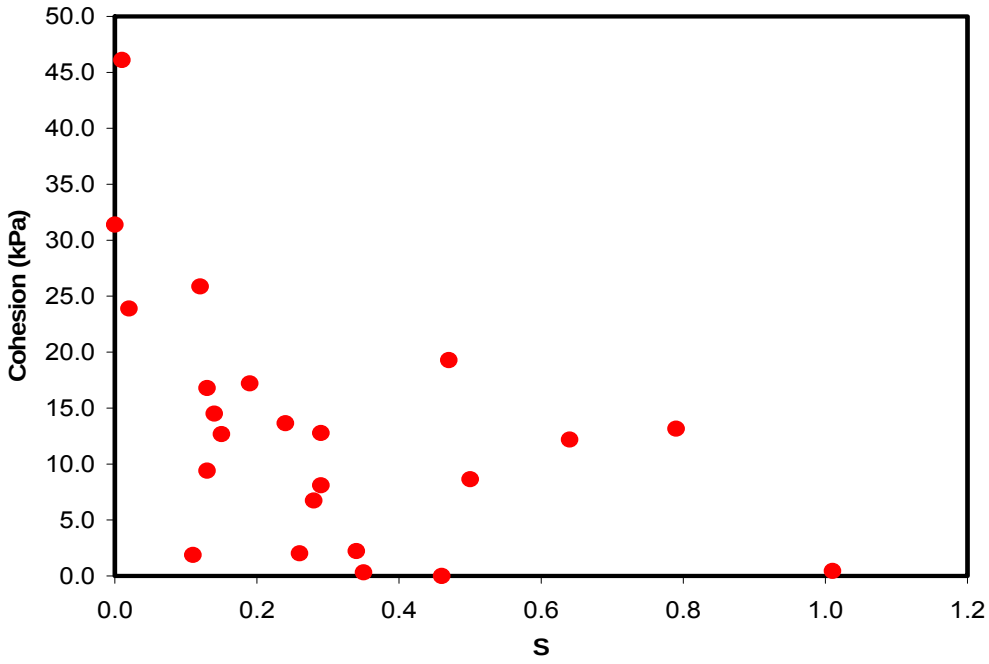

Figure 6.10. Correlation of cohesion with S**.**

6.4.4 Correlation of percent calcite with Cohesion

Figure 6.11 shows no correlation between cohesion and percent calcite, which supports the observation made earlier related to the correlation between cohesion and pyrite oxidation since these two mineral are reciprocal of each other. Figure 6.12 shows no correlation between cohesion and carbon.

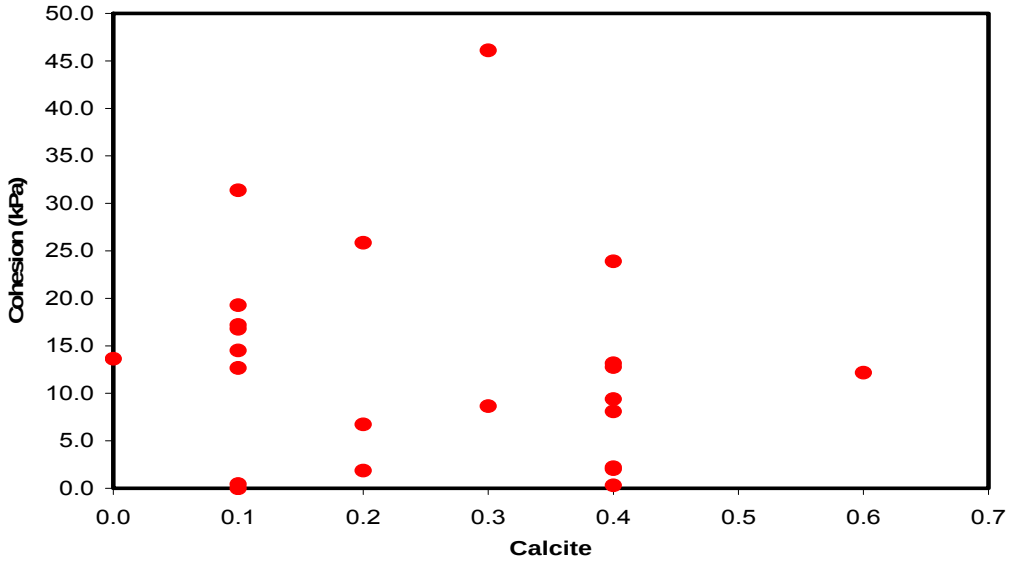

Figure 6.11. Correlation of cohesion with percent calcite.

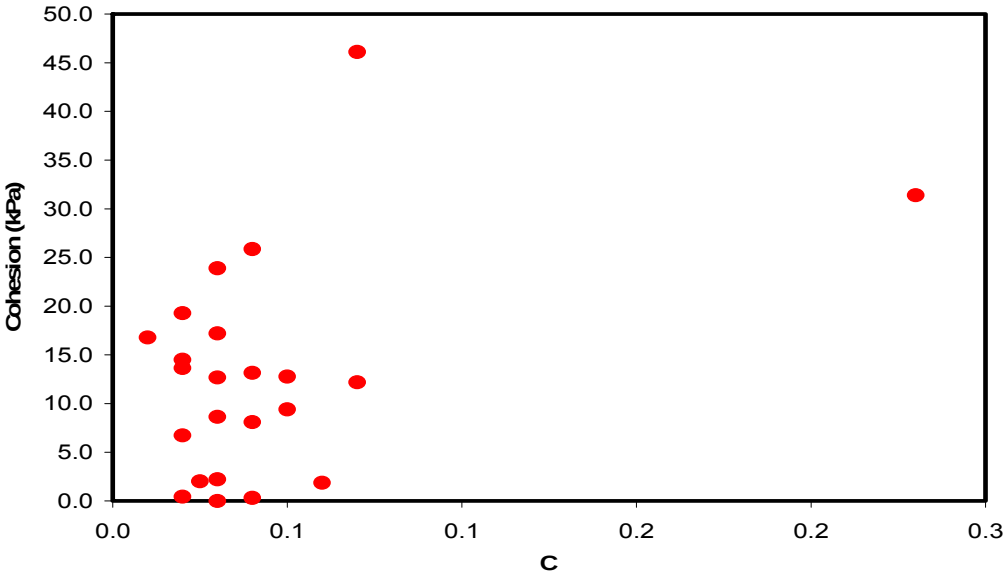

Figure 6.12. Correlation of cohesion with C.

6.4.5 Correlation of Clay minerals with Cohesion

Figure 6.13-6.16 shows little to no correlation between cohesion and individual clay minerals, which supports the fact that different combinations of minerals and other factors within the rock piles and analogs accounts for the existence of cohesion. Note that mong these four figures, the linear correlation between cohesion and chlorite is stronger.

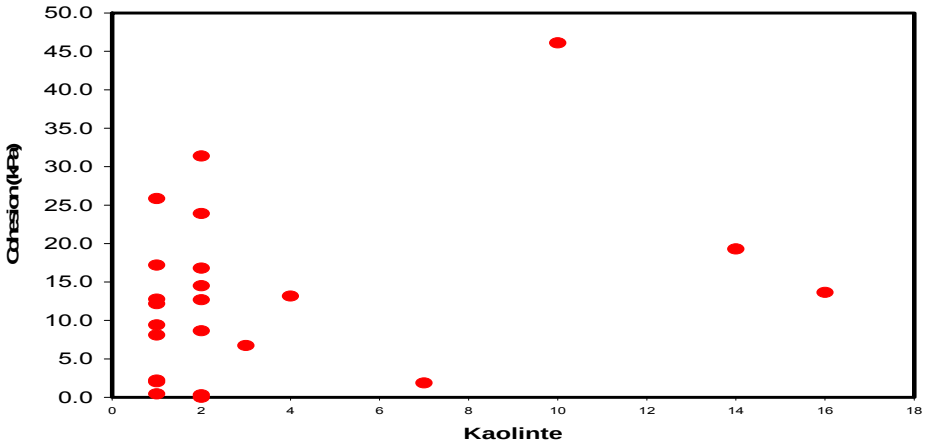

Figure 6.13. Correlation of cohesion with Kaolinte.

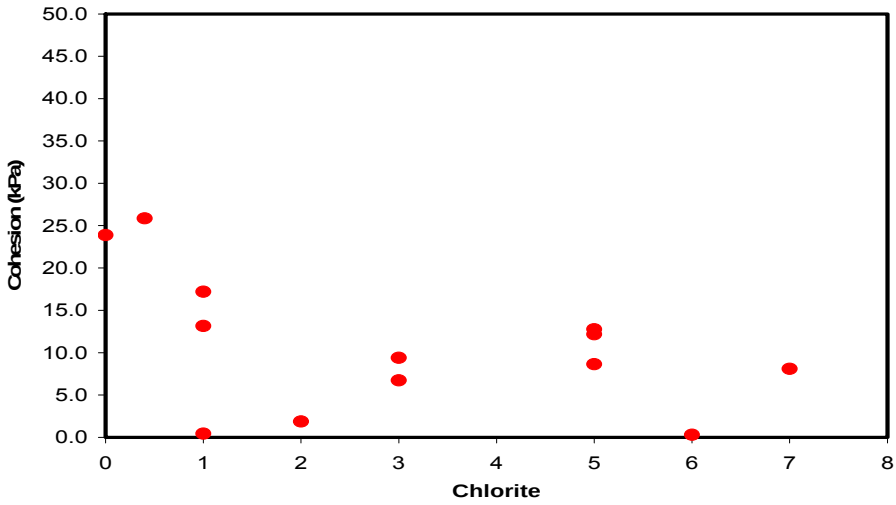

Figure 6.14. Correlation of cohesion with Chlorite.

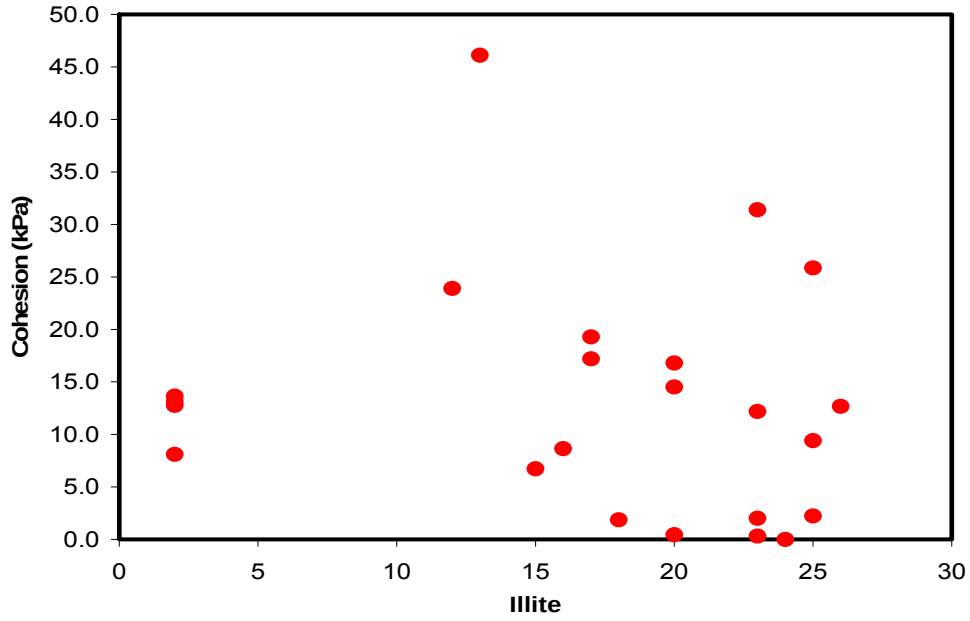

Figure 6.15. Correlation of cohesion with Illite.

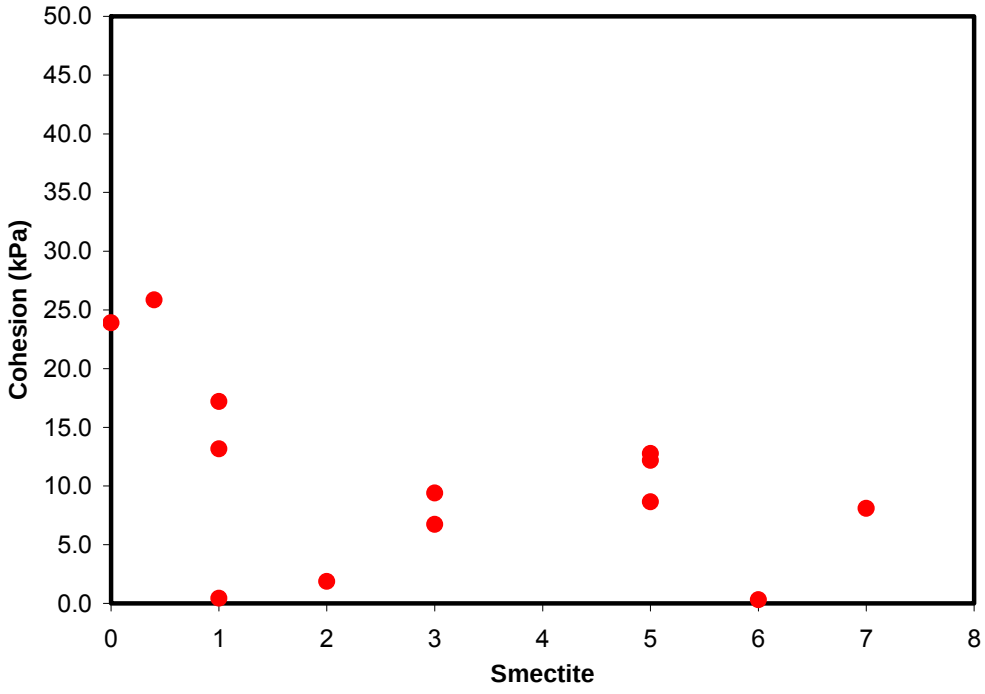

Figure 6.16. Correlation of cohesion with Smectite.

6.5 Effect of Degree Weathering on Shear Strength of Rock Piles and Analogs Samples

The effect of degree of weathering on cohesion is also investigated. It must be noted that as discussed previously, the specific minerals do not have strong correlation with cohesion. This means that cohesion within the rock piles and analogs is not a measure of only one mineral. Figure 6.17 and 6.18 shows the results of the field-measured cohesions of different rock piles and analogs versus the simple weathering index. Note that only the shear test results on rock pile blocks that contained rock fragments smaller than or equal to 1/5 the width of the shear box is shown in the Figures. Table 6.6 reports some geotechnical parameters of the rock piles and analogs such as %fine, PI, matric suction, and cohesion at the 24 places where successful in situ shear tests were conducted. In Table 6.6, means and standard deviations of cohesions corresponding to the SWI of 2, 3, and 4 are reported as well. The calculated cohesion values range between 0 to 46.1 kPa. In Table 6.7, the mean and standard deviation for cohesion of the rock piles and analogs have been reported separately. In order to evaluate the trend in cohesion change with time, t-tests were performed using the data in Table 6.7 and also Figure 6.19 that shows the cohesion versus time in a semi-logarithm plot. Since the rock piles were constructed using the end-dumping method with no mechanical compaction, it is reasonable to assume the cohesion of these materials was 0 at the time of construction. With this assumption, before and after pair t-tests were conducted to investigate the improvement in cohesion since the rock piles placement. The improvement in the mean of cohesion with a 95% confidence was between 6.2 to 13.1 kPa. Another t-test between the rock piles at the current situation and their natural analogs indicated that the present mean

cohesion of the rock piles of 9.6 kPa, in future will improve with 95% confidence to a value between 17.7 to 37.8 kPa. Note that the results of these two t-tests are approximate for the following reasons:

1. The number of data points, 20 cohesion values for the rock piles and 4 cohesion values for the analogs may not be great enough (especially for the analogs) to be statistically significant.
2. The measured cohesions on the rock piles belong to the locations where a shear test block could be made i.e. at the locations that the rock piles had cohesion. There were locations with no cohesion that a shear block could not be made to run the shear test. Therefore, the shear tests on the rock pile are biased toward to the locations that cohesion exists.

Note that Figures 6.17 and 6.18 suggest that higher cohesion values belong to more weathered samples but there are more weathered samples with low cohesion values.

Table 6.6 Some of the geotechnical properties of rock piles and analogs, and the descriptive statistics of field cohesion values.

Rock piles and Analogs	Test id	Matric Suction (kPa)	Fine (%)	PI (%)	USCS	SW I	Field Cohesion (kPa)	No. of Tests	Cohesion (kPa)	
									Mean	STD
Sugar Shack South Rock Pile	SSS-VTM-0600-1	1	6.9	8.7	GP-GC	2	1.9	**3**	**7.6**	**5.5**
Spring Gulch Rock Pile	SPR-AAF-0001-1	10	1.3	1.4	GP	2	8.1			
Spring Gulch Rock Pile	SPR-AAF-0001-2	9	0.6	9.5	GP	2	12.8			
Sugar Shack South Rock Pile	SSS-AAF-0001-1	1	1.8	7.3	GP	3	6.7	**7**	**11.2**	**10.6**
Sugar Shack South Rock Pile	SSS-AAF-0005-1	9	1.4	4.7	SP	3	17.2			
Sugar Shack South Rock Pile	SSS-AAF-0009-1	0	2.0	10.5	GP	3	2.0			
Sugar Shack West Rock Pile	SSW-AAF-0004-1	n/a	13.6	14.2	GP-GC	3	8.7			
Sugar Shack West Rock Pile	SSW-VTM-0026-1	13	0.7	7.1	SP	3	0.3			
Sugar Shack West Rock Pile	SSW-VTM-0030-1	3	0.7	7.1	GP	3	12.2			
Debris Flow	MIN-AAF-0001-1	25	3.6	3.6	GP	3	31.4			

Middle Rock Pile	MID-VTM-0002-1	1	1.0	1.9	GP	4	0.5	**13**	**14.8**	**12.6**
Debris Flow	MIN-AAF-0012-1	31	0.7	8.9	GP	4	46.1			
Sugar Shack West Rock Pile	SSW-AAF-0005-1	5	2.9	8.2	GP	4	25.9			
Sugar Shack West Rock Pile	SSW-AAF-0007-1	9	0.6	7.2	SP	4	13.2			
Sugar Shack West Rock Pile	SSW-VTM-0600-1	n/a	0.2	7.7	GP	4	19.3			
Sugar Shack West Rock Pile	SSW-VTM-0600-2	n/a	1.5	6.2	GP	4	13.6			
Sugar Shack West Rock Pile	SSW-VTM-0600-3	n/a	13.6	9.2	GC	4	2.2			
Spring Gulch Rock Pile	SPR-VTM-0012-1	2	8.4	2.5	GP-GM	4	12.7			
Spring Gulch Rock Pile	SPR-VTM-0012-2	0	6.7	6.2	GP-GC	4	4.0			
Spring Gulch Rock Pile	SPR-VTM-0012-3	0	7.9	4.3	GP-GC	4	0.0			
Spring Gulch Rock Pile	SPR-VTM-0019-1	5	10.0	7.3	SP-SC	4	14.5			
Spring Gulch Rock Pile	SPR-VTM-0019-2	2	8.5	6.9	GP-GC	4	16.8			
Questa Pit Alteration Scar	QPS-AAF-0001-3	0	6.8	16.4	GP-GC	4	23.9			
Questa Pit Alteration Scar	QPS-VTM-0001-1	11	4.2	5.3	GP	5	9.4	**1**		

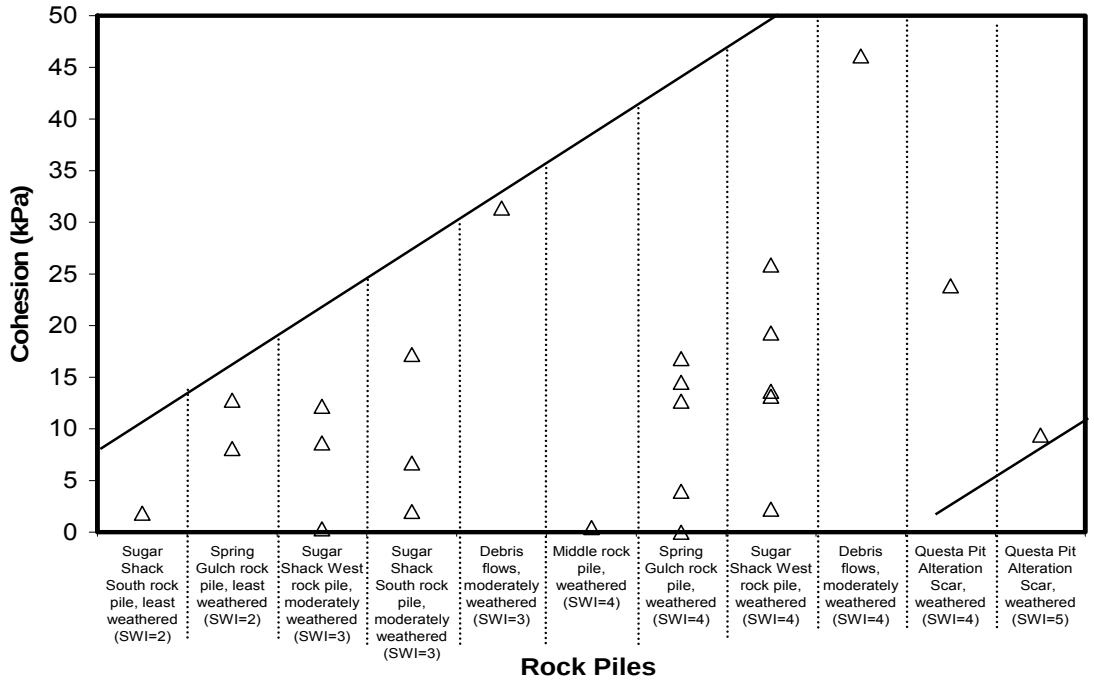

Figure 6.17. Correlation between cohesion and the degree of weathering (SWI). The sample locations and the SWI for each sample are indicated along the X-axis.

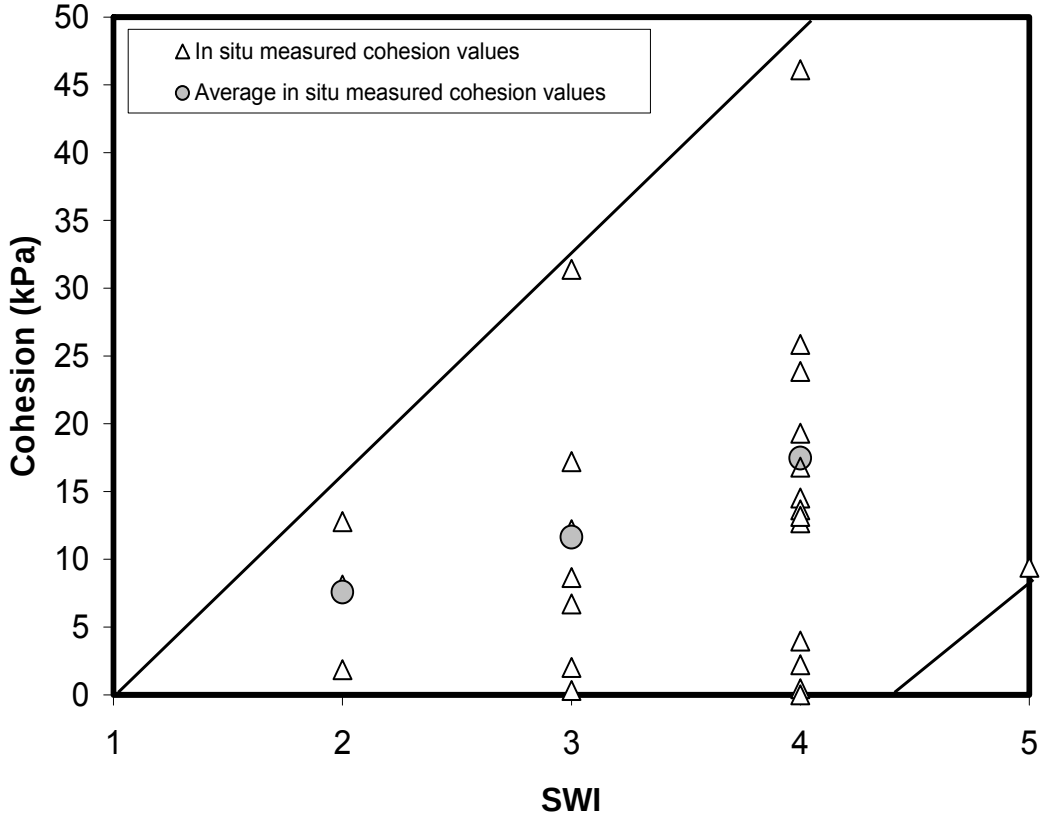

Fig. 6.18. Cohesion vs simple weathering index. . The average cohesion corresponding to each SWI is shown with a gray circular symbol.

Table 6.7 Descriptive statistics of field cohesion of the rock piles and analogs, reported separately.

State	Cohesion (kPa)		
	Mean	**STD**	**No. of *in situ* tests**
Rock piles at the placement time	0	0	N/A
Rock piles after 40 years (current situation)	9.6	7.3	20
Analogs (thousands of years old)	27.7	15.3	4

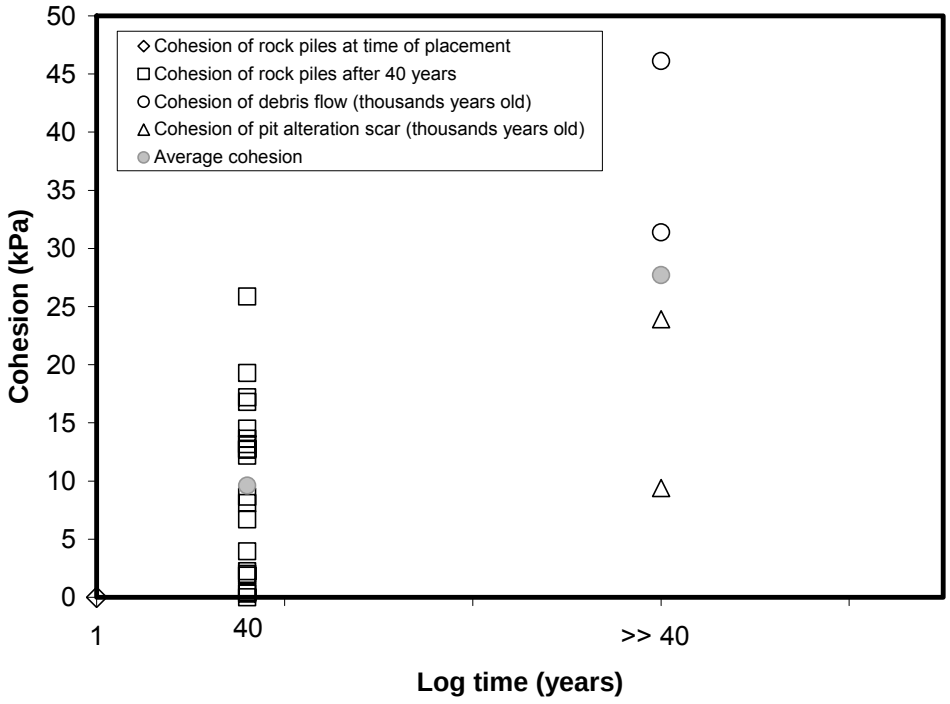

Fig. 6.19. Cohesion vs. age of the rock piles and analogs.

The intrinsic cohesions for matric suction of 0 kPa were calculated using Fredlund and Rahardjos' (1993) technique as indicated in Chapter 5 and plotted in Figure 6.20 where a relationship similar to that in Figure 6.18 is evident. As explained earlier, it is important to note that the initial cohesion of the rock piles was 0 at the time of dumping due to the particle separations caused by end-dumping the material. Therefore, all the cohesion that now exists, as documented by the in situ shear tests, must have been generated in the piles since the rock piles were initially placed. That is, there has been an increase in cohesion over time, although the cohesion change per unit time is not known.

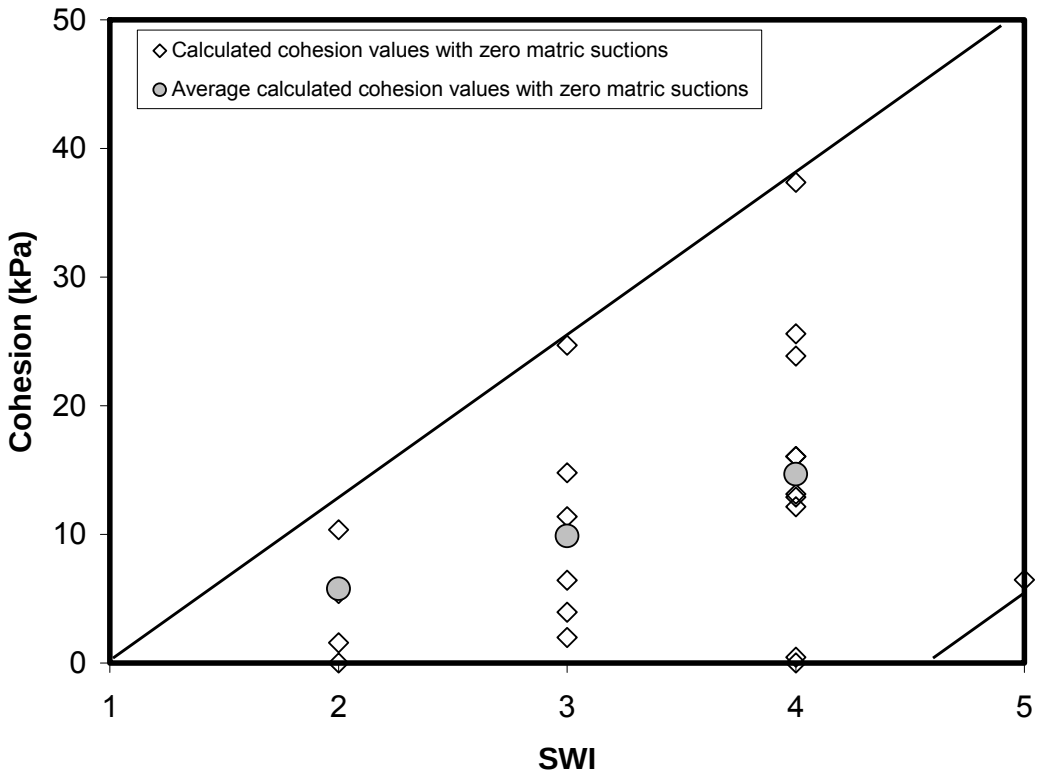

Figure 6.20. Correlation between cohesion with matric suction of zero with the degree of weathering. The average cohesion corresponding to each SWI is shown with a gray circular symbol.

Figure 6.21 illustrates a comparison between the measured in situ and the laboratory friction angles for each pile and the corresponding SWI of that pile. The comparison was made to find the effect of weathering on the friction angle of the rock pile and analog materials. In most published literature, authors have indicated that weathering reduces the friction angle of materials (see Chapter 3). It is important to note that most of these reported arguments are related to weak lithologies like coal and related sedimentary rocks. In Figure 6.22, the friction angles from this research are plotted versus the SWI without addressing the locations where the samples for the shear tests were collected. On

average, the friction angles obtained from shear tests with low normal stresses are higher than those obtained from shear tests with high normal stresses.

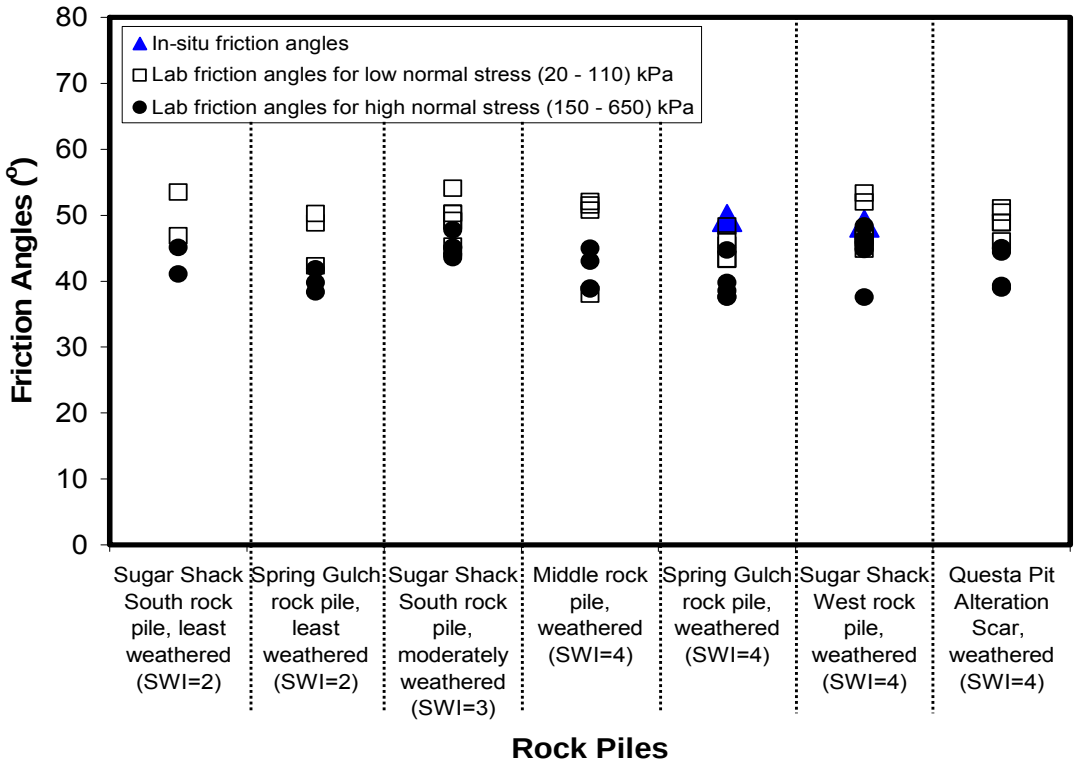

Figure 6.21. In situ and laboratory friction angles for samples from Questa rock pile and their natural analogs plotted for rock piles with different SWI**.**

An important observation from Figure 6.21 is that no reduction in friction angle has occurred due to the weathering at the test location since the construction of the rock piles. This could be due to the fact that rock fragments in the Questa mine rock piles are highly durable. For example, the slake durability index for 90 rock fragment samples from Goathill North Rock Pile ranged from 82 to 98% (Viterbo, 2007). Viterbo classified these samples as being highly to extremely highly durable based on Franklin's durability classification (Franklin and Chandra, 1972).

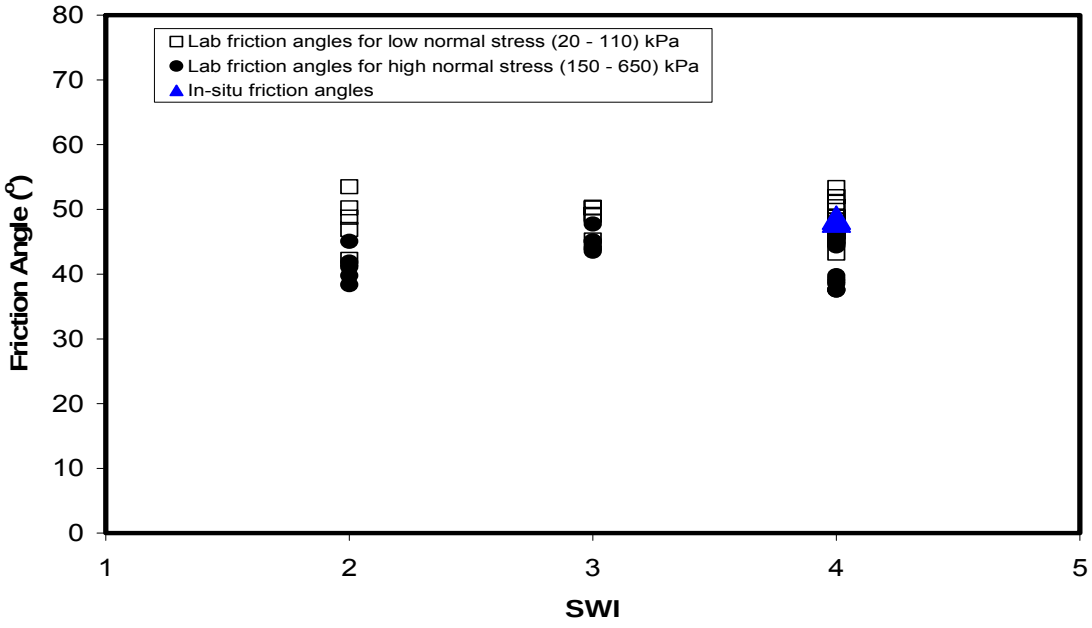

Figure. 6.22. In situ and laboratory peak friction angles vs. simple weathering index.

Inspection of Figure 6.22 indicates that the peak friction angle of the rock pile material at most of the locations is greater than 40º. A few factors, in addition to high slake durability mentioned earlier, are responsible for the high friction angle of Questa rock pile material as follows:

- The percentage of fine material is low at this stage of weathering at Questa mine. The amount of fine material is less that 20%. This allows the rock fragments in the rock piles to be directly in contact with each other with the consequence of having more frictional resistance.
- The rock fragments in the rock piles have relatively high compressive and tensile strengths. For example, test results on rock fragments from the Goathill North Rock Pile showed point load strength in the range of 1.1 to 5.8 MPa (Viterbo, 2007).

- The rock fragments in the rock piles are angular. Angularity causes greater interlocking of the particles and induces higher shearing resistance. The angularity of the rock fragments is shown in Figure 6.23 that is a close-up photo of the surface of the Spring Gulch Rock Pile.

Figure 6.23. A close-up photo of the surface of Spring Gulch Rock Pile showing the angularity of the rock fragments compared to a spherical ball 50 mm in diameter.

6.6 Effect of Normal Load on Shear Strength of Rock Pile Material

The effects of the variation in normal load in the case of direct shear tests or of confining pressure in triaxial tests on the shear strength and behavior of soils have been studied for many years. The detailed literature search on this topic is discussed in Chapter 3 of this thesis. To reiterate a few of these, Linero et al. (2007) concludes that there is a decrease in friction angle when the confining stresses are increased in triaxial testing of

rock pile material. The lower the normal stress the higher the friction angle. Hribar (1986) also made the observation that the friction angle reduces when the normal stress is increased. Marachi et al. (1969) indicates that when the confining pressure of a triaxial test is increased, the friction angle decreases. This effect was also investigated and confirmed during this research. Figure 6.24 shows the friction angles obtained for different ranges of applied normal stresses.

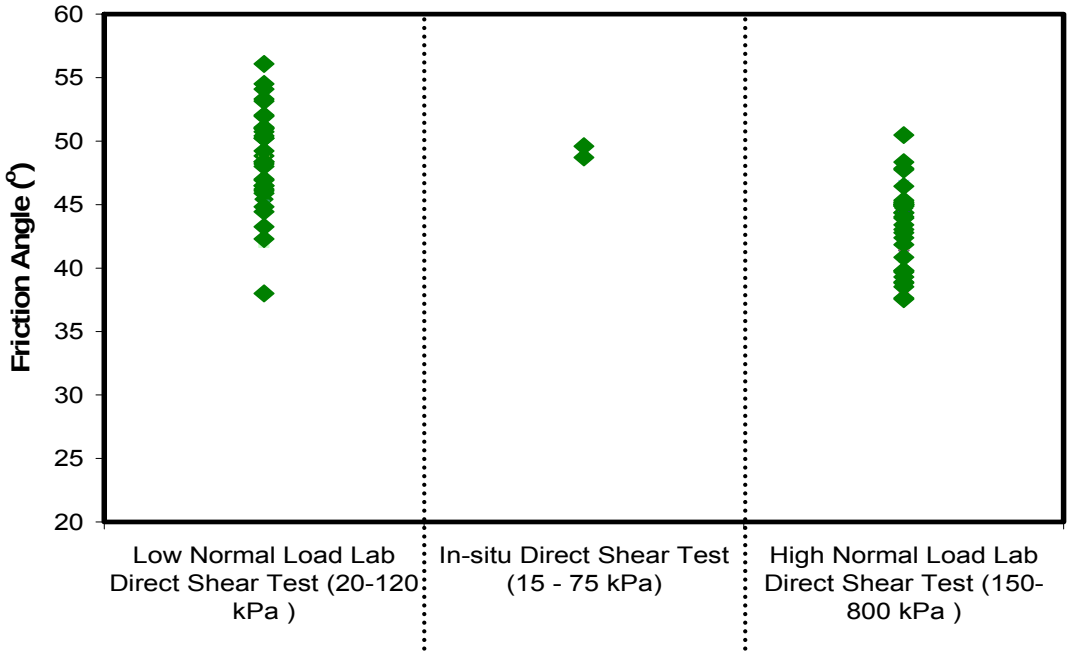

Figure 6.24. Friction angle with different normal load range for rock piles and analogs

Notice that low normal loads are associated with high friction angles and high normal loads are associated with decreased friction angles. This observation is similar to what Linero et al. (2007), Hriba (1986) and Marachi et al. (1969) reported. Linero et al. (2007) also reported that low normal stress friction angles are the true representation of shear strength of the top layer of rock piles, and that high normal load friction angles are

related to deep-seated layers of rock piles. Koerner (1970) explained the negative correlation between the friction angle and the applied normal load indicating that measured drained friction angles have two components, a friction factor (Φ_f) and a dilation factor (Φ_δ). For high normal loads the amount of soil dilation is small with particle breakages involved that result in the reduced friction angles. Marsal (1967) stated that the most important factor affecting both shear strength and compressibility is the phenomenon of particle fragmentation undergone by a granular body when subjected to changes in its state of stresses, both during the uniform compression stage and during deviator loading application. Linero et al. (2007) reported low friction angles with corresponding high particle breakage factors.

6.7 Nonlinear Shear Strength Model of Questa Mine Rock Pile and Analog Samples

Linero et al. (2007) used Charles and Watts' (1980) equation to describe the shear strength of copper porphyry rock pile material in Chile by performing triaxial tests. The findings of Linero et al. (2007) are of importance to this work because the rock piles they studied have similar lithology as that in the Questa mine area, so their results can be compared to these findings. Linero et al. (2007) report A and b (equation 3-8) values of 0.84 $MPa^{(1-b)}$ and 0.78 for parallel particle size distribution and 0.86 $MPa^{(1-b)}$ and 0.90 for scalped truncated particle size distribution. It must be noted that their triaxial testing cylinder size was 2m in height by 1m in diameter. The maximum particle size of the test was 1/5 the width of the sample. These particle sizes are far larger than those tested in our 5.08cm direct shear box in the laboratory. To ascertain if the Questa rock pile material

behaves according to linear or nonlinear failure criteria, Figure 6.25 was generated from a laboratory direct shear test performed on in situ sample of Spring Gulch rock pile. Figure 6.26 shows the nonlinear behavior of the Questa rock pile material samples over a range of applied normal loads.

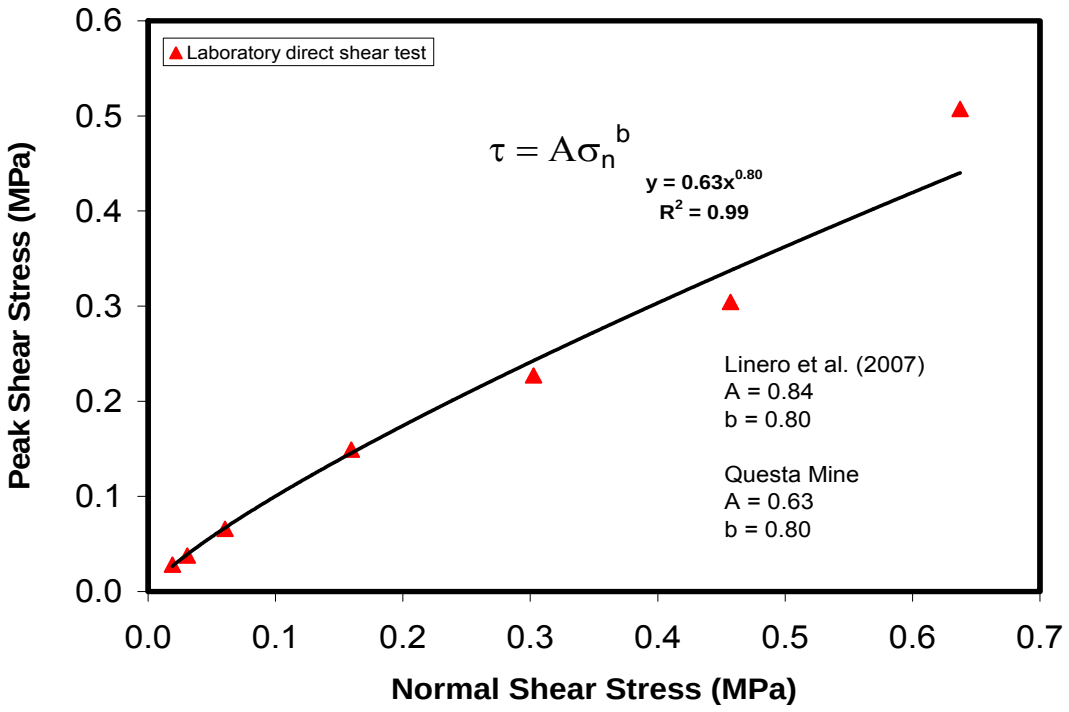

Figure 6.25. Nonlinear behavior of rock pile and analog materials over a range of normal loads.

From Figure 6.26, the values of the two constants A and b are 0.63 $MPa^{(1-b)}$ and 0.80, respectively. Material with higher resistance generally presents higher values of A. The b parameter determines the nature of the failure envelop. Comparing constant values from Questa rock pile with what Linero et al. (2007) reported, the Questa rock piles have a lower resistance and this corresponds to lower friction angles having been measured in the laboratory comparable to what Linero et al. (2007) reported for the large triaxial tests

performed. Another reason for our low values of A as compared to Linero et al. (2007) is that particle sizes tested in our laboratory direct shear tests as compared to those used by Linero et al. (2007) are very small, creating lower resistance and therefore a lower friction angle comparable what was reported by Linero et al. (2007). Table 6.8 is a summary of nonlinear criteria constants for Questa Materials tested. It is important to note that this values where obtained from

Table 6.8. Summary of nonlinear failure criteria constants form laboratory direct shear tests on materials collected from in situ direct shear test locations.

In situ Test id	A kPa $^{(1-b)}$	b
QPS-AAF-0001-1	5.10	0.72
QPS-AAF-0001-2	4.74	0.71
QPS-AAF-0001-3	2.66	0.84
QPS-AAF-0008-1	2.38	0.83
QPS-AAF-0009-1	4.81	0.74
QPS-AAF-0020-1	4.95	0.74
QPS-AAF-0022-1	8.84	0.61
QPS-VTM-0001-1	6.60	0.66
MIN-AAF-0001-1	9.68	0.61
MIN-AAF-0004-1	6.66	0.67
MIN-AAF-0010-1	9.7	0.63
MIN-AAF-0012-1	3.72	0.78
MIN-AAF-0015-1	4.7	0.77
MID-AAF-0001-1	5.91	0.69
MID-AAF-0002-1	7.19	0.63
MID-AAF-0002-2	3.50	0.76
MID-VTM-0002-1	7.42	0.66
SPR-AAF-0001-1	3.02	0.82
SPR-AAF-0001-2	4.02	0.77
SPR-VTM-0005-1	2.82	0.80
SPR-VTM-0008-1	4.19	0.75
SPR-VTM-0008-2	1.49	0.90
SPR-VTM-0012-1	4.87	0.73
SPR-VTM-0012-2	2.30	0.82
SPR-VTM-0012-3	8.52	0.61
SPR-VTM-0019-1	3.54	0.75
SPR-VTM-0019-2	2.98	0.78
SSS-AAF-0001-1	4.96	0.73
SSS-AAF-0001-2	3.14	0.81

SSS-AAF-0005-1	5.04	0.72
SSS-AAF-0005-2	4.74	0.74
SSS-AAF-0009-1	4.92	0.73
SSS-AAF-0009-2	3.75	0.79
SSS-VTM-0600-1	4.22	0.74
SSS-VTM-0601-1	3.35	0.80
SSW-AAF-0001-1	5.80	0.69
SSW-AAF-0002-1	2.42	0.85
SSW-AAF-0002-2	3.44	0.78
SSW-AAF-0002-3	2.60	0.84
SSW-AAF-0004-1	6.36	0.71
SSW-AAF-0005-1	3.57	0.78
SSW-AAF-0007-1	6.73	0.67
SSW-VTM-0016-1	6.32	0.70
SSW-VTM-0016-2	8.85	0.62
SSW-VTM-0023-1	9.10	0.62
SSW-VTM-0026-1	6.29	0.70
SSW-VTM-0030-1	9.72	0.63
SSW-VTM-0030-2	6.17	0.70
SSW-VTM-0600-1	2.86	0.78
SSW-VTM-0600-2	4.73	0.74
SSW-VTM-0600-3	2.90	0.83

7. Conclusions and Recommendations

7.1 Conclusions

Laboratory and in situ direct shear tests were conducted on the Questa rock pile materials to investigate the effect of weathering on the shear strength of these materials. To classify the rock-pile material based on the weathering intensity, a simple weathering index was used that was defined by color, mineralogy, and texture of the material. A series of geotechnical tests were completed on samples with different weathering intensities from four (4) of the Questa rock piles and from weathering analogs of the rock piles (alteration scar and debris flows on the Questa mine site). It should be noted that all in-situ tests were performed at or near the surfaces of the rock piles, and the conclusions made regarding the effect of weathering on the friction angle and cohesion are valid only for the shallow surface portion of the rock piles and not the interior. The synthesis of these analyses lead to the following conclusions:

- Friction angle decreases with increase in normal load; laboratory peak friction angles ranged from 38^o to 48^o for high normal loads and 38^o to 52^o for low normal loads. The two measured in-situ friction angles were around 48^o.
- The index properties have little to no correlation with cohesion. Cohesion shows a slight negative correlation with water content and a slight positive correlation with matric suction. The lower cohesion values tend to correlate with higher %fines, but some samples with lower cohesion also have low %fines.

- The mineralogy and chemistry have little or no correlation with cohesion which shows that no single mineral or chemical element affects cohesion within the rock piles and analogs
- A nonlinear failure criterion can be used to describe the shear strength of Questa rock pile material similar to that used for earth fill dam materials. If the range of applied normal load is narrow, a linear failure criterion is valid as well.
- The initial values of cohesion in the rock piles at the time of construction were near zero due to the disintegration of the particles caused by end dumping of the material. The shear tests indicate that the cohesion has increased from zero to a measurable value since the construction of the rock piles at the locations that in situ tests were conducted.
- The increase of cohesion of the rock pile material with time is attributed to the presence of cementing agents like clay, gypsum, iron oxides and jarosite, in the rock pile and the gradual compaction of the rock piles since their emplacement.
- Higher cohesion values belong to older samples, although not all of the older analog samples have the highest cohesion values.
- Higher cohesion values are in the most weathered samples, but not all weathered samples have high cohesion. In fact there are some weathered samples with very low cohesion.

7.2 Recommendations for future work include:

- Further laboratory direct shear tests need to be performed to investigate the effect of particle size on the shear strength of the rock pile materials.

- Further investigation and testing are required at greater depths into the interior of the rock piles to extend the conclusions made regarding the cohesion and friction angles to the whole structure of the rock piles. Reclamation of Sugar Shack West offers an excellent opportunity to perform these tests within the interior.
- Further investigation of cohesion with mineralogy and geochemistry needs to be completed to look at various chemical weathering indices and mineral combinations.

REFERENCES

Abramson L.W., Lee, T.S., Sharma, S. and Boyce, G.M., 2001, Slope Stability and Stabilization Methods: second edition, John Wiley and Son, Inc

Adams, R., Ahfeld, D., and Sengupta, A., 2007, Investigating the Potential for Ongoing Pollution from an Abandoned Pyrite Mine: Mine Water and the Environment, v. 26, p. 2-13.

ASTM, 1987, Standard Preparation of Soil Samples for Particle Size Analysis and Determination of Soil Constants (D421), Annual Book of ASTM Standards, American Society for testing and Materials (ASTM), West Conshohocken, PA.

ASTM, 1998, Standard Test Method for Direct Shear Test of Soils Under Consolidated Drained Conditions (D3080), Annual Book of ASTM Standards, American Society for Testing and Materials (ASTM), West Conshohocken, PA.

ASTM, 2001a, Standard Laboratory Determination of Water (moisture) Content of Soil, Rock, and Soil-Aggregate Mixtures (D2216), Annual Book of ASTM Standards. American Society for Testing and Materials (ASTM), West Conshohocken, PA.

ASTM, 2001b, Standard Test Method for Liquid Limit, Plastic Limit, and Plasticity Index of Soils (D4318). Annual Book of ASTM Standards, American Society for Testing and Materials (ASTM), West Conshohocken, PA.

ASTM, 2002a, Standard Test Method for Particle-Size Analysis of Soils (D422), Annual Book of ASTM Standards. American Society for Testing and Materials (ASTM), West Conshohocken, PA.

ASTM, 2002b, Standard Test Methods for Specific Gravity of Soil Solids by Water Pycnometer (D854), Annual Book of ASTM Standards, American Society for Testing and Materials (ASTM), West Conshohocken, PA.

Bell, F.G., 1996, Dereliction: Colliery Spoil Heaps and their Rehabilitation: Environmental and Engineering Geoscience, v. 2, p. 85-96

Bews, B.E., Barbour, S.L., Wilson, G.W., and O'Kane, M.A., 1997, The Design of Lysimeters for a Low Flux Cover System Over Acid Generating Waste Rock: unpublished report.

Bishop, A W., 1948, A Large Shear Box for Testing Sand and Gravels, Proceedings of the 2nd International Conference on Soil Mechanics and Foundation Engineering, Vol. 1, p. 207-211.

Blight, G. E., and Fourie, A. B., 2005, Catastrophe Revisited - Disastrous Flow Failures of Mine and Municipal Solid Waste: Geotechnical and Geological Engineering, v. 2005, no. 23, p. 219-248.

Blowes, D. W. and Jambor, J. L., 1990, The Pore-Water Geochemistry and the Mineralogy of the Vadose Zone of SulphideTailings, Waite Amulet, Quebec, Canada: Applied Geochemistry, v. 5, p. 327-346.

Brand, E. W., Phillipson, H. B., Borrie, G. W., and Clover, A. W., 1983, "In Situ Shear Tests on Hong Kong Residual Soils," International Symposium on In Situ Testing, Paris, France, Vol. 2, p. 13—17.

Caine, J. S., 2003, Questa Baseline and Pre-Mining Ground-Water Quality Investigation 6: Preliminary Brittle Structural Geologic Data, Questa Mining District, Southern Sangre de Cristo Mountains, New Mexico: U.S. Geological Survey, Open-file Report 02-0280.

Caldwell, J. A., and Moss, A. S. E., 1981, The Simplified Analysis of Mine Waste Embankments, AIME Fall Meeting 1981, *in* Symposium on Design of Non-Impounding Mine Waste Embankments, Denver, CO, USA.

Carpenter, R. H., 1968, Geology and ore deposits of the Questa molybdenum mine area, Taos County, New Mexico *In;* Ore deposits of the United States, 1933-1967, Granton-Sales, J.D., Ridge, *ed*. AIME, p.1328-1350.

Campbell A.R., and Lueth V.W., 2008, Isotopic and textural discrimination between hypogene, ancient supergene, and modern sulfates at the Questa Mine, New Mexico: Applied Geochemistry. Add v and p

Charles, J. A., and Watts, K. S., 1980, The Influence of Confining Pressure on the Shear Strength of Compacted Rockfill, Geotechnique 30, No. 4, p. 353 – 367.

Chigira M., and Oyama T., 1999, Mechanism and effect of chemical weathering of sedimentary rocks, Engineering Geology, 55, 3-14.

Cho, G. C., Dodds, J. and Santamarina, J. C., 2006, "Particle Shape Effects on Packing Density, Stiffness, and Strength: Natural and Crushed Sands," J. of Geotech. and Geoenv. Eng. ASCE, Vol. 132, No. 5, pp. 591—602

Clark, K. F., 1968, Structural controls in the Red River District, New Mexico. Economic Geology, v. 63, p. 553-566.

Coduto, D. P., 2001, Foundation Design: Principles and Practices, Upper Saddle River, New Jersey, Prentice-Hall, Inc. ISBN 0-13-589706-8, TA775.C63 2001.

Coker, I., and Flores, R., 2000, A Device for Extracting Large Intact Soil Samples Developed and Used in a Remote Region of Bolivia, Electronic J. of Geotech. Eng., Vol. 5, http://www.ejge.com/2000/Ppr0003/Ppr0003.htm, accessed November 20, 2006.

Collins, K., and McGown, A., 1974, The Form and Function of Microfabric Features in a Varuety of Natural Soils, Geotechnique, Vol. XXIV, No. 2, p.223-254

Das, B.M., 1983, Advanced Soil Mechanics, New York, McGraw-Hill Book Company, 511 p.

Dinelli, E., Lucchini, F., Fabbri, M., and Cortecci, G., 2001, Metal distribution and environmental problems related to sulfide oxidation in the Libiola copper mine area (Ligurian Apennines, Italy): Journal of Geochemical Exploration, v. 74, p. 141-152.

Herasymuik, G.M., 1996, Hydrogeology of a sulphide waste rock dump: M.S. Thesis, University of Saskatchewan, Saskatoon, Saskatchewan, Canada.

Duncan, J. M., and Chang, C. Y., 1970, Nonlinear Analysis of Stress and Strain in Soils, Proceedings of the America Society of Civil Engineers, Journal of the Soil Mechanics and Foundation Division, SM5, p. 1629-1653.

El-Sohby, M. A., El-Khoraibi, M. C., Rabba, S. A., and El-Saadany, M. M. A., 1987, "Role of Soil Fabric in Collapsible Soils, *VIII PCSMFE*, Cartagena, Columbia, p. 9-20.

Endo, T. and Tsurata, T., 1979, On the Effects of Tree Roots Upon the Shearing Strength of Soil, Annual report of the Hokkaido Branch, Forest Place Experimental Station, Sapporo, Japan, p. 167—183.

Fakhimi,A., Salehi,D. and Mojtabai, N., 2004, "Numerical Back Analysis for Estimation of Soil Parameters in the Resalat Tunnel Project," Tunneling and Underground Space Technology, Vol. 19, p. 57—67.

Fakhimi, A., Boakye, K., Sperling, D., and McLemore, V., 2008, Development of a modified in situ direct shear test technique to determine shear strength of mine rock piles: Geotechnical Testing Journal, v. 31, no. 3, p. 1-5.

Filipowicz, P. and Borys, M., 2005, Geotechnical properties of mining wastes and their utilization in civil engineering; in Proceedings of International Conference on Problematic Soils: May 25-27, 2005, Eastern Mediterranean University, Famagusta, N. Cyprus, p. 259-267.

Franklin, J.A., Chandra, A., 1972, The slake durability test, Int. J. Rock Mech. Min. Sci., 9, p. 325–341.

Fredlund D.G., and Rahardjo H., 1993, Soil mechanics for unsaturated soils, Wiley.
Gupta, A. S. and Rao, K. S., 1998, Index properties of weathered rocks: inter-relationships and applicability: Bulletin of Engineering Geology and Environment, v. 57, p. 161-172.

Fontes, M. P. F. and Carvalho, Jr., I. A., 2005, Color attributes and mineralogical characteristics, evaluated by radiometry, of highly weathered tropical soils: Soil Sci. Soc. Am. J. 69:1162–1172.

Gale, V. G., and Thompson, A. J. B., 2001, Reconnaissance study of waste rock mineralogy: Questa New Mexico, petrography, PIMA spectral analysis and Rietveld analysis: PetraScience Consultants, Inc.

Grow, A. J., Davidson, D. T., and Sheeler, J. B., 1961, Relative Effect of Chlorides, Lignosulfonates and molasses on Properties of a Soil-Aggregate Mix, Highway Research Board Bulletin 309, National Academy of Sciences-National Research Council, Washington.

Gupta, A. S. and Rao, K. S., 1998, Index properties of weathered rocks: inter-relationships and applicability: Bulletin of Engineering Geology and Environment, v. 57, p. 161-172.

Gutierrez, L. A. F., 2006, "The Influence of Mineralogy, Chemistry and Physical Engineering Properties on Shear Strength Parameters of the Goathill North Rock Pile Material, Questa Molybdenum Mine, New Mexico," M. S. thesis, New Mexico Institute of Mining and Technology, Socorro, 201 pp., http://geoinfo.nmt.edu/staff/mclemore/Molycorppapers.htm, accessed November 19, 2006.

Gutierrez, L.A.F., Viterbo, V.C., McLemore, V.T., and Aimone-Martin, C.T., 2008, Geotechnical and Geomechanical Characterisation of the Goathill North Rock Pile at the Questa Molybdenum Mine, New Mexico, USA; *in* Fourie, A., ed., First International Seminar on the Management of Rock Dumps, Stockpiles and Heap Leach Pads: The Australian Centre for Geomechanics, University of Western Australia, p. 19-32.

Hawley, P.M., 2001, Site Selection, Characterization, and Assessment. In: W.A. Hustrulid, M.K. McCarter and D.J.A. Van Zyl (Editors), Slope Stability in Surface Mining. Society for Mining, Metallurgy, and Exploration, Inc (SME). Littleton, p. 267-274.

Herasymuik, G.M., 1996, Hydrogeology of a sulphide waste rock dump: M.S. Thesis, University of Saskatchewan, Saskatoon, Saskatchewan, Canada.

Hockley, D.E., Noel, M., Rykaart, E.M., Jahn., S., and Paul, M., 2003, Testing of soil covers for waste rock in the Ronneburg WISMUT mine closure; 6th ICARD, Cairns, Australia, The Australasian Institute of Mining and Metallurgy, p. 273-279.

Holtz, W.G. and Gibbs, H.G., 1956, Triaxial Shear Tests on Previous Gravelly Soils. Journal of Soil Mechanics and Foundation Engineering Division, 82: 1-22.

Holtz, W.G., 1960, The Effect of Gravel Particles on Friction Angle, ASCE Research Conference on Shear Strength, p. 1000-1001.

Holtz, R.D. and Kovacs, W.D., 2003, An Introduction to Geotechnical Engineering. Civil Engineering and Engineering Mechanics Series. Pearson Education Taiwan Ldt., 733 p.

Hribar, J., Dougherty M., Ventura J., and Yavorsky P., 1986, Large Scale Direct Shear Tests on Surface Mine Spoil. International Symposium on Geotechnical Stability in Surface Mining, Calgary, November 1986.

Hutchinson, J. N., and Rolfsen, E. N., 1962, Large Scale Field Shear Box Test and Quick Clay, Geologie and Bauwesen, Vienna, Volume 28, Number 1, p. 31 – 42.

Hutchinson, J. N., 1988, General Report. Morphological and geotechnical parameters of landslides in relation to geology and hydrogeology, 5th International Symposium on Landslides: Switzerland, p. 3-35

Jaboyedoff, M., Baillifard F., Bardou E., and Girod F., 2004, The effect of weathering on Alpine rock instability, Quarterly Journal of Engineering Geology and Hydrogeology, 37, 2, 95-103.

John, S. B. P., 1980, In situ measurement of soil properties, Technical report documentation for California Department of Transportation Scramento, Report No. 19305-632136.

Kasmer, O., Ulusay, R., and Gokceoglu, C., 2006, Spoil pile instabilities with reference to a strip coal mine in Turkey: mechanisms and assessment of deformations: Environmental Geology, v. 49, p. 570-585.

Ke'zdi, A., 1975, Soil Mechanics, Tankonyvkiado', Budapest, (In Hung).

Kirkpatrick, W. M., 1965, Effect of Grain Size and Grading on the Shearing Behavior of Granular Material, Proceedings 6th International Conference on Soil Mechanics and Foundation Engineering, Vol. I, p. 273-277.

Klinedinst, L. G., 1972, Development and testing of a portable in-situ direct shear device, Maters Thesis, University of Idaho, Department of Civil Engineering, p.119.

Koerner, R. M., 1970, Effect of Particle Characteristic on Soil Strength, Proceedings of the American Society of Civil Engineers, Journal of the Soil Mechanics and Foundations Division, SM4, p. 1221-1235.

Knight, P. J., 1990, The flora of the Sangre de Cristo Mountains, New Mexico, *in* Bauer, P. W., Lucas, S. G., Mawer, C. K., and McIntosh, W. C., eds., Tectonic Development of the Southern Sangre de Cristo Mountains, New Mexico: New Mexico Geological Society Forty-First Annual Field Conference, September 12-15: Socorro, NM, New Mexico Geological Society, p. 94-95.

Kroeger, E.B., Huang, S.L., and Speck, R.C., 1991, Spoil pile failure and analysis in interior Alaska: Society of Mining Engineering, preprint 11 p.

Lambe, T. W., and Whitman, R. V., 1969, Soil Mechanics, Wiley, New York.

Lefebvre, R, Lamontagne, A, Wels, C and Robertson, A, MacG, 2002, ARD production and water vapor transport at the Questa Mine, in *Proceedings Ninth International Conference on Tailings and Mine Waste, Tailings and Mine Waste '02*, pp 479-488 (AA Balkema Publishers: Lisse).

Leps, T.M., 1970, Review of Shearing Strength of rockfill. Journal of Soil Mechanics and Foundation Engineering Division, 96(SM4): 1159-1170.

Leslie, D. D., 1963, Large Scale Triaxial Tests on Gravelly Soils, Proceedings, 2nd Pam Am Conference on Soil Mechanics and Foundation Engineering, Vol. I, p. 181-202.

Lewis, J. G., 1956, Shear Strength of Rockfill, Proceedings of the 2nd Australia-New Zealand Conference on Soil Mechanics and Foundation Engineering, p, 181-202.

Li, M., 1999, Hydrochemistry of oxidized waste rock from Stratmat site, N.B.: MEND 1.36.2a, 81 p.

Little, A. L., 1969, The engineering classification of residual tropical soils; in Proceedings 7th International Conference Soil Mechanics Foundation Engineering: Mexico City, vol. 1, p. 1-10.

Linero, S., Palma, C., and Apablaza, R., 2007, Geotechnical Characterization of Waste Material in Very High Dumps with Large Scale Triaxial Testing, Proceedings of International Symposium on Rock Slope Stability in Open Pit Mining and Civil Engineering, 12-14, September 2007, Perth, Australia, p. 59-75.

Lipman, P. W. and Reed, J. C., Jr. 1989, Geologic map of the Latir volcanic field and adjacent areas, northern New Mexico. U. S. Geological Survey, Miscellaneous Investigations Map I-1907, scale 1:48,000.

Lohnes R.A. and Demirel T., 1973, Strength and structure of laterites and lateritic soils,

Engineering Geology, 7, 13-33.

Lucia, P.C., 1981, Review of experiences with flow failures of tailing dams and waste impoundments: PhD dissertation, University of California, Berkeley, 234 p.

Maquaire O., Malet J.P., Remaitre A., Locat J., and Guillon J., 2003, Instability conditions of marly hillslopes: towards landsliding or gullying? The case of Barcelonnette Basin, South East France, Engineering Geology, 70, 109-130.

Marachi, D. N., Chan, C. K., Seed, B. H., and Duncan, J. M., 1969, Strength and Deformation Characteristics of Rockfill materials, Department of Civil Engineering, University of California, Berkeley, California, Report No. Te-69-5, 139p.

Marsal, R. J., 1965a, Discussion, Proceedings, 6th International Conference on Soil Mechanics and Foundation Engineering, Vol. 3, p. 310-316.

Marsland, A., 1971, "The Use of In Situ Tests in a Study of the Effects of Fissures on the Properties of Stiff Clays," *First Australian-New Zealand Conference on Geomechanics*, Melbourne, Australia, Vol. 1, p. 180—189.

Martin, V., Aubertin, M., Zhan, G., Bussière, B., and Chapuis, R.P., 2005, An investigation into the hydrological behaviour of exposed and covered waste rock dumps: SME Preprint 05-109, 10 p.

Martín-Garcia, J. M., Delgado, G., Parraga, J. F., Gamiz, E., and Delgado, R., 1999, Chemica, mineralogical and (micro)morphological study of coarse fragments in Mediterranean red soils: Geoderma, v.90, p. 23-47.

McCarthy, D. F., 1993, Essential of Soil Mechanics and Foundations: Basic Geotechnics. Prentice Hall, New Jersey. 200 p.

McLemore, V. T., Walsh, P., Donahue, K., Gutierrez, L., Tachie-Menson, S., Shannon, H. R., and Wilson, G. W., 2005, Preliminary Status Report On Molycorp Goathill North Trenches, Questa, New Mexico, *in* 2005 National Meeting of the American Society of Mining and Reclamation, Breckenridge, Colorado, p. 26.

McLemore, V.T., 2008, Evaluation of weathering indices for the Questa rock piles: unpublished report to Chevron, Task B1.1.

Mellinger, F.M., 1966, Laboratory and In-situ Tests of Scale, Proceedings, America Society of Civil Engineers Water Resources Engineering Conference, Denever, Colorado.

Meyer, J. W., 1991, Volcanic, plutonic, tectonic and hydrothermal history of the southern Questa Caldera, New Mexico. University Microfilms, Ph.D. dissertation, 348 p.

Meyer, J. and Leonardson, R., 1990, Tectonic, hydrothermal, and geomorphic controls on alteration scar formation near Questa, New Mexico: New Mexico Geological Society, Guidebook 41, p. 417-422.

Mitchell, J. K., 1993, Fundamentals of Soil behavior, John Wiley and Sons, New York

Molycorp Inc., 2002, Request for Letters of Intent, Questa, NM. http://www.infomine.com/consultants/doc/mcrliaun.pdf

Morin, K.A., Gerencher, E., Jones, C.E., and Konasewich, D.E., 1991, Critical review of acid drainage from waste rock: MEND report 1.11.1, 193 p.

Morin, K.A., Hutt, N.M., and Hutt, S.G., 1997, History of Eskay Creek mine's waste-rock dump from placement to disassembly: MEND Project 1.44.1, 419 p.

Mutschler, F. E., Wright, E. G., Ludington, S. D., and Abbott, J. T., 1981, Granitic molybdenite systems: Economic Geology, v. 76, p. 874-897.

Nichols, R. S., 1987, Rock Segregation in Waste Dumps, *in* Flow-through Rock Drains: Proceedings of the International symposium convened at the Inn of the South, Cranbrook, B. C.

Nolan, Davis, and Associates, Limited, 1991, Heath Steele Waste Rock Study: MEND project 2.31.1(a), 187 p.

Nordstrom, D. K., McCleskey, R. B., Hunt, A. G., and Naus, C. A., 2005, Questa Baseline and Pre-mining Ground-Water Quality Investigation. 14. Interpretation of 123 Ground-Water Geochemistry in Catchments Other than the Straight Creek Catchment, Red River Valley, Taos County, New Mexico, 2002-2003: U.S. Geological Survey, Scientific Investigations Report 2005-5050.

Norwest Corporation, 2004, Goathill North Slide Investigation, Evaluation and Mitigation Report: unpublished report to Molycorp Inc., 99 p., 3 vol.

Norwest Corporation, 2005, Questa Roadside Rockpiles 2005 Operation Geotechnical Stability Evaluation: unpublished report to Molycorp Inc., 210 p., 3 vol.

Okagbue C.O., 1986. An Investigation of Landslide Problems in Spoil Piles in a Strip Coal Mining Area, West Virginia (USA), Engineering Geology, 22, 317-333.

O'Loughlin, C .L. and Pearce, A .J., 1976, "Influence of Cenozoic Geology on Mass Movement and Sediment Yield Response to Forest Removal, North Westland, New Zealand'" Bulletin of the International Association of Engineering Geology, Vol. 14, p. 41—46.

Pa'lossy, L., Scharle, P., and Szalatkay, I., (1993), Earth Walls, Ellis Horwood, New York, ISBN 0-13-223876-4, 246 p.

Pasamehmetoglu, A.G., Karpuz, C. and Irfan, T.Y., 1981, The Weathering Characteristics of Ankara Andesites from the Rock Mechanics Point of View; in Weak Rock, Soft, Fractured and Weathered Rock: Proceedings of the International Symposium on Weak Rock; v. I, A.A. Balkema, Rotterdam, Netherlands, p. 185-190 .

Pereira, J. H. F., 1996, "Numerical Analysis of the Mechanical Behavior of Collapsing Earth Dams During First Reservoir Filling," Ph.D. thesis, University of Saskatchewan, Saskatoon, Saskatchewan, Canada, 449 p.

Pereira, J. H. F. and Fredlund, D. G., 1999, "Shear Strength Behavior of a Residual Soil of Gneiss Compacted at Metastable-Structured Conditions," *11th* Pan Anmerican Conference on Soil Mechanics and Geotechnical Engineering, Iguazu Falls, Brazil, Vol. 1, pp. 369—377.

Pernichele A.D. and Kahle M.B., 1971, Stability of waste dumps at Kennecott's Bingham Canyon mine, Society of Mining Engineers, AIME, transactions, Vol. 250, 363-367.

Powers, M.C., 1982, Comparison chart for estimating roundness and sphericity: AGI (American Geological Institute), Alexandria, Va., data sheet 18.1

Pusch, R. R., 1973, General Report on Physico-Chemical Processes which affect Soil Structure and Visa Versa, Proceeding of the International Symposium on Soil Struture, Gothenburg, Sweden, Appendix pp. 33.

Robertson, A.M., 1982, Deformation and Monitoring of Waste Dump Slopes, pp. 16.

Robertson, A. M., 1985, Mine Waste Disposal: An Update on Geotechnical and Geohydrological Aspects.

Rowe, P. W., 1962, The Stress-Dilatancy Relation for Stastic Equilibrium of an Assembly of Particles in Contact, Proceedings of the Royal Society of London, Vol. 269, pp. 500-527.

Robertson GeoConsultants Inc., 2000, Progress Report: Questa Mine Rock Pile Monitoring and Characterization Study: Robertson Geo Consultants Inc., Report No. 052007/3 For Molycorp Inc

Saretzky, G.T., 1998, Hydrological Characterization of a Sulfide Waste Rock Dump: M.S. thesis, Univ. of Saskatchewan, Saskatoon, SK.

Savci, G. and Williamson, A.L., 2002, Hydrologic Assessment of Waste Rock Stockpiles: A case study from Ajo mine, Arizona: SME proceedings, Phoenix

Scheinost, A. C. and Schwertmann, U., 1999, Color identification of iron oxides and hydroxysulfates: use and limitations: Soil Science Society of America Journal, v. 63, pp. 1463-1471.

Schilling J.H., 1956, Geology of the Questa molybdenum (Moly) mine area, Taos County, New Mexico, State Bureau of Mines and Mineral Resources, New Mexico Institute of Mining and Technology, Campus Station, New Mexico, Bulletin 51:87.

Schultze, E.,1957, Large Scale Shear Tests, Proceeding of 4th International Conference on Soil Mechanics and Foundation Engineering, London, England, Voulme 1, p.193.

Seedman, R. W., and Emerson, W. W., 1988, The Role of Clay-rich Rocks in Spoils Pile Failure at Goonyella, Queensland, Austria, International Journal of Rock Mechanocs and Mining Science, 22, p. 113 – 118.

Shannon, H. R., 2006, Fluid Transport through a Variably Saturated Rock Pile hill slope system .M.S. thesis, Department of Mineral Engineering, New Mexico Tech, New Mexico.

Shaw S., Wels C., Robertson A., and Lorinczi, G., 2002, Physical and Geochemical Characterization of Mine Rock Piles at the Questa Mine: an Overwiew, 9th International Conference on Tailings and Mine Waste, Balkema, Rotterdam.

Shum, M. G. W., 1999, Characterization and Dissolution of Secondary Weathering Products from the Gibraltar Mine Site [M. S. thesis]: University of British Columbia, 310 p.

SigmaStat for Windows Version 3.10 Copyright, 2004, Systat Software, Inc.

Skempton, A. W., 1958, Arthur Langtry Bell (1874 – 1956) and His Contribution to Soil Mechanics, Geotechnique, Voulme 8, Number 4, p. 143-157.

Sracek, O., Choquette, M., Gelinas, P., Lefebvre, R., and Nicholson, R. V., 2004, Geochemical Characterization of Acid Mine Drainage from a Waste Rock Pile, Mine Doyon, Quebec, Canada: Journal of Contaminant Hydrology, v. 69, p. 45-71.

Stormont, J.C., and Farfan, E., 2005, Stability Evaluation of a Mine Waste Pile: Environmental and Engineering Geoscience, v. 11(1), p. 43-52.

Swanson, D.A, Savci, G., Danzier, G., Williamson, A., and Barnes, C., 2000, Unsaturated hydrologic assessment of waste rock stockpiles in semi-arid climates; in ICARD 2000: Proceedings from the 5th International Conference on Acid Rock Drainage, Society for Mining, Metallurgy, and Exploration, Inc, Littleton, Co., v. 2, p. 1273-1282.

Terzaghi, k., Peck, R.B. and Mesri, G.M., 1996, Soil Mechanics in Engineering Practice. John Wiley and Sons, Inc., New York, 549 p.

Tobias, S, 1990, "Auswertung der Direkt-Schwerversuche, " unpublished Ph.D. Thesis, Zurich University.

URS Corporation, 2000, "Interim Mine Rock Pile Erosion and Stability Evaluations, Questa Mine," Unpublished report to Molycorp, Inc., 6800044388.00, December 1, http://www.molycorp.com/hes/MolycorpQuestaReports/InterimReport052007_1.pdf (accessed on February 14, 2007).

Vallerga, B. A., Seed, H. B., Monismith, C. L., and Cooper, R. S., 1957, Effect of Shape Size and Surface Roughness of Aggregate Particles on the Strength of Granular Materials, Special Technical Publication No. 212, ASTM, pp.

Varadarajan, A., Sharma, K. G., Venkatachalam, K., and Gupta, A. K., 2003, Testing and Modeling Two Rockfill Materials, Journal of Geotechnical and Geoenvironmental Engineering, Vol. 129, No. 3, ISSN 1090-0241, p. 206-218.

Viterbo, V.C., 2007, Effects of pre-miming hydrothermal alteration processes and post-mining weathering on rock engineering properties of Goathill North rock pile at Questa mine, Taos County, New Mexico: M. S. thesis, New Mexico Institute of Mining and Technology, Socorro, 274 p., http://geoinfo.nmt.edu/staff/mclemore/Molycorppapers.htm, accessed December 06, 2007.

Western Regional Climate Center, 2003, Historical Climate Information: New Mexico Climate Summaries, Red River, New Mexico (297323).

Williams, D. J., 2000, Assessment of Embankment Parameters, Slope Stability in Surface Mining, Society for Mining, Metallurgy, and Exploration, Inc. (SME), ISBN 0-87335 194-0, TN291 .S56 2001. p. 275 – 284.

WinSTAT Statistics for Windows, Version 3.1, Copyright, 1991-1996 Kalmia Co. Inc

Wu, T. H., McKinnell, III, W. P. and Swanston, D. N., 1979, "Strength of Roots and Landslides on Prince of Wales Island, Alaska," Canadian Geotechnical Journal, Vol. 16(1), p. 19—33.

Yokota S. and Iwamatsu A., 1999, Weathering Distribution in a Steep Slope of Soft Pyroclastic Rock as an Indicator of Slope Instability, Eng. Geology, 55: p. 57-68.

Yokoyama, T. and Nakashima, S., 2005, Color development of iron oxides during rhyolite weathering over 52,000 years: Chemical Geology, v. 219, p. 309-320.

Yilmaz, I., 2001, Gypsum/anhydrite: some engineering problem, Bull Engineering Geology Enviorment, Volume 59. p. 227-230.

Young, R. N., and Sheeran, D. E., 1973, Fabric Unit Interaction and Soil Behaviour, Proceedings of the International Symposium on Soil Struture, Gothenburg, Sweden, p. 176-183.

Zahl, E. G., Biggs, F., Boldt, C. M. K., Connolly, R. E., Gertsch, L., and Lambeth, R. H., 1992, Waste Disposal and Contaminant Control, *in* Hartman, H. L., ed., SME Mining Engineering Handbook: Littleton, CO, Society for Mining, Metallurgy and Exploration Inc., p. 1170-1180.